UNIVERSITY OF PIEMONTE ORIENTALE
"AMEDEO AVOGADRO"

Department of Translational Medicine

PhD PROGRAM IN BIOTECHNOLOGY FOR HUMAN HEALTH

XXVI cycle

Academic years 2010-2013

PhD THESIS

THE DIACYLGLYCEROL KINASE ALPHA IS A KEY REGULATOR OF EPITHELIAL CELLS POLARIZATION

Supervisor:

Prof. Andrea Graziani

PhD Coordinator:

Prof. Claudio Santoro

PhD Student:

Valentina Bettio

Table of contents

Summary

During these three years of PhD fellowships I have been studying how the lipid kinase Diacylglycerol kinase alpha regulates epithelial cells polarization. All the results were obtained under the supervision of Prof. Andrea Graziani, in the laboratory of Biochemistry of the Department of Translational Medicine in Novara (Italy).

The main purpose of my PhD project was to elucidatethe Diacylglycerol kinase alpha downstream signalling in 3D-high polarized MDCK cells, which organize in structures known as cysts. MDCK cysts are a key tool to understand the molecular pathways that regulate cystogenesis and tubulogenesis. The Diacylglycerol kinase alpha is a central player during MDCK cystogenesis and the data obtained in MDCK cysts strongly correlates its enzymatic activity to proper cystogenesis and luminogenesis, as well as to mitotic spindle orientation during cell mitosis.

These new findings further confirm that the Diacylglycerol kinase alpha is a key regulator of different biological processes and provide a strong link between Diacylglycerol kinase alpha catalytic activity and cystogenesis, targeting of protein at different cellular compartments and proper orientation of the mitotic spindle.

Introduction

Epithelial tissues organization

All metazoa show a common feature: their cells are organized in multicellular tissues and organs. Metazoa epithelial tissues are the most important model of organization *in vivo*. Indeed, epithelia are the most archetypal polarized tissues in metazoa and more than 60% of mammalian cell types belong to the epithelial cluster or derive from it (1). Epithelial tissues are formed by sheets of adherent cells that divide the organism into topologically and physiologically distinct spaces. Despite some rare exceptions, epithelial tissues cover the entire organism and are the interface trough different biological compartments and with the external environment.

Epithelial tissues can be classified using their morphological features as discriminants. Based on this classification, there are:

- glandular epithelia are involved in secretion processes and are organized in structures known as glands. There are different kinds of glands. The first type are simple invaginations of the epithelial surface that can secrete their contents through their ducts. This kind of glands are called exocrine glands. Otherwise, epithelial cells can give rise to solid organs or islands that secrete hormones into other tissues. This glands are known as endocrine glands;
- simple epithelia are formed by a monolayer of cells. Usually, they feature absorption and secretion functions. This kind of epithelia provide a poor protection against mechanical insults and their cells show different specialized structures, such as cilia;
- stratified epithelia comprise multiple layers of cells. They are really thick and feature a protective function against mechanical stresses and insults. Indeed, stratified epithelia, such as skin, cover the outside of the organism.

Epithelial cells can be organized in tubes that infiltrate the whole organism, carrying liquid and gases containing nutrients, waste and other materials. In certain tissues, such as lung and kidney, these tubes form elaborate networks and glands.

Role of EMT and MET in tissue morphogenesis

Epithelial to mesenchymal transition (EMT) is widely recognized as an essential biological process to allow dispersion of mesenchymal cells and organogenesis in

embryo. Moreover, EMT also plays a crucial role in the dispersion of malignant cells in patients with carcinomas. Indeed, the plasticity of cancer cells relies on their ability to adapt to the selective pressure existent during tumour development and aberrant reactivation of EMT can promote cancer cell plasticity (2; 3).

During EMT epithelial cells lose their epithelial characteristics and acquire typical properties of mesenchymal cells. Indeed, epithelial cells are usually strongly associates with their neighbours, so they barely move or dissociate from the epithelial layer. In contrast, mesenchymal cells do not form a regular layer of adjacent cells or specialized intracellular adhesion complexes, but they feature an elongated shape and an high migratory capacity. Nevertheless, migrating mesenchymal cells are still polarized, as well as when they interact with neighbour cells, and migrate easily within tissues. For example, they can cross large distances along the embryo to give rise to a particular organ. In the adult, instead, their main function is to maintain structural integrity by secreting extracellular matrix. Moreover, in tumour cells EMT-induced lost of cell polarity and cell-cell interactions increase the migratory and invasive properties (3;4).

EMT is essential to allow the generation of new tissue types during development, but also contributes to the pathogenesis of diseases. For example, in the context of renal disease epithelial cells can undergo EMT and usually it correlate with a poor renal outcome; moreover, in adult epithelial structures EMT contributes to organ scarring as a result of the loss of epithelial function and matrix production (5).

To allow tube formation, epithelial cells undergo EMT and lose the apical-basolateral polarization, downregulate cell-cell adhesion, change their cytoskeleton composition and invade the ECM. Then, during EMT epithelial cells adopt a mesenchymal phenotype, although they could be still polarized and display the classic planar cell polarity of migrating cell. Afterwards, epithelial cells undergo mesenhymal to epithelial transition (MET) and restore their apical-basolateral polarity.

Cell polarity and epithelia

The main feature of epithelial cells is their polarized phenotype. Cell polarization is a complex feature that involves the asymmetric organization of most of the physical aspects of the cell. This asymmetric polarization must be finely coordinated to obtain structured tissues. The final properties of the derived tissue are a consequence of the properties of the cells involved in its development.

Today, it is known that different groups of cells or tissues can be organized into different polarized arrangements by coordinating their polarity in space and time. It is also clear that their diversity is due to conserved design principles. Nonetheless, the formation of a tissue is truly complex: several biological processes – such as cell division, cell death ecc. – must be coordinated in space and time in the tissue itself.

Evolutionary, the polarized phenotype allows cell specialization and can be found in a lot of cell types. For example, the neuronal synapses show specialized sites in which neurotransmitters are released and captured (6). Another example are migrating cells, that show a front-rear polarization during the external-stimuli induced cell migration (7). For single epithelial cells, the polarized phenotype is obtained through the asymmetric organization of their components, such as Golgi apparatus, centrosome and cytoskeleton. Indeed, every single cell in the monolayer lining a tubule features the same orientation, with its apical surface facing the central lumen and its basal surface facing the outside of the structure.

The most studied polarized epithelial tissues are the simple epithelium of mammalian intestine and kidney. Their cells show a columnar shape and their apical surfaces provide the luminal interface; instead, their lateral surface is in contact with adjacent cells. Specialized junctions and cell-cell adhesion structures are localized in the cell-cell contact area. In particular, in epithelial cells intracellular junctions allow the formation of a continuous layer of cells and can be use to move metabolites from cell to cell. There are three different types of intracellular junctions: *i)* tight junctions, that localize just below the apical membrane and isolate the intracellular spaces from the lumen, forming the *zonula occludens* and limiting paracellular permeability, *ii)* anchoring junctions, that link cytoskeletons of adjacent cells, allowing the formation of a single functional unit and *iii)* gap junctions, which contains hundreds of small pores that allow the exchange of small molecules between adjacent cells.

Finally, the basal surface of epithelial cells contacts the underlying basement membrane, extracellular matrix and underlying blood vessels. The basal and the lateral surfaces are similar in composition and organization and together are called “basolateral” domain.

The peculiar organization of epithelial cells define their apical-basolateral polarization. In order to establish the apical-basolateral polarity, epithelial cells must segregate proteins and lipids asymmetrically to the apical and basolateral domains. Furthermore, the delivery of membrane and secretory proteins to defined intracellular

compartments and membranes is a crucial and mandatory step to define and maintain the identity and the functions of epithelial cells. Indeed, intracellular vesicular trafficking and protein localization is finely regulated in order to ensure the proper apical-basolateral polarization.

In vitro models to study cystogenesis and tubulogenesis

Today, there are some *in vitro* systems that allow to study tube formation and could be useful to understand common mechanism underlying tubular organ formation and development. One of the most used is represented by MDCK cells, which derive from the dog kidney distal tubule and collecting ducts and preserve their properties. MDCK cells self-organize into hollow spheres called cysts. These cysts are formed by a monolayer of polarized cells and resemble the complex organization that epithelial cells display *in vivo*. When treated for some days with Hepatocyte Growth Factor (HGF), these cysts produce branching tubules. This branching tubulogenesis is reminiscent of the structures found in many epithelial organs (8; 9).

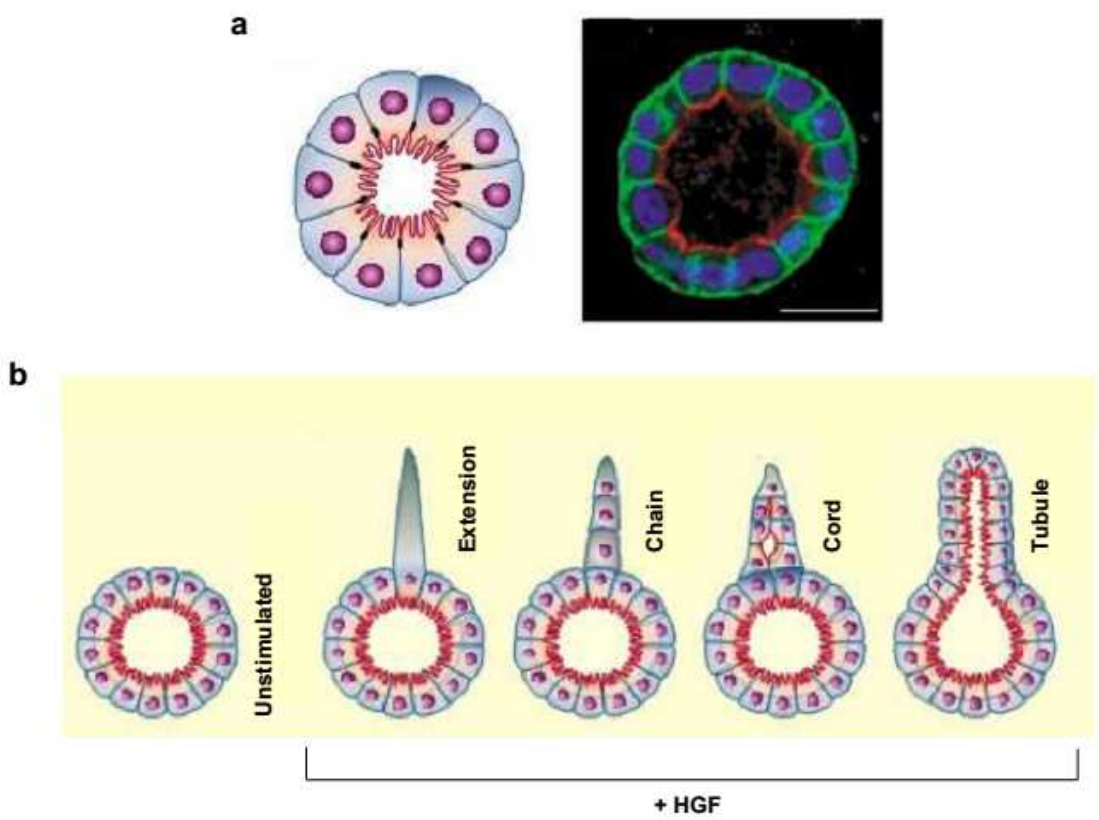

Figure 1: Cystogenesis and tubulogenesis *in vitro*.

a) Typical cysts embedded in extracellular matrix. The left panel shows a representation of a cyst, with the basolateral domain in blue and the apical domain in red. The right panel shows a confocal

image of an MDCK cysts. Here, the apical domain is marked with GP135 in red, the basolateral domain is marked with β-catenin in green and nuclei are blue. **b)** Tubulogenesis induced by HGF administration. When treated with HGF, MDCK cysts undergo branching tubulogenesis through three intermediate states, named extension, chain and cord (10).

Obviously, these culture systems are still a gross simplification of the high complex architecture founded *in vivo* and present some limits, but their use might be appropriate for many studies, such as to investigate the involvement of external stimuli and intracellular signalling in organ development – in healthy or pathological conditions – or in response to an injury.

As described before, the most important feature of *in vivo* epithelial structures is that they are generally lined by a monolayer of well polarized epithelial cells, which have an apical surface facing the lumen and a basolateral surface in contact with neighbour cells and with the extracellular matrix. When cultured in 3D matrix gels, such as type I collagen and Matrigel, MDCK cells form the previously cited cysts, 3D monolayer structures with well defined apical (AP) and basolateral (BL) domains. A crucial step during cystogenesis is to create the central lumen. Today, two main mechanisms are known: cavitation and hollowing (1).

Cavitation starts during the first phases of cystogenesis, when cells are not so polarized and begin to proliferate. As a consequence of proliferation, some daughter cells will not be in contact with the extracellular matrix and undergo apoptosis, leaving the hollowed central lumen (Figure 2a). This mechanism is used *in vivo* by the cells of the mammary acini and involves the pro-apoptotic BCL2-family factors, while is contrasted by the oncogene ERBB2 (1).

The hollowing process is a peculiarity of cells displaying a fast rate of polarization and relies on vesicular trafficking to the apical domain. Indeed, small vesicles containing liquid and apical proteins are generated by endocytosis at the basolateral domain and recruited both to specific intracellular membrane compartments and to the apical domain. Their fusion with the apical membrane induces the formation of a rudimental lumen between two adjacent cells (Figure 2b). Now, these two cells are able to orientate around the lumen and to define the classic apical-basolateral polarization. The derived cyst will preserved in time this polarized organization around the central lumen (1).

Once formed, cysts and tubules must maintain their structure and their polarized organization. Different settings of proteins and pathways are involved in cystogenesis

and are also necessary to preserve epithelial cells polarization and organization in the 3D context.

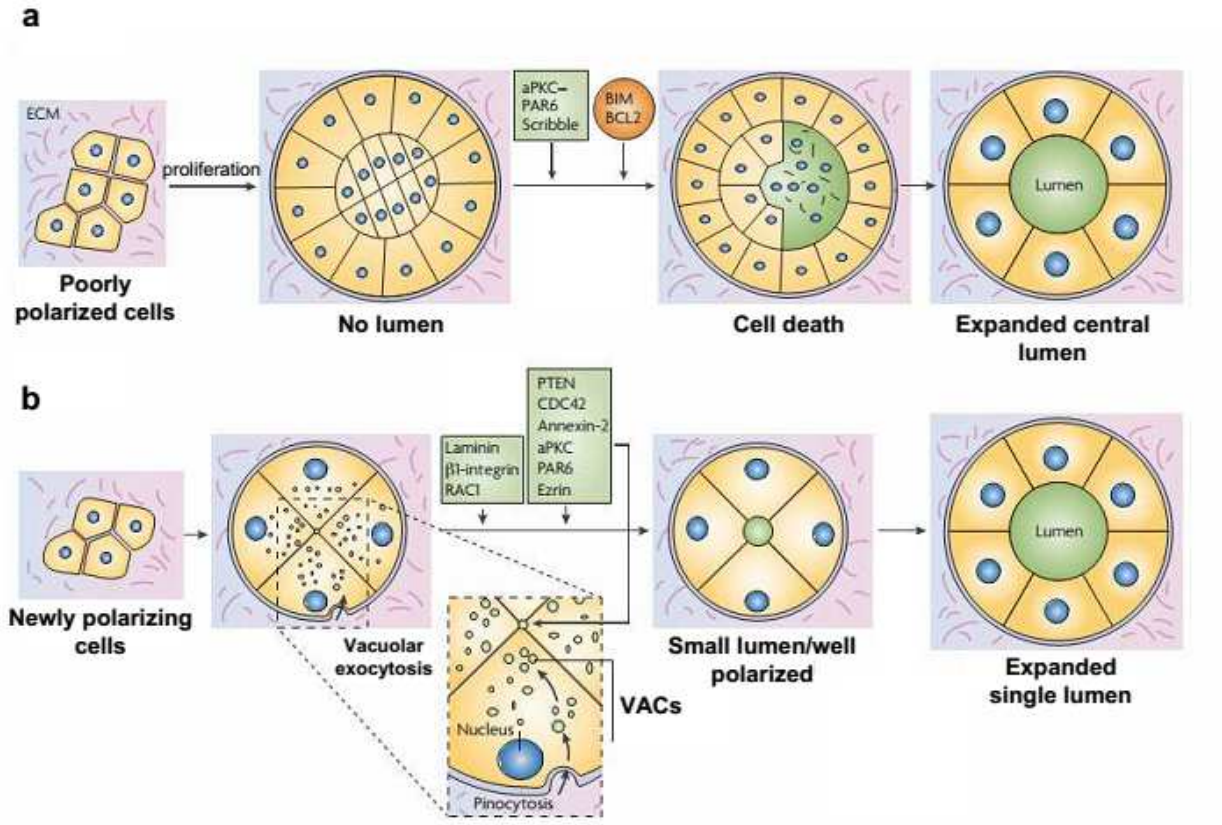

Figure 2: Cavitation and hollowing.

a) Cavitation. Poorly polarized cells proliferate and the cells not in contact with the extracellular matrix undergo apoptosis, resulting in lumen clearing and polarized cyst formation **b)** Hollowing. Intracellular vesicles are delivered to regions between cells. Once rudimental lumens are formed, tight junctions, pump proteins and the polarity complexes promote the formation of a single expanded lumen (Adapted from 1).

Master regulators of cell polarity

During the cell polarization process a cell respond to an extracellular stimulus and redistribute its proteins and organelles in an asymmetrical layout, preserving this organization in time. The polarized phenotype is mandatory for many cellular processes, such as cell migration, differentiation an morphogenesis and is regulated by some important family of proteins. As described before, epithelial cells are characterized from their apical-basolateral polarization, which most important regulators are represented by the polarity complexes. Today, three major polarity complexes are known:

1. Par complex. The PAR family of proteins was first identified in *C. Elegans* during a screening for lethal mutants of early developmental genes. In this study, it has been established that mutants of the PAR-family proteins lose their apical-basolateral polarized localization. Their delocalization perturbs asymmetric cell division of blastomeres in early gastrulating embryonic cells, leading to the formation of a defective body pattern (11). Four different proteins compose the Par complex: Cdc42, Par-3 (Bazooka), Par-6 and the atypical protein kinase C (aPKC). The Par complex is involved in induction and maintenance of the apical-basolateral polarity and can be further divided into other two complexes: *i*) the Cdc42/Par-6/aPKC complex, which is important to define the apical domain identity, and *ii*) the Par-3/aPKC complex, that is involved in tight junctions formation (12).
2. Crumbs complex. It is composed by three proteins, Crumbs (Crb), Pals and PATJ and is conserved from invertebrates to vertebrates. This complex was first identified in *Drosophila Melanogaster* (13) and it plays a pivotal role in defining apical-basolateral domains of epithelial cells. Indeed, The Crumbs complex localizes at the apical domain and regulates apical polarity together the Par complex, providing a central regulatory pathway for the establishment of polarity and epithelial functions.
3. SCRIB complex. It has three members, Scribble (SCRIB), Dlg (Discs Large) and Lgl (Lethal Giant Larvae). SCRIB was first identified in *Drosophila Melanogaster* as a regulator of epithelial cell septate junctions. SCRIB acts in combination with Lgl, Dlg and also with the PAR complex both in *Drosophila Melanogaster* and in mammals (14; 15). Here it is necessary to establish the polarization of epithelial cells and to preserve the polarization of the basolateral domain. The SCRIB complex is important for adherence junction and cell–cell contact integrity and may play an important role in the regulation of E-cadherin at the anchoring junctions (16).

There is a crosstalk between these three polarity complexes. Indeed, Par-6 acts as a targeting subunit for aPKC and recruits both Crumbs complex and Lgl as substrates (1).

The Par, Crumbs and SCRIB polarity complexes regulate the asymmetric localization of the Rho family small GTPases, that in some cases are components of the complexes themselves – such as for Cdc42 in the Par complex. Mammalian Rho

GTPases are master regulators of cell polarity and membrane dynamics and are a family of 20 proteins which most important role is to regulate actin cytoskeleton dynamics and remodelling. As any classic GTPase, also Rho GTPases switch between an active form, bound to GTP, and an inactive one, bound to GDP. The cycling between these two states is finely tuned by guanine nucleotide-exchange factors (GEFs), GTPase-activating proteins (GAPs) and guanine nucleotide-dissociation inhibitors (GDIs). GTP-bound Rho GTPases can interact with and activate downstream effectors, regulating a wide range of processes, such as morphogenesis, cell migration, cell adhesion, vesicle transport and microtubule dynamics (17). The most important members of this family are Rac, Cdc42 and Rho.

Today, three Rac isoforms have been described, based on sequence similarity: Rac1, Rac2 and Rac3. These proteins stimulate lamellipodium and membrane ruffles formation and, despite their high sequence similarity, they show different expression patterns and non-redundant functions. Indeed, Rac1 is ubiquitously expressed, while Rac2 is expressed in cells from haematopoietic origin and Rac3 is high expressed in the brain (17).

Cdc42 has a conserved role in the regulation of cell polarity, cell migration and fate specification during cell division in many eukaryotic organisms. Cdc42 also regulates filopodium formation in many cell types and chemotaxis and direct cell migration both *in vivo* and *in vitro*. Moreover, Cdc42 affects tight junctions formation and polarized trafficking of proteins (17).

The Rho subfamily is composed by three isoforms – RhoA, RhoB and RhoC – that show a high homology. They are responsible for stress-fibres formation, vesicle trafficking and cancer development. Indeed, RhoB function as a tumour suppressor: its expression is reduced in tumours and its overexpression inhibits cell growth, survival, invasion and metastasis. Moreover, RhoC expression correlates with metastasis in several cancer types and it is sufficient to induce metastasis in poorly metastatic cells (17).

The Rho GTPases are also involved in the epithelial apical-basolateral polarization and they accomplishes different functions. As described before, Cdc42 is a member of the Par polarity complex and localizes at the apical domain. Rac1 localizes at the basolateral domain and to the tight junctions. Its function is important to maintain the polarized phenotype together Integrins and E-cadherin. RhoA is

targeted to the whole plasma membrane and its activity is essential for proper tubulogenesis (1).

Membrane lipids and polarity

In the past years, phosphoinositides (PtdIns) have emerged as markers of membrane identity. In particular, in mammalian cells phosphatidylinositol-4,5-biphosphate – PI(4,5)P_2 – and phosphatidylinositol-3,4,5-triphosphate – PI(3,4,5)P_3 – are key determinants of the apical and basolateral surface respectively. PtdIns are lipidic signals which allow the proper localization of different proteins at distinct cellular domains. They play a key role during apical-basolateral polarity establishment and maintenance, as well as during *in vitro* cystogenesis. Indeed, in MDCK cysts it has been demonstrated that the lipid phospatase PTEN mediates PI(4,5)P_2 and PI(3,4,5)P_3 proper segregation. Par-3 recruits PTEN to the apical domain and here PTEN dephosphorylates the PI(3,4,5)P_3 to PI(4,5)P_2. As a consequence, the apical membrane results enriched in PI(4,5)P_2, which in turn recruits different proteins at the apical domain (18).

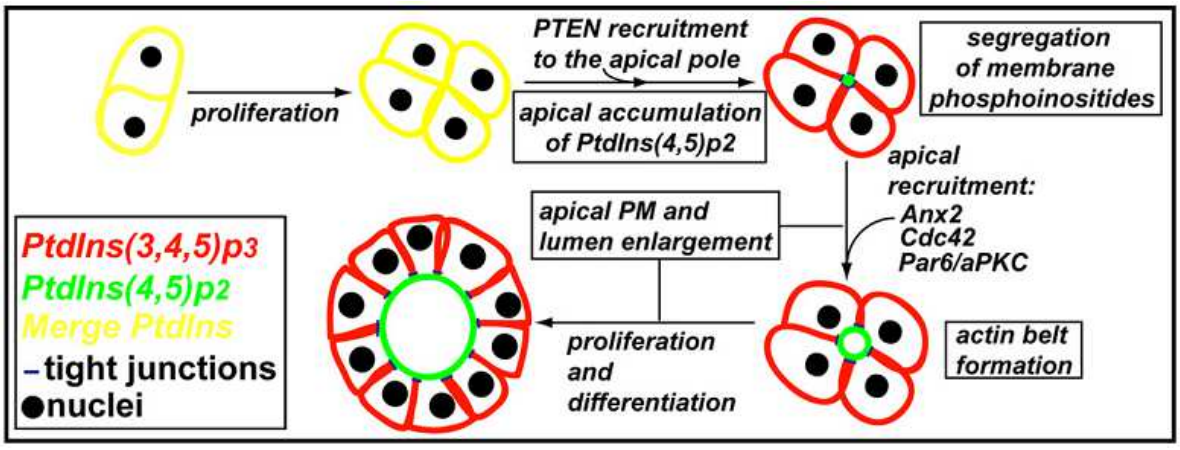

Figure 3: PI(4,5)P_2 and PI(3,4,5)P_3 segregation during cystogenesis. PI(4,5)P_2 and PI(3,4,5)P_3 colocalize in unpolarized cells (yellow). Apical recruitment of PTEN leads to PI(4,5)P_2 enrichment at this domain (green). PI(4,5)P_2 recruits the Par complex to form apical plasma membrane and lumen. (18).

PI(4,5)P_2 enrichment at the apical domain is mandatory during morphogenesis because it is the key signal that recruits the Par complex – in particular Cdc42, Par-6 and aPKC – at the apical domain. Instead, PI(3,4,5)P_3 is a landmark of specialized

regions of the basolateral plasma membrane and can determine the orientation of the mitotic spindle during mitosis.

Together $PI(4,5)P_2$ and $PI(3,4,5)P_3$ are key regulators of epithelial cells polarity and plasma membrane identity.

Mitotic spindle orientation, membrane lipids and polarity

Proper mitotic spindle orientation along a predetermined axis, which confines the plane of cell division, is essential for morphogenesis and embryogenesis and occurs in many types of cells. In most cases, spindle alignment along the predetermined axis requires both astral microtubules and the actin cytoskeleton. The interaction between microtubules plus ends and actin cytoskeleton is mediated by a family of proteins known as microtubules plus-end-tracking proteins (+Tips). The most important members of this family are EB1, Adenomatous Polyposis Coli (APC), CLIP associating proteins (CLASPs) and the dynein/dynactin complex.

In polarized cells, during mitosis astral microtubules interact with cortical factors in specific cortical regions and determine the proper orientation of the mitotic spindle. Dynein-dependent microtubule pulling forces are the most important players in this process. In 2D cultured cells, mitotic spindles are oriented parallel to the substratum through a mechanism involving Integrin-mediated cell-substrate adhesion and $PI(3,4,5)P_3$ restriction to specific membrane domains. In particular, $PI(3,4,5)P_3$ accumulates at the midcortex, where it recruits dynactin and induce the dynein-dependent spindle orientation in parallel to the substratum (19).

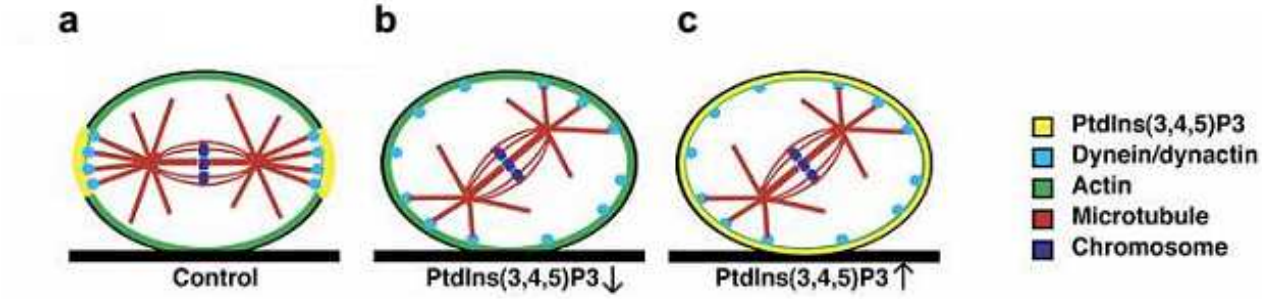

Figure 4: Mitotic spindle orientation in 2D cultured cells. $PI(3,4,5)P_3$ enrichment at the midcortex drives the orientation of the mitotic spindle in parallel to the substratum (a). $PI(3,4,5)P_3$ depletion (b) or delocalization (c) leads to mitotic spindle misorientation (19).

However, in 3D polarized epithelial cysts mitotic spindle can be oriented in parallel or perpendicularly to the apical-basolateral polarity plane.

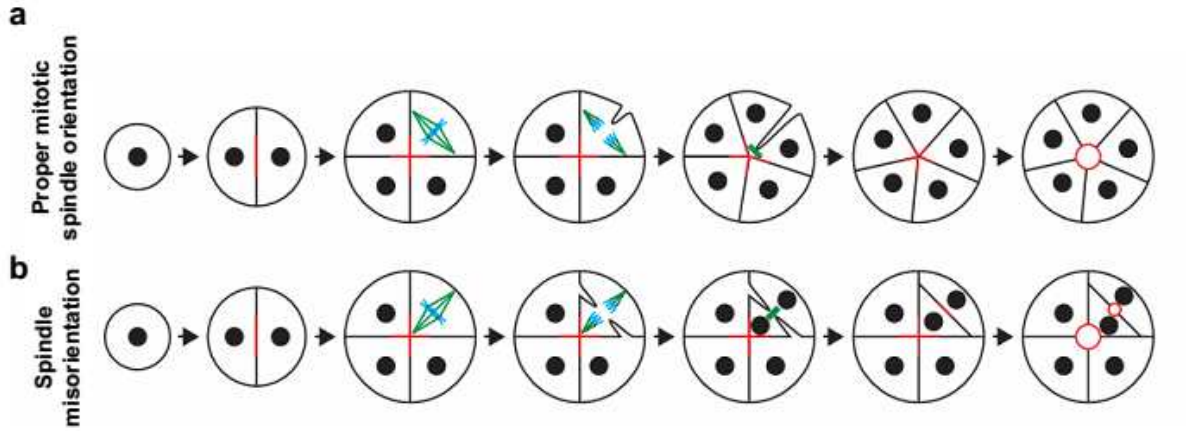

Figure 5: Mitotic spindle orientation in cysts. a) During normal cystogenesis, the mitotic spindle is oriented perpendicularly to the apical-basal axis and the mitotic cell divides in the plane of the monolayer. b) When the mitotic spindle is misoriented, the mitotic cell divides in the wrong plane, leading to the formation of aberrant cysts with multiple lumens. The apical surface (red), microtubules (green), and chromosomes (blue) are indicated (Adapted from 22).

The oriented cell division is a key step in different biological processes. For example, oriented cell division allows the stem cells to divide symmetrically or asymmetrically, along the parallel or perpendicular cell-substrate axis respectively. Here, the substrate is represented by their attached niche or the extracellular matrix.

Cell geometry, cell polarity and cell-cell adhesion have been proposed to be the determinants for the spindle axis orientation. Cell-cell adhesions provide a cortical cue to orient the mitotic spindle parallel to the epithelial plane. In particular, it has been demonstrated that the Gαi-LGN-NuMa complex is one of the most important regulators of astral microtubules anchorage to cell cortex. This complex localizes at the basolateral domain and is evolutionary conserved (in *Drosophila Melanogaster* its members are called Mud, Pins and Gαi respectively). GDP-loaded Gαi recruits LGN through its GoLoco motifs at the C-terminus. Moreover, LGN binds also microtubules-associated NuMA through the tetratricopeptide repeats (TPR) at its N-terminal portion (20). This interaction is essential for microtubules anchorage to the cell cortex. Furthermore, cortical NuMa also associates with the microtubule motor Dynein/Dynactin (21) providing a sliding anchorage for depolymerising microtubules, whose shrinkage pulls towards the cell cortex the connected spindle pole.

Cortical factors are not the only regulators of mitotic spindle orientation. Indeed, Cdc42 controls mitotic spindle orientation acting on the spindle machinery that controls the orientation of the mitotic spindle itself. Moreover, Cdc42 is required to properly position the apical surface by controlling spindle orientation during cell division (22; 23; 24).

Polarized cell division must be finely tuned and affects some physiological and pathological behaviours. The balance between symmetric and asymmetric cell division defines the number of indifferentiated stem cells, as well as the bulk of differentiated cells in a given tissue. The deregulation of spindle orientation in proliferating cells has been shown to cause abnormal stem cell differentiation, aberrant organ structures and functions and lead to the onset of disorders that include tumorigenesis and polycystic kidneys.

Diacylglycerol kinase alpha: diacylglycerol and phospatidic acid balance and their involvement in cell polarity

Diacylglycerol kinases (DGKs) are a family of lipid kinases that phosphorylates the membrane lipid diacylglycerol (DAG) into phosphatidic acid (PA), both lipid second messengers. Thus, DGKs tuned the transduction pathway of two seconds messengers, shutting down the DAG pathway and activating the PA one.

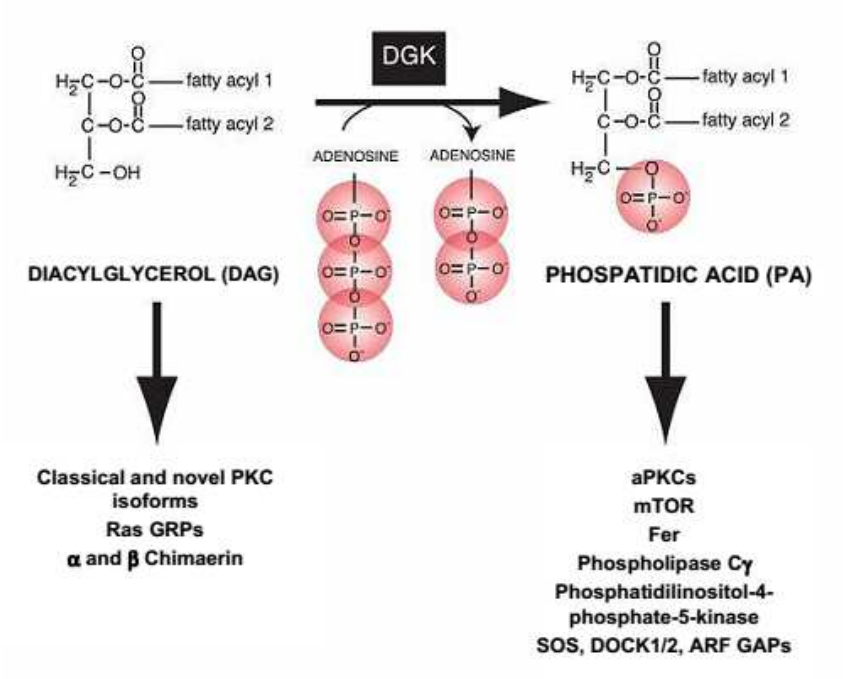

Figure 6: DGKs enzymatic activity regulates DAG and PA levels at the plasma membrane. DAG (left) and PA (right) downstream effectors are shown (27).

DAG is an activator of C1 domain-containing proteins, such as classic and novel protein kinase C (PKC), Ras guanine-nucleotide releasing factors (Ras GRPs) and alpha and beta Chimaerin (Rac1- and- Cdc42-GAP protein) (25).

PA binds to several proteins, although a specific PA binding domain has not been identified. It binds to and regulates the localization and function of several protein kinases (aPKC, mTOR, Fer), lipid metabolizing enzymes (Phospholipase Cγ, Phosphatidilinositol-4-phosphate 5-kinase) and small GTPase regulators (SOS, DOCK1/2 and ARF GAPs) (25, 26).

DGKs are cytosolic enzymes and they translocate to membrane compartments where DAG is produced. Some DGKs isoforms have been identified in unicellular organisms, such as bacteria and yeast. However, these isoforms are structurally different from those identified in higher eukaryotes. Indeed, the bacterial DGK is a small, integral membrane protein, unlike mammalian DGKs, and it can phosphorylate other lipids in addition to DAG (25).

There are 10 isoforms of DGKs in mammalian, divided into 5 classes basing on structural motifs. All the isoforms show two common structural domains: *i)* the catalytic domain, which contains the ATP binding site, and *ii)* two cysteine-enriched domains, homologous to the DAG-binding C1A and C1B domains of PKCs. The C1 domain closest to the catalytic domain contains an extended region of fifteen amino acids that contributes to DGKs activity. Indeed, mutations in this domain significantly reduce the kinase activity of DGK enzymes. Moreover, it seems that the C1 domains of some DGKs could act as protein-protein interaction sites and it suggest that these domains might bind not only DAG. For example, the C1 domain of DGKζ binds directly to the Rho GTPase Rac1 (25).

Every single DGK class also features some characteristics structural domains:

1. type I DGKs comprehends the α, β and γ isoforms. They show calcium-binding EF-hand motifs, that make them more active in presence of calcium, and a Recoverin Homology Domain;
2. type II DGKs class is composed by the δ, η and κ isoforms. They have pleckstrin homology domains at their amino-termini, which are able to weakly bind PtnIns in DGKδ. They also feature a sterile alpha motifs (SAM) at their carboxy-termini that might act as a localization cue and can also induce their homo- and hetero-oligomerization;

3. the only type III DGK is DGKε. It shows a strong specificity toward arachidonate in the sn-2 position of the acyl chains of DAG. This preference suggests that DGKε may be a key component of the pathway that induces the enrichment of PtdIns with arachidonate;
4. type IV DGKs are the ζ and ι isoforms. They have domains similar to the phosphorylation site of MARCKS proteins that act as localization cues. Moreover, these isoforms show four ankyrin repeats and a carboxy-terminal PDZ binding domain;
5. the only type V DGK is DGKθ. It has three C1 domains and a putative PH domain that contains a Ras association domain, though DGKθ do not associate with Ras (25).

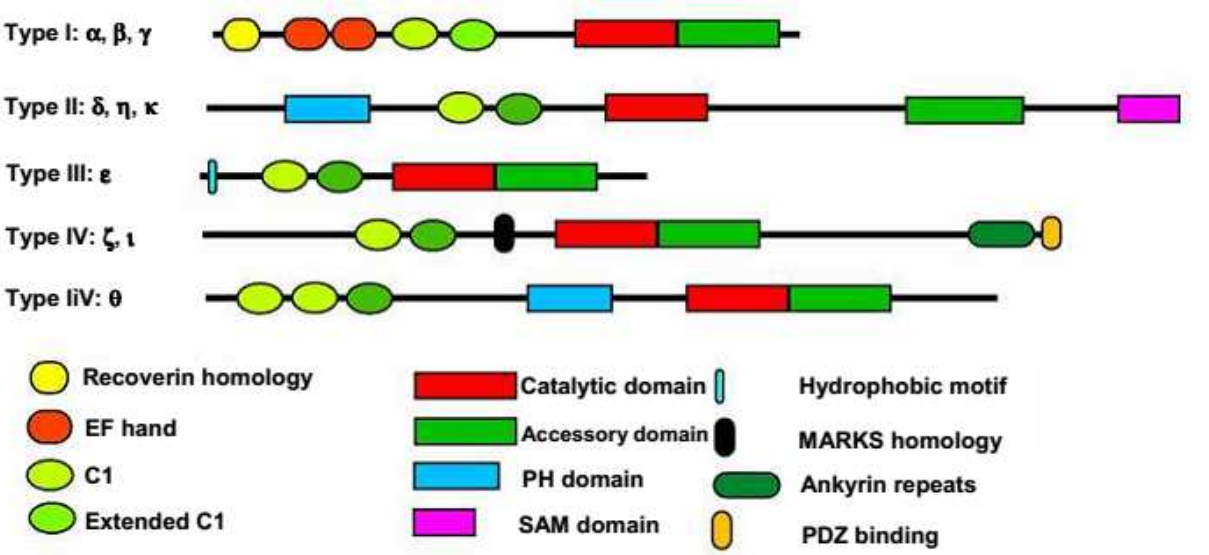

Figure 7: Structure of mammalian DGKs. The ten DGKs isoforms are grouped by sequence homology into five subtypes. Protein motifs common to several DGKs are shown (24).

DGKs structural diversity indicates that these enzymes modulate numerous important biological events likely independently. In this regard, in our laboratory it has been demonstrated the alpha isoform – which belongs to the type I DGKs – is specifically involved in cell migration, invasion and angiogenesis. In particular, DGKα is activated downstream growth factors stimulation – such as HGF and Vascular Endothelial Growth Factor (VEGF) – by Src kinase, that phosphorylates DGKα on Tyr^{335}. Moreover, expression of the oncogenic constitutive-active v-Src is sufficient to induce DGKα phosphorylation and consequent activation (28; 29; 30). In epithelial

MDCK cells, DGKα regulates HGF and v-Src-induced cell migration as well as focal adhesions and cytoskeletal actin remodelling. In MDCK cells, HGF acts as an EMT modulator and induces cell scatter: after a few minutes of HGF stimulation, MDCK cells remodel their actin cytoskeleton and start to elongate dynamic ruffles, that eventually evolve in lamellipodia, leading to the consequent cell migration. In our laboratory it has been demonstrated that in MDCK epithelial cells, upon HGF stimulation, DGKα activation provides a lipidic signal, PA, which recruits to the plasma membrane a complex containing Rac1, RhoGDI – a guanine nucleotide dissociation inhibitor of the Rho GTPases family members – and the atypical protein kinase Cζ/ι (aPKCζ/ι), which are activated by acidic lipids, such as PA. After its activation, aPKCζ/ι phosphorylates RhoGDI, with the consequent release of Rac1 from the complex and its activation. Rac1 itself can activate downstream effectors, leading to cortical actin remodelling and ruffles formation, triggering cell migration as a final effect (31; 32). Similarly, in this cell model DGKα controls membrane localization of Cdc42 through a mechanism independent from aPKCζ/ι.

All these findings demonstrate that DGKα is a key regulator of epithelial cells polarization and migration. Indeed, DGKα is a regulator of some members of the Rho family of small GTPases – Rac1 and Cdc42 at least – which are key determinants of cell polarity (17). As described before, both Rac1 and Cdc42 functions are necessary to trigger cell migration and actin cytoskeleton remodelling. They also regulates cystogenesis in 3D polarized epithelial cells, which is strongly perturbed upon both Rac1 and Cdc42 silencing (1, 18). Together, all these observations suggests that DGKα may be an important regulator of epithelial cells cystogenesis and polarization in a 3D context, where membrane lipids and Rho GTPases are key determinants of the polarized phenotype. Indeed, DGKα is both a regulator of lipidic signals, metabolizing membrane DAG to PA, and of Rac1 and Cdc42 intracellular localization.

Aim of the thesis

Data previously obtained in our laboratory demonstrate that in epithelial cells DGKα is an important regulator of cell migration and of the front-rear polarized phenotype of migrating cells. Indeed, DGKα catalytic activity is necessary to trigger actin cytoskeleton remodelling, ruffles elongation and cell scatter (30; 31). Active DGKα metabolizes membrane DAG to PA, which is a lipidic signal that recruits Rac1 and Cdc42 at specific sites of the plasma membrane. Rac1 and Cdc42 are then activated at the leading edge of epithelial cells, where they mediates the elongation of protrusions and the consequent cell migration (31; 32; 37). DGKα is also involved in Integrin recycling and in β1-Integrin-dependent elongation of protrusions. DGKα is recruited at the tip of the emerging pseudopods, where PA enrichment allows RCP- and α5β1-Intergin-containing vesicles docking to the plasma membrane (42). DGKα catalytic activity is necessary to trigger all these cellular functions, suggesting that during cell migration, actin remodelling and Integrin recycling DGKα acts primarily as a regulator of lipidic signals than as a scaffolding protein.

Rho GTPases and Integrins are also key regulator of epithelial cells polarization in a 3D environment. Indeed, in cysts derived from epithelial cells Integrins are localized at the basolateral domain, where they mediate the interaction with the extracellular matrix and the consequent laminin deposition (39; 41). Conversely, Rho GTPases are involved both downstream Integrins signalling and in apical recruitment of vesicles (1; 18; 36; 39; 41).

Today, DGKα is a well demonstrated regulator of cell migration and front-rear polarization. Previous observations also demonstrated that DGKα regulates both Rho GTPases and Integrins (31; 32; 37; 42). Thus, we hypothesized that DGKα can be involved also in epithelial cells 3D polarization and cystogenesis. Indeed, we demonstrated that in MDCK cysts DGKα catalytic activity is necessary for the formation of a single central lumen because both its specific siRNA-mediated silencing and its pharmacological inhibition leads to the formation of multiple lumens.

The aim of this work is to elucidate the role of DGKα during epithelial cells polarization and cystogenesis. DGKα is a regulator of two important lipidic second messengers, DAG and PA: they act as docking sites/localization signals for vesicles and proteins and DGKα catalytic activity is strictly necessary to trigger their

downstream signalling,. Here I analyzed DGKα involvement in apical and basolateral recruitment of proteins, in particular of Cdc42 and Rac1. Moreover, I analyzed the role of DGKα in the orientation of the mitotic spindle during mitosis, as multiple lumen are a direct consequence of mitotic spindle misorientation in epithelial cysts (22; 23; 24).

The final purpose of this thesis is to dissect the signalling pathways underlying cell polarization in 3D systems and, at a larger extend, in complex tissues and organs *in vivo* and to determine if DGKα is involved in important physiological and pathological processes that involve cell migration/polarization and mitotic spindle orientation.

Materials and methods

Cells

MDCK cells were grown in MEM (Minimal Essential Medium) supplemented with 5% fetal bovine serum, antibiotics and antimycotics in humid atmosphere at 37°C with 5% CO_2.

MDCK stably expressing Cdc42-GFP, CBD-GFP, Annexin A2-GFP, PH-Akt-GFP, PH-PLD-GFP and Rab11-GFP are a Keith Mostov's kind gift.

MDCK stably expressing the inducible OST-tagged DGKα were obtained by lentiviral transduction. After 3 weeks in selective medium, cells were analyzed by immunofluorescence and western blot.

HeLa cells were grown in DMEM (Dulbecco's modified essential medium) with 10% fetal bovine serum, antibiotics and antimycotics in humid atmosphere at 37°C with 5% CO_2.

3D cells culture and cystogenesis

To obtain MDCK cysts in Matrigel, cells were trypsinized to a single cell suspension of $2x10^4$ cells/ml in MEM media plus 5% fetal bovine serum and 2% Matrigel. The obtained cell suspension was plated in 8-well coverglass chambers covered with Matrigel. Cells where feed every 2 days and grown for 4 days until cysts with large lumen formed.

Inhibitors and treatments were added in the culture media.

Cell synchronization: double thymidine block

HeLa cells were synchronized by a double-thymidine block. 2.5 mM thymidine was added into the medium 24h after plating. After 18 hours, thymidine was washed out and cells were grown in complete medium for 8 hours, then 2.5 mM thymidine was added again into the medium for 18 hours. Cells were then washed twice with PBS and released in complete medium for 8 hours. Cells were then fixed and processed for immunofluorescence.

Inhibitors and treatments were added directly in the culture media before the fist thymidine block and kept during both the synchronization and release steps.

In all the experiments, HeLa cells were cultured on fibronectin-coated coverslips for more than 90 hours to allow polarization and synchronization.

Microscopy

MDCK cysts and HeLa cells were fixed in 4% paraformaldehyde (pH 7.4) and stained with specific antibodies. Pictures from the processed cysts and cells were acquired with a Leica SP2 confocal microscope. Different cellular parameters were then analyzed, such as number of single/multiple lumens and apical/basal protein staining for MDCK cysts and mitotic spindle orientation for both MDCK cysts and HeLa cells.

For each condition, more than 20 cysts or cells/experimental point were analyzed and standard deviation or standard error were calculated. Statistical significance was determined by student's T test.

Spindle orientation analysis

1. MDCK cysts: to determine mitotic spindle orientation, cysts were fixed in paraformaldehyde and stained with an anti-acetylated-α–tubulin antibody. Pictures of metaphase cells from the processed cysts were acquired and two main polarity axis were determined: *i*) spindle axis, highlighted by drawing a line that connects the two spindle poles, and *ii*) apical-basolateral axis. The angle formed by the apical-basolateral axis and the spindle axis were then analyzed: angles <45° were considered abnormal.

   More than 20 cysts/experiment were analyzed for each condition and standard deviation was calculated. Statistical significance was determined by student's T test.

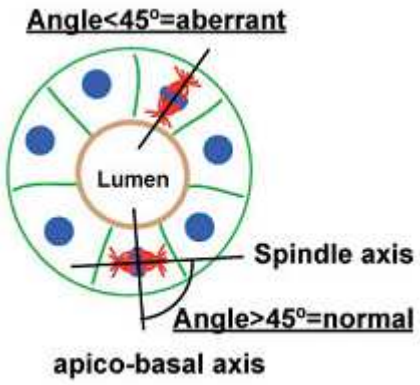

Figure 8: schematic representation of the analysis of mitotic spindle orientation in MDCK cysts. The spindle axis and the apical-basolateral axis are shown (23).

2. HeLa cells: to determine mitotic spindle orientation, synchronized HeLa cells grown on fibronectin-coated coverslips were fixed in paraformaldehyde and

stained with an anti-acetylated-α–tubulin antibody. Pictures of metaphase cells from the processed cells were acquired and the spindle axis has been highlighted drawing a line that connects the two spindle poles. The α angle formed by the spindle axis and the horizontal substratum was then analyzed: angles >10° were considered abnormal.

More than 20 cells/experiment were analyzed for each condition and standard deviation or standard error were calculated. Statistical significance was determined by student's T test.

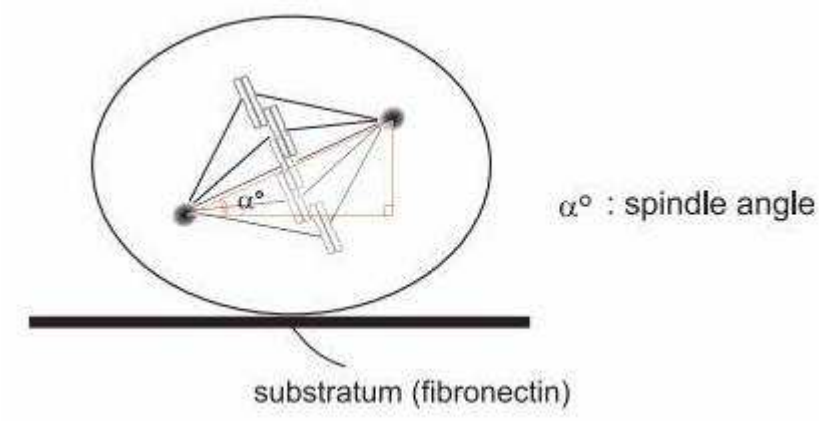

Figure 9: schematic representation of the analysis of mitotic spindle orientation in HeLa cells. The α angle and the substratum are shown (55).

Pulldown assay

Four days old cysts (cultured in 6 wells-matrigel coated plates in presence or not of DGKα pharmacological inhibitor R59022, 1μM final concentration) were lysed in an equal volume of gold lysis buffer (2% Triton X-100, 40 mM Tris-HCl, 100 mM NaCl, 20 mM $MgCl_2$, 30% glycerol, 1 mM dithiothreitol and protease inhibitors), then centrifuged at 15,000 rpm for 5 minutes. A 50 μl sample from the supernatant was set aside for determination of Cdc42 and Rac1 levels in the total lysates. GTP loading on Cdc42 and Rac1 was determined by GST-PAK beads pulldown and revealed by western blot.

RNAi

Three different custom siRNAs against the canine DGKα isoform were synthesized as double strand RNA:

- c1: sense GCUCAGAAGUGGACAGGAUtt and antisense AUUCUGUCCACUUCUGAGCtg;

- c2: sense CCCAGACAUCCUGAAAACCtt and antisense GGUUUUCAGGAUGUCUGGGtg;
- c3: sense CCUUCCACACCACAAAAACtt and antisense GUUUUUGUGGUGUGGAAGGtg.

MDCK cells plated at low density were transfected with 200 pM of DGKα siRNAs or with a control siRNA using Lipofectamine 2000. Then cells were plated in Matrigel for 4 days to allow cysts formation and processed for immunofluorecence analysis and Western Blot.

The siRNA against the Human DGKα is a validated siRNA and was buy from Ambion. HeLa cells plated at low density were transfected with 12.5 pM of DGKα siRNA or with a control siRNA using Lipofectamine 2000. After synchronization by double thymidine block cells were processed for immunofluorecence analysis and Western Blot.

The control siRNA is a validated negative control and was buy from Ambion. This siRNA sequence do not target any gene product and have been designed to have no significant sequence similarity to mouse, rat or human transcript sequence. Moreover, the control siRNA have been tested in multiple cell lines and show to have no significant impact on cell proliferation, apoptosis and morphology.

Results

Lack of Diacylglycerol kinase alpha activity leads to the multiple lumen phenotype

In order to examine the role of DGKα activity during cyst development in 3D cultures of epithelial cells, we used MDCK cells either silenced for DGKα by specific siRNAs (Figure 10a) or treated with a DGKα pharmacological inhibitor. The specificity of the custom siRNAs and of the pharmacological inhibitor R59022 for DGKα have been previously demonstrated (31; 33).

When grown in matrigel for 4 days upon DGKα silencing, MDCK cells developed polarized cysts with multiple, large, intercellular, hollow lumens instead of a single central lumen as in control cysts (Figure 10d). Nevertheless, despite their multiple lumen phenotype, the polarized architecture of epithelial cells surrounding each lumen within the cyst is well preserved, as every lumen shows a strong apical actin enrichment as in control cysts (Figure 10b). DGKα expression was analyzed by western blot and it is still quite knocked down after 4 days from the transfection with the DGKα specific siRNAs (Figure 10a). Moreover, the same phenotype was obtained by pharmacological inhibition of DGKα by cell treatment with R59022. Indeed, following DGKα inhibition we can observe large, intercellular, hollowed, actin-rich lumen in the 70% of the cysts (Figure 10e and 10h).

This findings demonstrate that DGKα enzymatic activity is required for the formation of cysts whit a single central lumen.

Then, we have investigated whether silencing/inhibition of DGKα affects the localization of polarity markers. The apical marker GP135 strongly accumulates at the apical plasma membrane both in control and in DGKα silenced cysts (Figure 10b). E-cadherin staining is also preserved: we can detect a strong basolateral E-cadherin staining both in control and DGKα silenced cysts (Figure 10c). Similar results were obtained following DGKα pharmacological inhibition with R59022. Indeed, GP135 (Figure 10e) and E-cadherin (Figure 10f) localize at apical and basolateral domain respectively in MDCK cysts treated with DGKα pharmacological inhibitor for 4 days.

In order to further analyze single cell polarization in our system, we looked at the Golgi apparatus polarization by GM130 localization, a peripheral cytoplasmic protein tightly bound to Golgi membranes (34). In MDCK cysts, the Golgi apparatus localizes

toward the central lumen, between the nucleus and the apical membrane. As shown in Figure 10g, also the Golgi orientation is preserved when DGKα is pharmacological inhibited: the Golgi apparatus is still located among nucleus and apical membrane as in control cysts.

Overall, these data indicate that DGKα is a key player during cystogenesis. Indeed, either its siRNA-mediated silencing or its pharmacological inhibition lead to aberrant cystogenesis and to the multiple lumen phenotype. Moreover, data obtained using the pharmacological inhibitor suggest that DGKα enzymatic activity is strictly required for proper single lumen formation. These data support the hypothesis that generation of a single central lumen during cystogenesis requires DGKα enzymatic function leading to either downregulation of DAG or generation of PA or reciprocal regulation of both signalling lipids.

Figure 10: the enzymatic activity of DGKα is necessary for single lumen formation.

a) DGKα silencing in MDCK cysts. MDCK cells were transfected with a control siRNA or with siRNAs specific for DGKα (c1, c2 and c3) and cultured as described in material and methods. DGKα silencing was analyzed by western blot. A Jurkat A3 lysate was used as a positive control for DGKα expression **b and c)** DGKα silencing leads to the multiple lumen phenotype without affecting single cell polarization. MDCK cysts transfected with a control siRNA or with siRNAs against DGKα (c1, c2 and c3) were fixed and stained for actin (red), nuclei (blue) and GP135 (green) or E-cadherin (green). Representative single confocal sections through the middle of the cysts are shown. Scale bar 20μM. **d)** Quantification of multiple lumen due to DGKα silencing. MDCK cysts transfected with a control siRNA or with siRNAs against DGKα (c1, c2 and c3) were fixed, stained and analyzed by concofal microscopy. Percentage above control of single vs multiple lumen has been evaluated and the graph shows the mean value of 3 independent experiments ± SE. *** t-test vs control $p<0.0005$. **e and f)** DGKα inhibition induces the multiple lumen phenotype without affecting single cell polarization. MDCK cysts cultured in presence or not of DGKα pharmacological inhibitor R59022 at 1μM final concentration were fixed and stained for actin (red), nuclei (blue) and GP135 (green) or E-cadherin (green). Representative single confocal sections through the middle of the cysts are shown. Scale bar 20μM. **e)** DGKα inhibition doesn't affect the polarized localization of the Golgi apparatus. MDCK cysts cultured in presence or not of DGKα pharmacological inhibitor R59022 at 1μM final concentration were fixed and stained for actin (red), nuclei (blue) and GM130 (green). Representative single confocal section through the middle of the cysts are shown. Scale bar 20μM. **h)** Quantification of the percentage of multiple lumen due to DGKα inhibition. MDCK cysts cultured in presence or not of DGKα pharmacological inhibitor R59022 at 1μM final concentration were fixed, stained and analyzed by concofal microscopy. The percentage above control of single vs multiple lumen has been evaluated

and the graph shows the mean value of 3 independent experiments ± SE. *** t-test vs control p<0.0005.

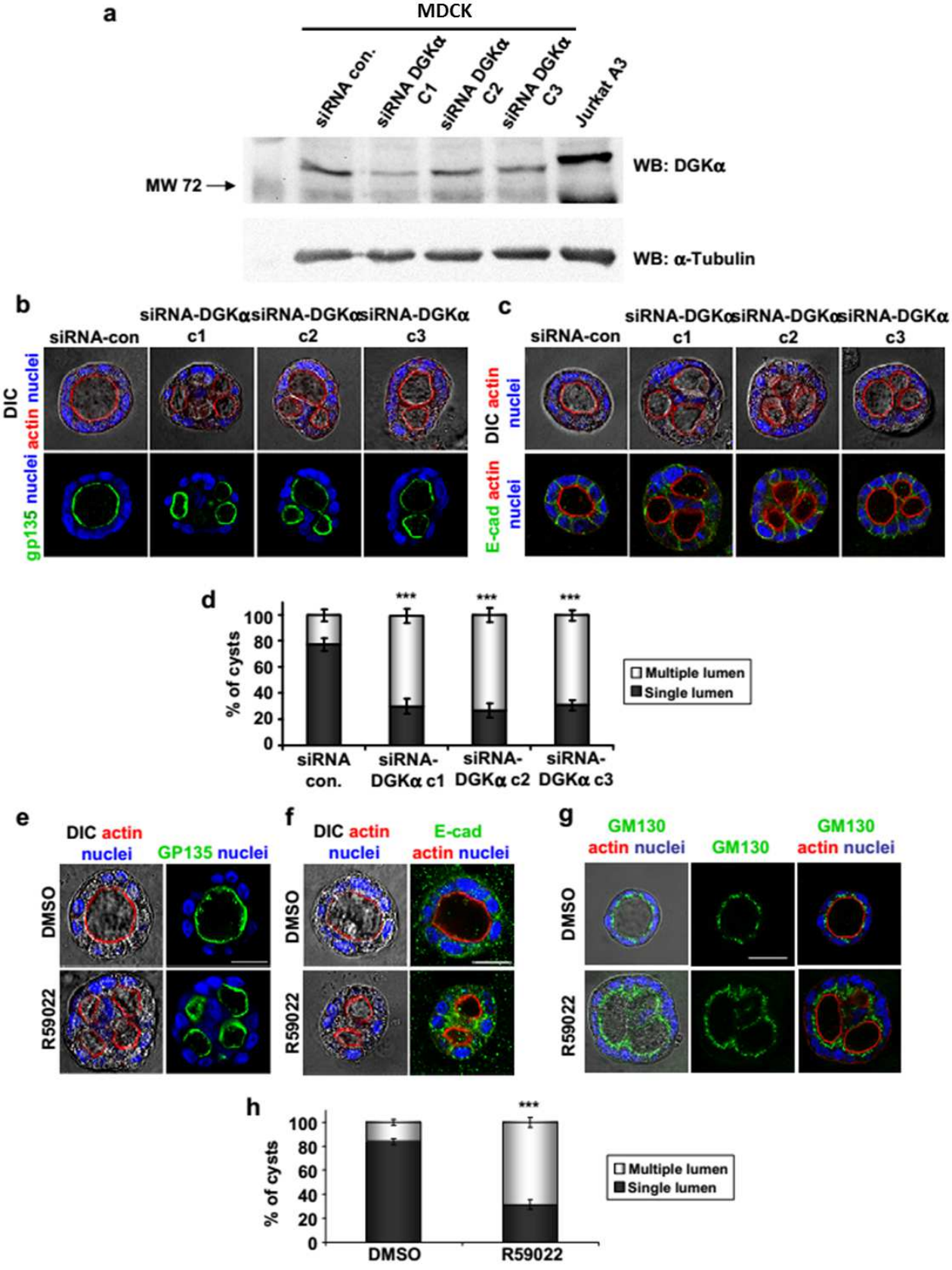

Diacylglycerol kinase alpha localization in MDCK cysts

We have investigated DGKα localization in MDCK cyst and we have found that endogenous DGKα is localized predominantly at the basolateral domain (Figure 11a), accumulated in dot-like structures, suggesting that it piles up in intracellular vesicles.

DGKα basolateral localization was further confirmed using MDCK cells that stably express an inducible OST-tagged form of DGKα. In these cells, OST-DGKα is expressed upon doxycycline administration to either 2D or 3D MDCK cultures (Figure 11b and 11c). Unexpectedly, OST-DGKα is not expressed with the same efficiency in 2D and 3D conditions: as shown in Figure 11b, the administration of 100 ng/ml of doxycycline is sufficient to induce OST-DGKα expression in MDCK cells cultured in 2D but not in 3D Matrigel-embedded cells (Figure 11b vs Figure 11c). In MDCK cysts, OST-DGKα is expressed only upon the administration of higher concentration of doxycycline (Figure 11c, 1000 ng/ml doxycycline). This behaviour can be due to the different context-dependent bioavailability of the doxycycline itself, since it perhaps reaches with less efficiency the Matrigel embedded cysts.

Only doxycycline-treated MDCK cysts show a basolateral staining of OST-DGKα. Moreover, OST-DGKα basolateral localization is comparable to the endogenous DGKα one (figure 11f).

Meticulous analysis of several pictures revealed that following its pharmacological inhibition DGKα accumulates at the apical domain (Figure 11f arrows and 11g). The finding that DGKα activity keeps its own localization at the basolateral domain suggests that accumulation of DAG or lack of PA drives it to the apical domain.

During cystogenesis, the apical-basolateral polarization is ensured by the asymmetric localization of proteins and membrane lipids. Lipidomic studies in MDCK cells grown upon porous filters, which feature the same apical-basolateral polarization of the cells that compose hollowed cysts, revealed that also PA and DAG are polarized. In particular, DAG is enriched at the apical domain while PA is more abundant in basolateral membranes (35). However, our data suggests that DGKα might act both at the apical and basolateral domains of MDCK cysts, regulating vesicular trafficking to different cellular compartments, leading to the establishment of the apical-basolateral polarized phenotype.

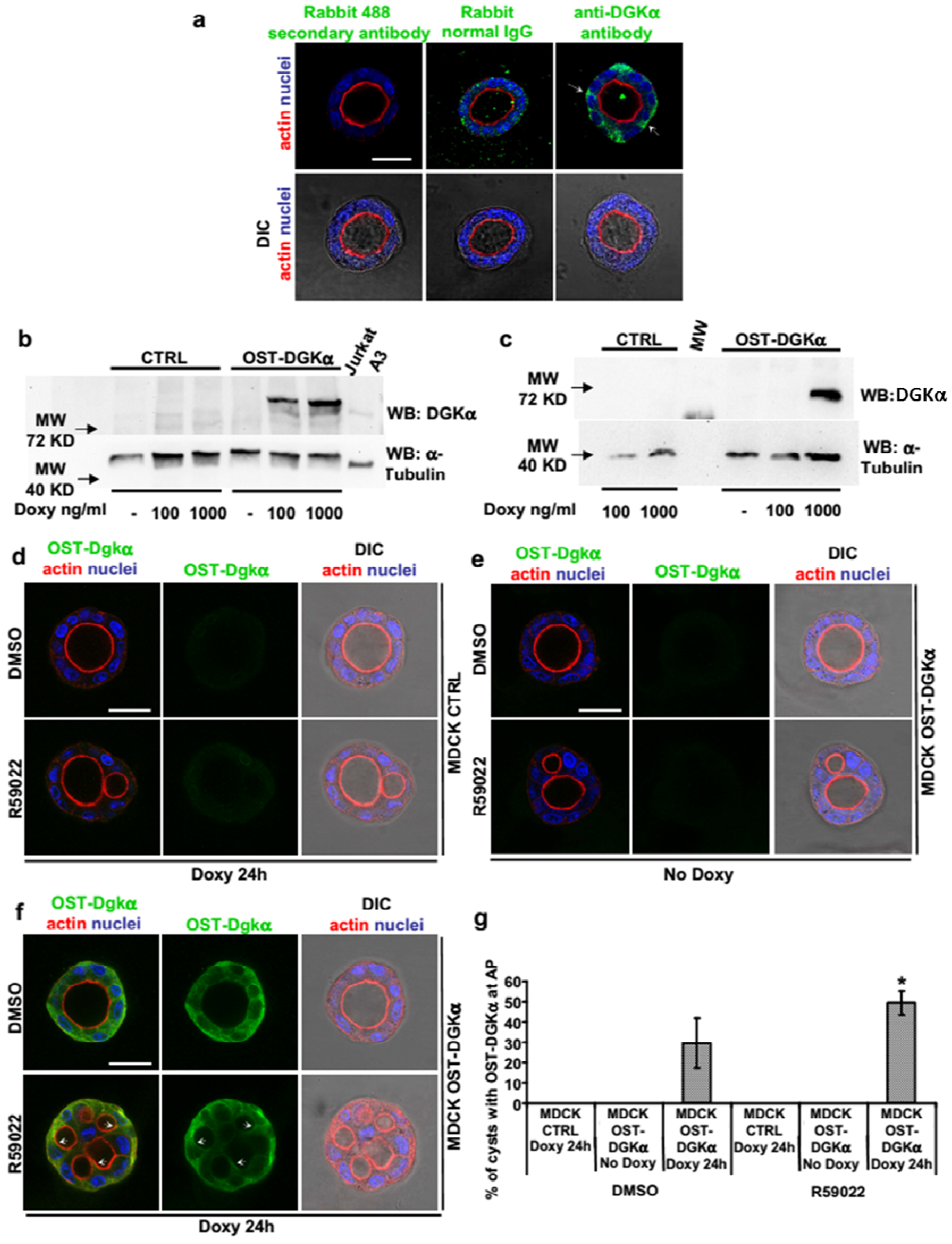

Figure 11: DGKα localization in MDCK cysts.

a) Endogenous DGKα accumulates in small vesicles at the basolateral domains. MDCK cysts were fixed and stained for DGKα (green), actin (red) and nuclei (blue). Representative single confocal sections through the middle of the cysts are shown. Scale bar 20μM. **b and c)** OST-DGKα expression. MDCK CTRL or OST-DGKα cells were cultured as a monolayer (b) or as cysts (c) and treated with

100-1000 ng/ml doxycycline for 24 hours. Cells were then lysed and cell lysates were analyzed by western blot. A Jurkat A3 lysate was used as a positive control for DGKα. **d, e and f)** OST- DGKα localization at the basolateral domain is catalytic activity-dependent. MDCK CTRL or OST-DGKα cysts were treated with 1000 ng/ml doxycycline for 24 hours, fixed and stained for OST-DGKα (green), actin (red) and nuclei (blue). Representative single confocal section through the middle of the cysts are shown. Scale bar 20μM. Arrows indicates apical OST-DGKα staining. **g)** DGKα inhibition induces its apical accumulation. The graph shows the percentage of cysts with apical OST-DGKα mean value of 3 independent experiments ± SE. * t-test vs control $p<0.05$

Diacylglycerol kinase alpha controls mitotic spindle orientation

The most significant event downstream DGKα signalling in MDCK cysts is the multiple lumen phenotype. In particular, DGKα pharmacological inhibition or its siRNA-mediated silencing induces the formation of clear, intercellular, multiple lumen (Figure 10e and 10f). This phenotype suggests a possible effect on the mitotic spindle orientation.

In the past few years, it has been demonstrated that in cysts multiple lumen appear when the mitotic spindle is misaligned during cell mitosis (22; 24). Indeed, in polarized cysts also mitosis is polarized and must be properly oriented. In particular, the two daughter cells must divide in parallel to the central lumen and perpendicularly to the apical-basolateral axis. When mitosis is not properly oriented, the two daughter cells will recognize the cytokinetic furrow as a newly formed apical domain (Figure 5). Consequently, they will redirect their vesicular trafficking to create a new lumen (22; 36).

Evaluation of mitotic spindle orientation in MDCK cysts revealed that it is misoriented upon DGKα silencing or pharmacological inhibition (Figure 12a and 12c). Spindle orientation was analyzed as described in material and methods, revealing that in cyst where DGKα was silenced by specific siRNAs more than 60% of mitotic cells display a mitotic spindle angles <45° (Figure 12a and 12b), which is considered abnormal (23). The same phenotype is observed when DGKα is pharmacological inhibited (Figure 12c and 12d). Moreover, a strong mitotic spindle misalignment is observed also when the lipid kinase is pharmacological inhibited for only 24 hours (Figure 12c and 12d).

These observations suggest that DGKα controls the orientation of the mitotic spindle in MDCK cysts. Moreover, mitotic spindle misorientation is an early event upon DGKα pharmacological inhibition, since it can be observed after only 24 hours

of treatment with the DGKα pharmacological inhibitor. Indeed, at least 60% of mitotic cells display a strong misorientation of the mitotic spindle alignment upon DGKα inhibition for 24 hours, as shown in figure 12d. Thus, in most cases the first cell mitosis occurring following DGKα inhibition is not oriented, suggesting a very strong link between DGKα catalytic activity and the orientation of the mitotic spindle.

Overall, these data support the hypothesis that the control of mitotic spindle orientation is the major mechanisms relying on DGKα activity in MDCK cysts.

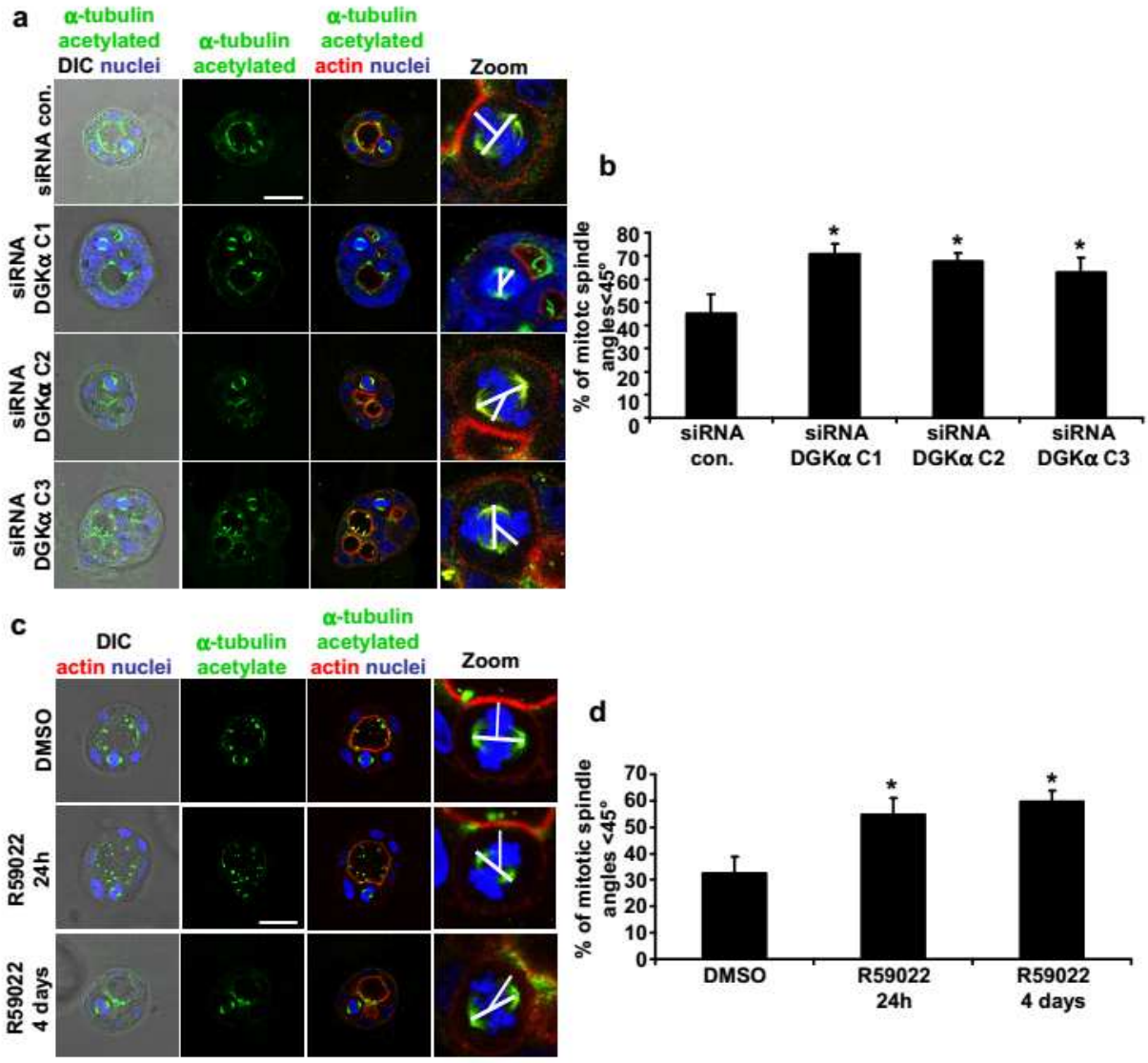

Figure 12: DGKα regulates mitotic spindle orientation.

a) DGKα silencing induces mitotic spindle misorientation. MDCK cells transfected with a control siRNA or with siRNA specific for DGKα were grown in matrigel for four days, fixed and stained for α-tubulin acetylated (green), actin (red) and nuclei (blue). Representative single confocal sections of metaphase cells are shown. The magnifications show the spindle axis and the apical-basolateral axis as white lines. Scale bar 20μM. **b)** Quantification of the percentage of misoriented mitotic spindle upon

DGKα silencing. The graph shows the percentage of mitotic spindle angles<45° mean value of 3 independent experiments ± SE. * t-test vs control p<0.05. **c)** DGKα pharmacological inhibition leads to spindle misorientation. MDCK cysts grown in presence or not of the DGKα pharmacological inhibitor R59022 at 1μM final concentration were fixed and stained for α-tubulin acetylated (green), actin (red) and nuclei (blue). Representative single confocal sections of metaphase cells are shown. The magnifications show the spindle axis and the apical-basolateral axis as white lines. Scale bar 20μM. **d)** Quantification of the percentage of misoriented mitotic spindle upon DGKα inhibition. Graph showing the percentage of mitotic spindle angles<45° mean value of 3 independent experiments ± SE. * t-test vs control p<0.05.

Cdc42 and mitotic spindle orientation

In polarized epithelial cells, Rho GTPases are key regulators of the polarized phenotype and their activity is mandatory to maintain it. Indeed, in MDCK cysts Cdc42 depletion strongly perturbs cell polarization and leads to the formation of small lumens with decreased apical F-actin staining. Moreover, apical markers accumulate in large intracellular vesicles (18). Cdc42 is also one of the most important regulators of mitotic spindle orientation during cystogenesis (22; 24). Indeed, the mitotic spindle is misoriented when Cdc42 is silenced. Moreover, two GEFs regulate Cdc42 activation in cysts: Tuba and Intersectin. In particular, Intersectin activates the Cdc42 pole responsible for mitotic spindle alignment (23).

DGKα is a key regulator of the polarized protrusive activity during migration and invasion of epithelial and endothelial cells. The lipid kinase is able to trigger cell migration because is a key regulator of Rac1 (30) and Cdc42 (37) localization during cell migration. Since Cdc42 regulates mitotic spindle orientation in MDCK cysts, we decided to analyze its localization and activation status in this context. At this end, we used an MDCK cell line that stably expresses a GFP-tagged Cdc42 (MDCK Cdc42-GFP). As expected, Cdc42-GFP localization is perturbed when DGKα is silenced or inhibited (Figure 13a and 13c). In these cysts Cdc42-GFP is more diffuse in the cytoplasm than enriched at the apical plasma membrane as in control cysts (Figure 13a and 13c) and in some cells also localizes at the basolateral domain (Figure 13a, arrows). This result was further confirmed looking at the localization of the CRIB domain of WASP (CBD), a probe for active GTP-Cdc42, using an MDCK cell line that stably expresses GFP-CBD. In control MDCK cysts, the CBD-GFP probe localizes predominantly at the apical domain, indicating that Cdc42 is strongly active at this site. When DGKα is silenced or pharmacological inhibited, also the CBD-GFP probe

is diffused in the cytoplasm (Figure 13b and 13d) as Cdc42-GFP. Moreover, in some cysts the CBD-GFP probe accumulates at the basolateral domain (Figure 13c and 13d, arrows). This basolateral GFP-CBD enrichment is peculiar of DGKα silenced or inhibited cyst and hardly detectable in control cysts.

However, despite DGKα clearly regulates Cdc42 localization, it does not regulate its activation status, measured biochemically as total Cdc42-GTP (Figure 13g), though we can not rule out that DGKα may affect the activation state of a small-hardly detectable pool of Cdc42 molecules.

As DGKα regulates Cdc42 localization, we then analyzed whether it regulates the pool of Cdc42 that is recruited and activated at the mitotic spindle (23). Unfortunately, we were not able to rule out it because no clear Cdc42-GFP or CBD-GFP staining at the mitotic spindle was detected (Figure 13e and 13f).

Taken together, these results demonstrate that Cdc42 is a downstream effector of DGKα in MDCK cysts. They also suggest that DGKα regulates Cdc42 localization but not its activation. The still open question is if the lipid kinase controls also the Cdc42 amount responsible for mitotic spindle orientation, which could provide a mechanism for the regulation of mitotic spindle orientation itself.

Figure 13: DGKα regulates Cdc42 localization.

a and c) DGKα silencing/inhibition affects Cdc42 localization. MDCK Cdc42-GFP cysts transfected with siRNAs against DGKα or grown in presence or not of DGKα pharmacological inhibitor R59022 at 1μM final concentration were fixed and stained for actin (red) and nuclei (blue). Representative single confocal sections through the middle of the cysts are shown. Arrows indicates Cdc42-GFP accumulation at the basolateral domain. Scale bar 20μM. **b and d)**. DGKα silencing/inhibition affects active Cdc42 localization. MDCK CBD-GFP cysts transfected with siRNAs against DGKα or grown in presence or not of DGKα pharmacological inhibitor R59022 at 1μM final concentration were fixed and stained for actin (red) and nuclei (blue). Representative single confocal sections through the middle of the cysts are shown. Arrows indicates CBD-GFP accumulation at the basolateral domain. Scale bar 20μM. **e and f)** Cdc42 localization at the mitotic spindle. MDCK Cdc42-GFP or CBD-GFP cysts grown in presence or not of DGKα pharmacological inhibitor R59022 at 1μM final concentration were fixed and stained for α-tubulin acetylated (red) and nuclei (blue). Representative single confocal sections of metaphase cells are shown. Scale bar 20μM. **g)** Cdc42 activation is not controlled by DGKα activity. MDCK cysts grown in presence or not of DGKα pharmacological inhibitor R59022 at 1μM final concentration were lysed and a GTS-PAK pulldown assay was performed. Total lysates were used as loading controls. Proteins were analyzed by western blot.

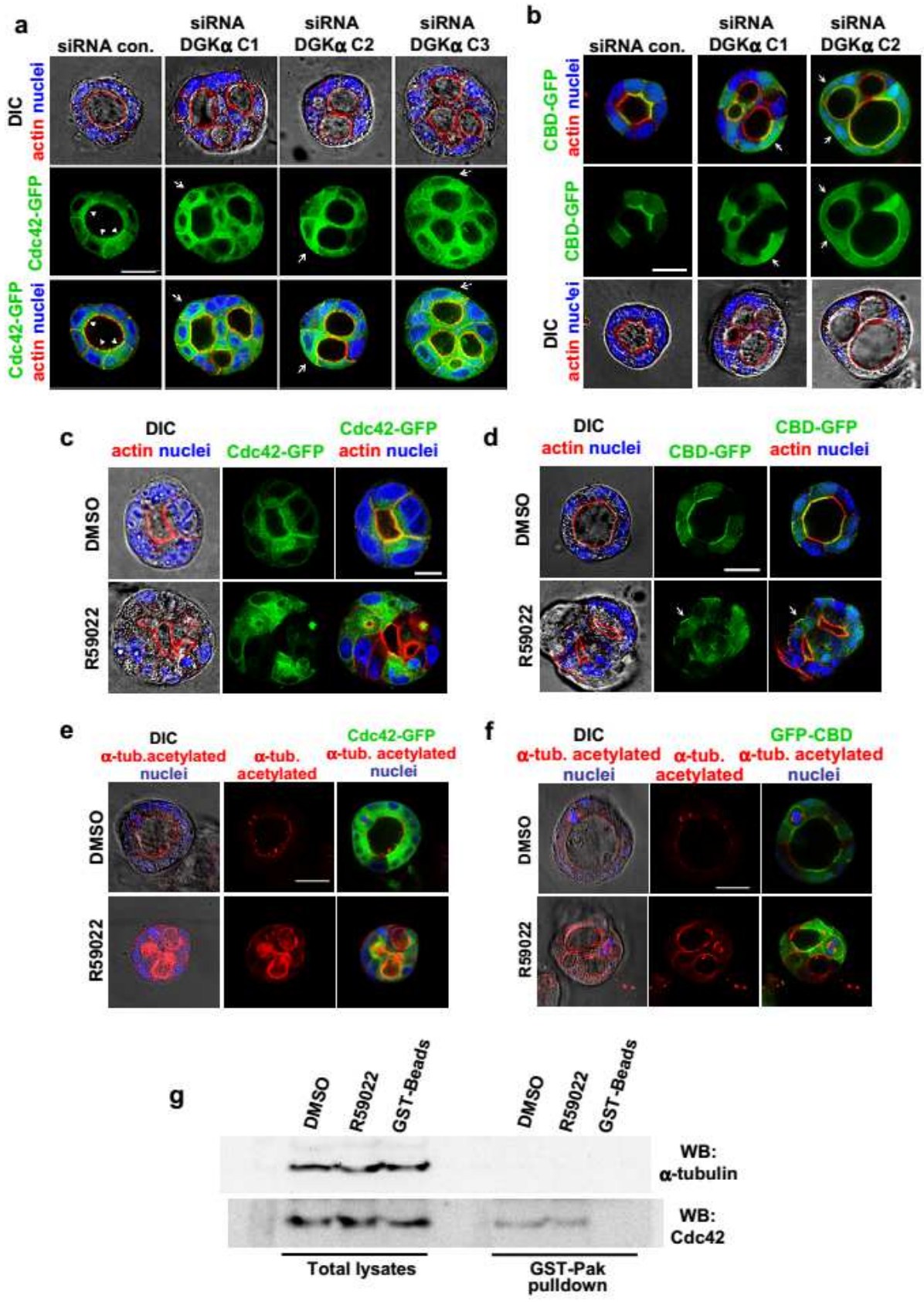
a
siRNA con.
siRNA DGKα C1
siRNA DGKα C2
siRNA DGKα C3
DIC actin nuclei
Cdc42-GFP
Cdc42-GFP actin nuclei
b
siRNA con.
siRNA DGKα C1
siRNA DGKα C2
CBD-GFP actin nuclei
CBD-GFP
DIC actin nuclei
c
DIC actin nuclei
Cdc42-GFP
Cdc42-GFP actin nuclei
DMSO
R59022
d
DIC actin nuclei
CBD-GFP
CBD-GFP actin nuclei
DMSO
R59022
e
DIC α-tub.acetylated nuclei
α-tub. acetylated
Cdc42-GFP α-tub. acetylated nuclei
DMSO
R59022
f
DIC α-tub. acetylated nuclei
α-tub. acetylated
GFP-CBD α-tub. acetylated nuclei
DMSO
R59022
g
DMSO
R59022
GST-Beads
DMSO
R59022
GST-Beads
WB: α-tubulin
WB: Cdc42
Total lysates
GST-Pak pulldown

Membrane lipids and mitotic spindle orientation

Membrane lipids are key determinants of cell polarity. In the polarized cysts context, apical and basolateral domains feature different lipid signatures. In particular, the apical domain is enriched in $PI(4,5)P_2$, while $PI(3,4,5)P_3$ concentration is higher at the basolateral domain. $PI(4,5)P_2$ apical enrichment is important to direct vesicular trafficking at this domain, through a mechanisms involving PTEN, Annexin A2, aPKC, Cdc42 and Rab11-containing vesicles (18; 36). On the other hand, basolateral $PI(3,4,5)P_3$ plays an important role in mitotic spindle orientation. Most studies were carried out in HeLa human cervical cancer cells plated on fibronectin. In this model it has been demonstrated that astral microtubules bind the midcortex membrane, which is enriched of $PI(3,4,5)P_3$, thus determining the orientation of the mitotic spindle in parallel to the substratum (19; 36). DGKα regulates mitotic spindle orientation also in this experimental system: following treatment with DGKα pharmacological inhibitor, HeLa cells plated on fibronectin-coated coverslips fail to properly orientate their mitotic spindle in parallel to the substratum (Figure 14a and 14b). The same phenotype is observed when DGKα is silenced using a specific siRNA (Figure 14c).

As in both HeLa cells and MDCK cysts, both DGKα and PI3K enzymatic activities regulate multiple lumen and mitotic spindle orientation, we assayed whether inhibition of DGKα affects $PI(4,5)P_2$/ $PI(3,4,5)P_3$ polarization in 3D MDCK cysts.

We investigated the localization of PH-Akt-GFP, a probe for $PI(3,4,5)P_3$ and $PI(3,4)P_2$, and the localization of PH-PLC-GFP, a probe for $PI(4,5)P_2$. In DGKα silenced 3D cysts, $PI(3,4,5)P_3$ segregation at the basolateral domain is perturbed, as the PH-Akt-GFP probe is more diffuse in the cytoplasm and is also recruited at the apical domain in some cysts (Figure 15a, arrows). The PH-Akt-GFP probe localization is perturbed also upon DGKα pharmacological inhibition (Figure 15), indicating that the catalytic activity of DGKα is required to maintain the proper segregation of membrane lipids in MDCK cysts.

Conversely, inhibition of the DGKα does not affect the localization of the $PI(4,5)P_2$ probe, which properly localizes at the apical domain as in control cysts (figure 15c). Indeed, no significant PH-PLC-GFP basolateral or cytoplasmic localization was detected upon DGKα inhibition, indicating that $PI(4,5)P_2$ segregation is not affected.

Overall, these data suggest that DGKα can regulate mitotic spindle orientation by regulating the localization of Cdc42 and of PI(3,4,5)P_3. The molecular mechanisms by which DGKα regulates the localization of both Cdc42 and PI(3,4,5)P_3 still await to be investigated.

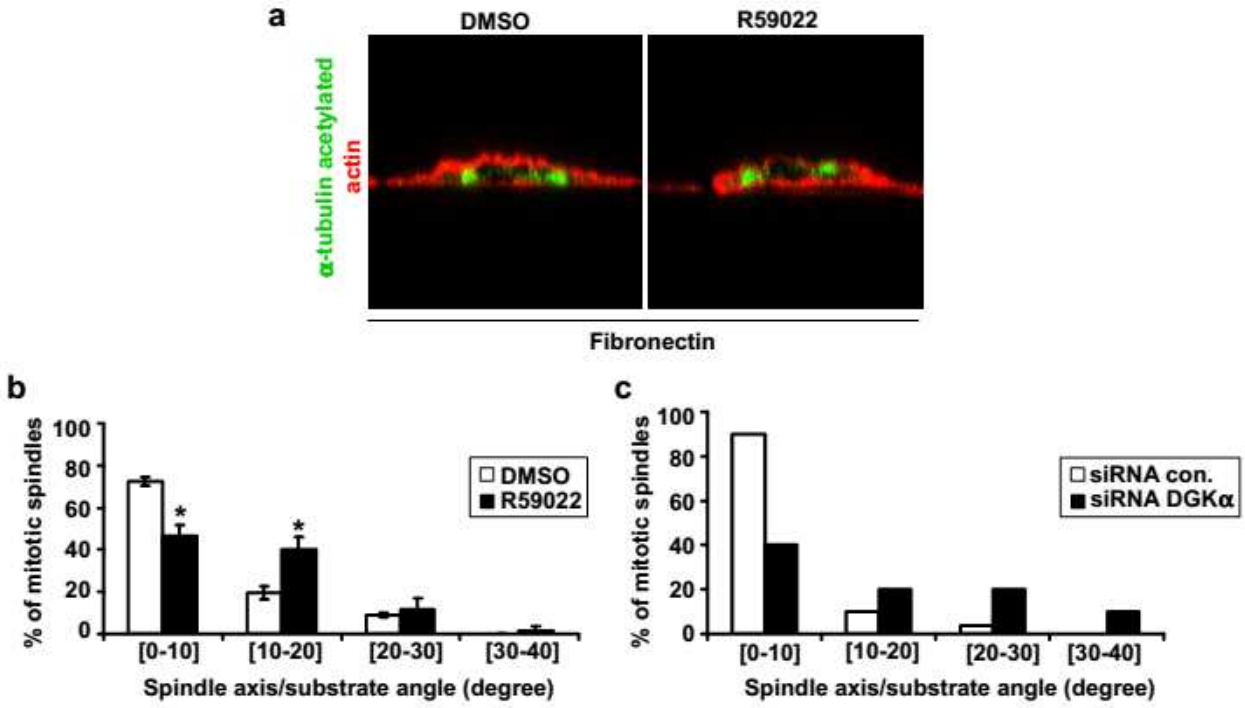

Figure 14: DGKα regulates mitotic spindle orientation in HeLa cells.

a) DGKα pharmacological inhibition induces spindle misorientation. HeLa cells plated on fibronectin coated coverslips (5μg/cm^2) grown in presence or not of DGKα pharmacological inhibitor R59022 at 1μM final concentration and synchronized by double thymidine block were fixed and stained for actin (red) and α-tubulin acetylated (green). Representative single confocal section (xz axis) of metaphase cells are shown. **b)** Quantification of the percentage of misoriented mitotic spindle upon DGKα inhibition. Graph showing the percentage of mitotic spindle angles divided into 4 groups. Mitotic spindle angles were considered normal in the [0-10] interval. The mean value of 3 independent experiments ± standard error is shown. * t-test vs control $p<0.05$. **c)** Quantification of the percentage of misoriented mitotic spindle upon DGKα silencing. Graph showing the percentage of mitotic spindle angles divided into 4 groups of a single experiment is shown. The mitotic spindle angles were considered normal only in the [0-10] interval.

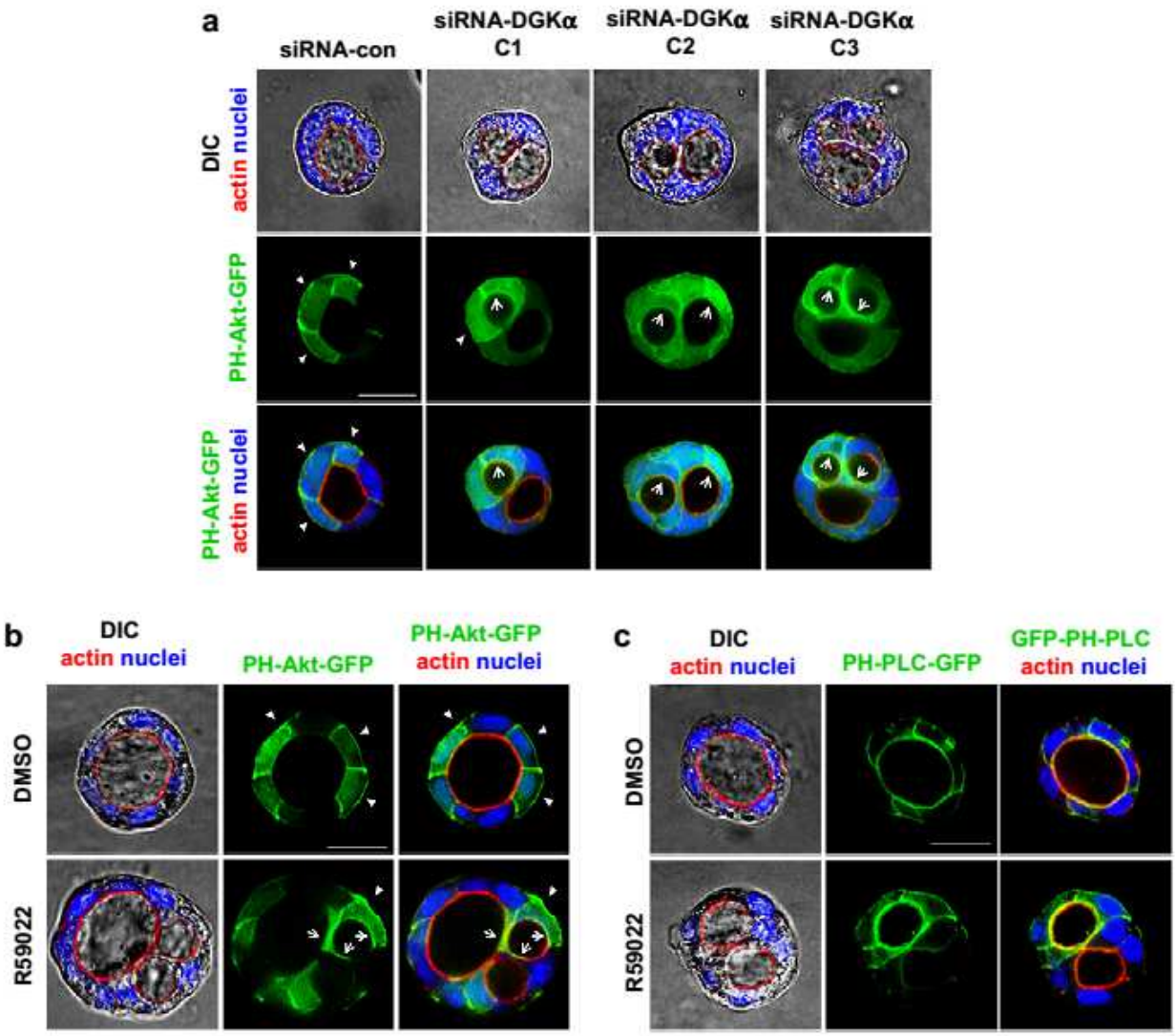

Figure 15: DGKα regulates PI(3,4,5)P_3 segregation at the basolateral domain but not PI(4,5)P_2 enrichment at the apical domain.

a and b) DGKα silencing/inhibition affect PH-Akt-GFP localization. MDCK PH-Akt-GFP cysts transfected with siRNAs against DGKα (a) or grown in presence or not of DGKα pharmacological inhibitor R59022 at 1μM final concentration (b) were fixed and stained for actin (red) and nuclei (blue). Representative single confocal sections through the middle of cysts are shown. Arrows indicates PH-Akt-GFP accumulation at the apical domain. Scale bar 20μM. **c)**. PH-PLC-GFP apical localization is independent from DGKα activity. MDCK PH-PLC-GFP cysts grown in presence or not of the DGKα pharmacological inhibitor R59022 at 1μM final concentration were fixed and stained for actin (red) and nuclei (blue). Representative single confocal sections through the middle of cysts are shown. Scale bar 20μM.

DGKα and Rac1 regulation: β1-Integrin signalling at the basolateral domain

In MDCK cysts also Rac1 is a key regulator of apical-basolateral polarity. Indeed, Rac1 localizes at the basolateral domain, where it mediates β1-Integrin signalling to induce laminin deposition (39). Moreover, suppression of Rac1 activity at the apical plasma membrane is critical for the maintenance of the cysts structure: upon constitutive activation of Rac1 at the apical membrane, the morphology of the cyst is disrupted, the central lumen is filled with live cells and the mitotic spindle is misoriented (40). Moreover, different Integrin pathways contribute independently to cystogenesis, regulating both Rac1 and Cdc42. Indeed, while α2β1- and α6β4-Integrins are required to establish a Rac1-dependent basal cue, leading to apical-basolateral polarization, α3β1-Integrin was found to regulate the orientation of mitosis, likely through Cdc42 (41).

DGKα regulates Rac1 (31) and Cdc42 (37) localization during growth factor and chemokine-induced induced cell migration and Cdc42 apical enrichment during cystogenesis (Figure 13). Moreover, in ovarian cancer cells DGKα is involved in α2β1-Integrin recycling and consequent elongation of protrusions (41). In MDCK cysts, DGKα localizes at the basolateral domain (Figure 11), which is more rich in PA than the apical domain (35). Together, these observations suggest that DGKα acts mainly at the basolateral domain, where it could drive *i*) Rac1 and Integrin-α2β1 laminin deposition, leading to apical-basolateral polarization, and/or *ii*) Integrin-α3β1-dependent Cdc42 regulation.

Despite DGKα is a well demonstrated Rac1 regulator in MDCK cells grown in 2D (32), in MDCK cysts its pharmacological inhibition has no effect on Rac1 basolateral localization (Figure 16a and 16b). However, when we looked at the activation status of Rac1 – measuring biochemically the Rac1-GTP level by a pulldown assay – we found that it is less active in presence of the DGKα pharmacological inhibitor respect to control untreated cysts (Figure 16c).

These data suggest that in polarized MDCK cysts DGKα acts on two Integrin-dependent pathways responsible for mitotic spindle orientation: *i*) the α2β1-Integrin and Cdc42-mediated pathway and *ii*) the α3β1-Integrin and Rac1-mediated pathway. Further experiments will rule out both hypothesis.

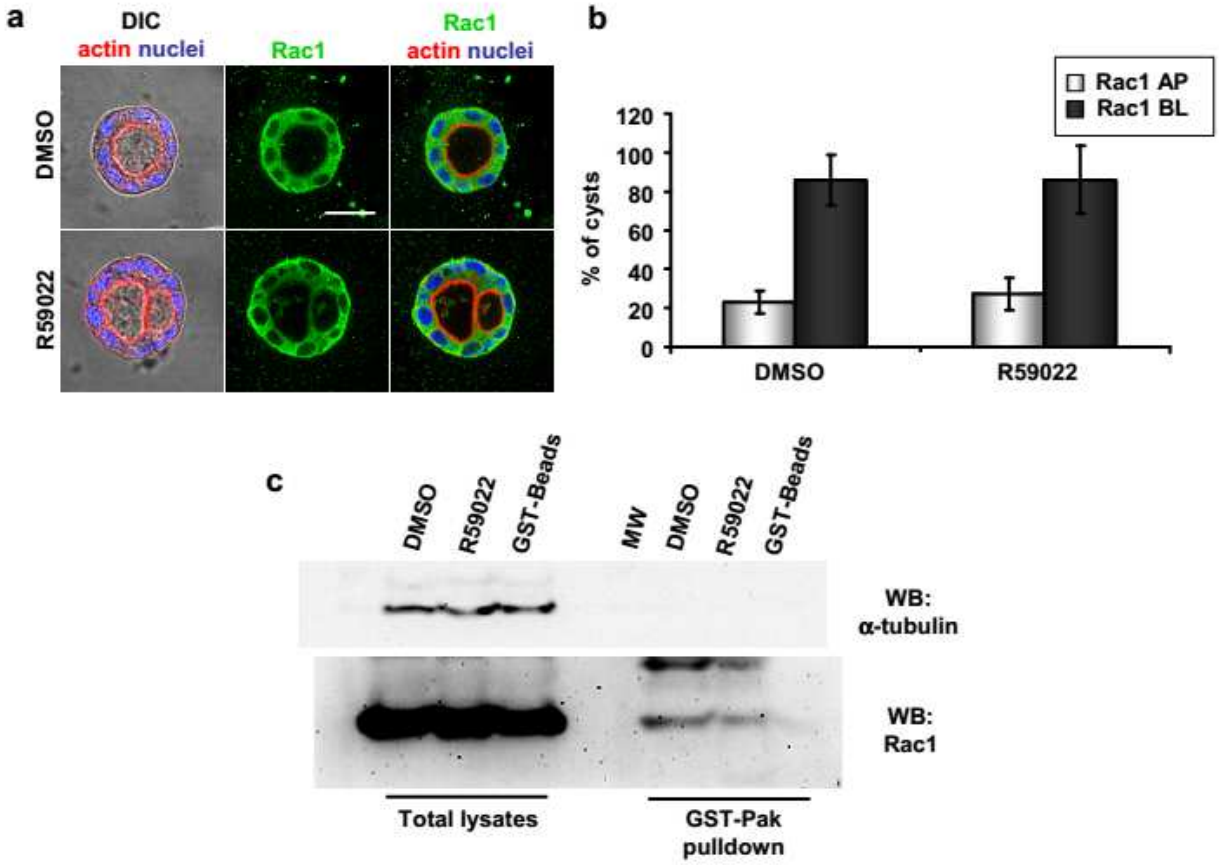

Figure 16: DGKα regulates Rac1 activation but not its localization.

a) DGKα inhibition doesn't perturb Rac1 basolateral localization. MDCK cysts grown in presence or not of DGKα pharmacological inhibitor R59022 at 1μM final concentration were fixed and stained for actin Rac1 (green), actin (red) and nuclei (blue). Representative single confocal sections through the middle of the cysts are shown. Scale bar 20μM. **b)** Rac1 apical and basolateral localization. The graph show the percentage of cysts whit apical (AP) and basolateral (BL) Rac1 staining. The mean value of 3 independent experiments ± standard error is shown. **c)** Rac1 activation is DGKα–dependent. MDCK cysts grown in presence or not of DGKα pharmacological inhibitor R59022 at 1μM final concentration were lysed and a GTS-PAK pulldown was performed. Total lysates were used as loading controls. Proteins were analyzed by western blot.

Phosphatidic acid and multiple lumens: Diacylglycerol kinase alpha and Phospholipase D crosstalk

DGKα acts as a key regulator of membrane compartments lipidic identity, modulating $PI(3,4,5)P_3$ segregation at the basolateral domain and metabolizing DAG into PA.

While DGKs generate PA by consuming DAG, PA is also generated by PLD-mediated hydrolysis of phospholipids, without affecting DAG level in cellular membranes (43). The mammalian PLD family consists of two related gene products: *i)*

PLD1, which is directly regulated by classic DAG-dependent PKC, Arf6, Rho GTPases and PI(4,5)P_2 and *ii)* PLD2, that is constitutively active and localizes to the plasma membrane in most cell types (44).

PLDs are emerging as important players during tumorigenesis: elevation of both isoforms is able to transform fibroblast and to contribute to cancer progression. Moreover, elevated PLDs activity is present in a wide variety of cancers and affects cells migration and invasion. In leucocytes, PLD has been associated with phagocytosis, degranulation, microbial killing and maturation (45). In intestinal epithelial cells, PLD1 is involved in brush border formation through a mechanism that involves the small G protein Rap2A and its downstream effector Ezrin (46).

In order to investigate whether PA generated by PLD may also contribute to cystogenesis, we inhibited both PLD1 and PLD2 by 1-butanol administration. This alcohol acts as a PLDs inhibitor because PLDs can use primary alcohols, such as 1-butanol, in place of water during the hydrolysis of phosphatidylcholine, producing phosphatidylbutanol instead of PA. Looking at the cyst morphology upon PLDs inhibition, we saw that none of the two isoforms is necessary for proper cystogenesis: their inhibition by 1-butanol administration doesn't perturb cystogenesis or cysts morphology (Figure 17a). Indeed, when treated whit 1-butanol for four days, MDCK cysts preserve their structure, whit a single central lumen surrounded by an actin-rich apical domain (Figure 17a and 17b). Moreover, also PI(3,4,5)P_3 segregation at the basolateral domain in not perturbed (Figure 17a and 17c).

Surprisingly, simultaneous inhibition of PLDs and DGKα restores the normal phenotype (figure 17a and 17b). Indeed, cysts treated with both DGKα and PLDs inhibitors show a single, actin-rich central lumen (Figure 17a). Moreover, also basolateral PI(3,4,5)P_3 segregation, which is lost upon DGKα inhibition or silencing (Figure 15a and 15b), is restored (Figure 17a and 17c).

These observations indicates that PLDs activity is dispensable during cystogenesis and that their activity is required only when DGKα is inhibited to give rise to the multiple lumen phenotype induced by inhibition of DGKα activity, i.e. by either DAG up-regulation and/or reduction of DGKα-generated PA.

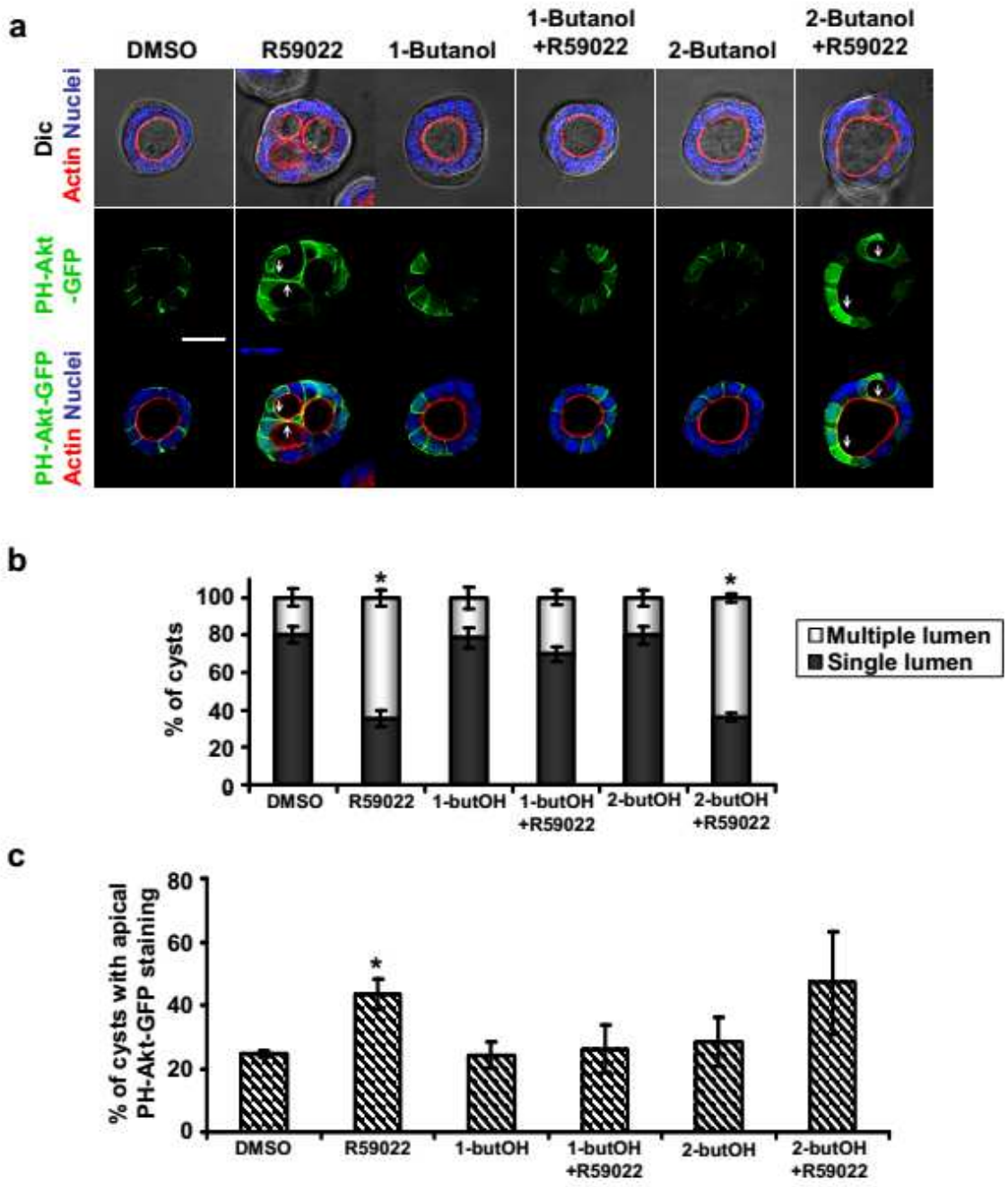

Figure 17: PLDs mediate the lack of DGKα activity-dependent multiple lumen phenotype.

a) DGKα and PLDs are necessary for single lumen formation and PI(3,4,5)P_3 basolateral enrichment. MDCK PH-Akt-GFP cyst grown in presence or not of DGKα pharmacological inhibitor R59022 at 1μM final concentration and/or 1-butanol or 2-butanol at 0,5% final concentration were fixed and stained for actin (red) and nuclei (blue). Representative single confocal sections through the middle of the cysts are shown. Scale bar 20μM. **b)** DGKα and PLDs inhibition together restore the single lumen phenotype. Graph showing the percentage of cysts with single or multiple lumen mean value of 3 independent experiments ± SE. * t-test vs control $p<0.05$. **c)** DGKα and PLDs inhibition together restore PI(3,4,5)P_3 enrichment at the basolateral domain. Graph showing the percentage of cysts with basolateral PH-Akt-GFP localization mean value of 3 independent experiments ± SE. * t-test vs control $p<0.05$.

Vesicular trafficking and apical targeting of Cdc42: role of Annexin A2

We have demonstrated that DGKα is a regulator of Cdc42 localization in polarized MDCK cysts (Figure 13) and during cell migration in different cell types (36). In particular, both Cdc42-GFP and CBD-GFP probes are more diffuse in the cytoplasm and recruited to the basolateral plasma membrane when DGKα is silenced or inhibited (Figure 13a, 13b, 13c, 13d) and not only strongly apical enriched as in control cysts. In the cysts polarized context, Cdc42 is an important regulator of mitotic spindle orientation (22, 23, 24), but its apical recruitment is also mandatory to define the apical membrane identity and to ensure the proper apical-basolateral polarization. In particular, Cdc42 is a member of the Par polarity complex, composed also by Par-3, Par-6 and aPKC. This complex is recruited to the tight junctions. Here aPKC is activated and phosphorylates Par-3, that dissociates from the complex and binds to the tight junctions (47). The remaining Par-6-aPKC complex is recruited to the apical plasma membrane through the interaction with Cdc42 and with the apical protein Annexin A2, which binds to acidic lipids and is then recruited to the $PI(4,5)P_2$ rich apical domain (18).

In order to define how DGKα regulates Cdc42 apical enrichment, we analyzed its involvement in the well described Annexin A2 and Par complex-drive pathway. Significantly, Annexin A2 is recruited to the apical domain by acidic lipids, such as DGKα product, PA. We used an MDCK cell line that stably expresses a GFP-tagged form of Annexin A2 (Anx A2-GFP). Looking at Anx A2-GFP localization, we found that its apical enrichment is DGKα-dependent. Indeed, when the lipid kinase is silenced or pharmacologically inhibited Anx A2-GFP is not only apical enriched, as in control cysts (Figure 18a and 18b), but it is also recruited to the basolateral domain (Figure 18a and 18b, arrows). Moreover, exogenous PA administration is sufficient to induce Anx A2-GFP basolateral localization (Figure 18c arrows). In control untreated cysts, Anx A2-GFP accumulates at the apical domain, as expected, but in PA treated cysts we can se a strong basolateral enrichment of Anx A2-GFP (Figure 16e, 78% of cysts in PA treated cysts vs 40% of cysts in controls). The strong basolateral Anx A2-GFP localization was confirmed measuring its fluorescence intensity at the apical and basolateral domain. As shown in Figure 18d, the ratio between basolateral and apical fluorescence intensity is higher only in PA treated cysts.

The Anx A2-GFP apical relocalization is strictly PA-dependent as it is not present in lysophosphatidic acid (LPA) and DAG treated cysts. Moreover, exogenous PA

administration induces strong morphological changes in the cyst structures, with an evident shrinkage of the central lumen and a general collapse of the cyst structure (Figure 18c and 18e). These morphological changes are evident also in the 40% of DAG treated cysts. This effect can be due to the physiological conversion of DAG in PA in these cysts.

These observations suggests that the apical recruitment of Annexin A2 is not only PI(4,5)P_2-dependent, as already known (18), but also driven by the PA product by DGKα. This data is in contrast with the well demonstrated PA basolateral enrichment in polarized MDCK cysts (35). However, we have demonstrated that endogenous DGKα localizes at the basolateral domain and also in dot-likes structures that reminds recycling vesicles (Figure 11a). Thus, it is possible that DGKα and its product PA are involved in the vesicular trafficking responsible for Annexin A2 apical recruitment and not directly to its apical docking itself. On the other hand, DGKα localizes at the basolateral domain, but it is also enriched at the apical domain when pharmacologically inhibited (Figure 11f, arrows, and 11g). This behaviour suggests that DGKα is transiently activated at the apical domain, where a PA enrichment for a short time could drive Annexin A2-enriched vesicles docking at the apical domain.

Overall, these data demonstrate that DGKα regulates Annexin A2 enrichment at the apical domain. Thus, the lipid kinase maybe regulates also the Par complex-drive Cdc42 apical enrichment.

Figure 18: DGKα regulates Annexin A2 apical recruitment.

a and b) DGKα silencing/pharmacological inhibition induces Annexin A2 basolateral relocalization. MDCK Anx A2-GFP cysts transfected with siRNAs against DGKα (a) or grown in presence or not of DGKα pharmacological inhibitor R59022 at 1μM final concentration (b) were fixed and stained for actin (red) and nuclei (blue). Representative single confocal sections through the middle of the cysts are shown. Arrows indicates Anx A2-GFP accumulation at the basolateral domain. Scale bar 20μM. **c)** Exogenous PA administration induces Anx A2-GFP basolateral localization. MDCK Anx A2-GFP cysts were grown in Matrigel for 4 day and treated for 30' with PA or LPA or DAG at 250 μM final concentration. Cysts were fixed and stained for actin (red) and nuclei (blue). Representative single confocal sections through the middle of the cysts are shown. Arrows indicates Anx A2-GFP accumulation at the basolateral domain. Scale bar 20μM. **d)** Anx A2-GFP is enriched at the BL domain of PA treated cysts: fluorescence intensity quantification. The graph shows the ratio of the fluorescence intensity of Anx A2-GFP at the basolateral and at the apical domain (BL/AP) mean value of 3 independent experiments ± SE. ** t-test vs control $p<0.005$. **e)** Quantification of exogenous

PA-induced Anx A2-GFP basolateral localization. Graph showing percentage of cysts with basolateral Anx A2-GFP localization mean value of 3 independent experiments ± SE. * t-test vs control p<0.05. *** t-test vs control p<0.0005

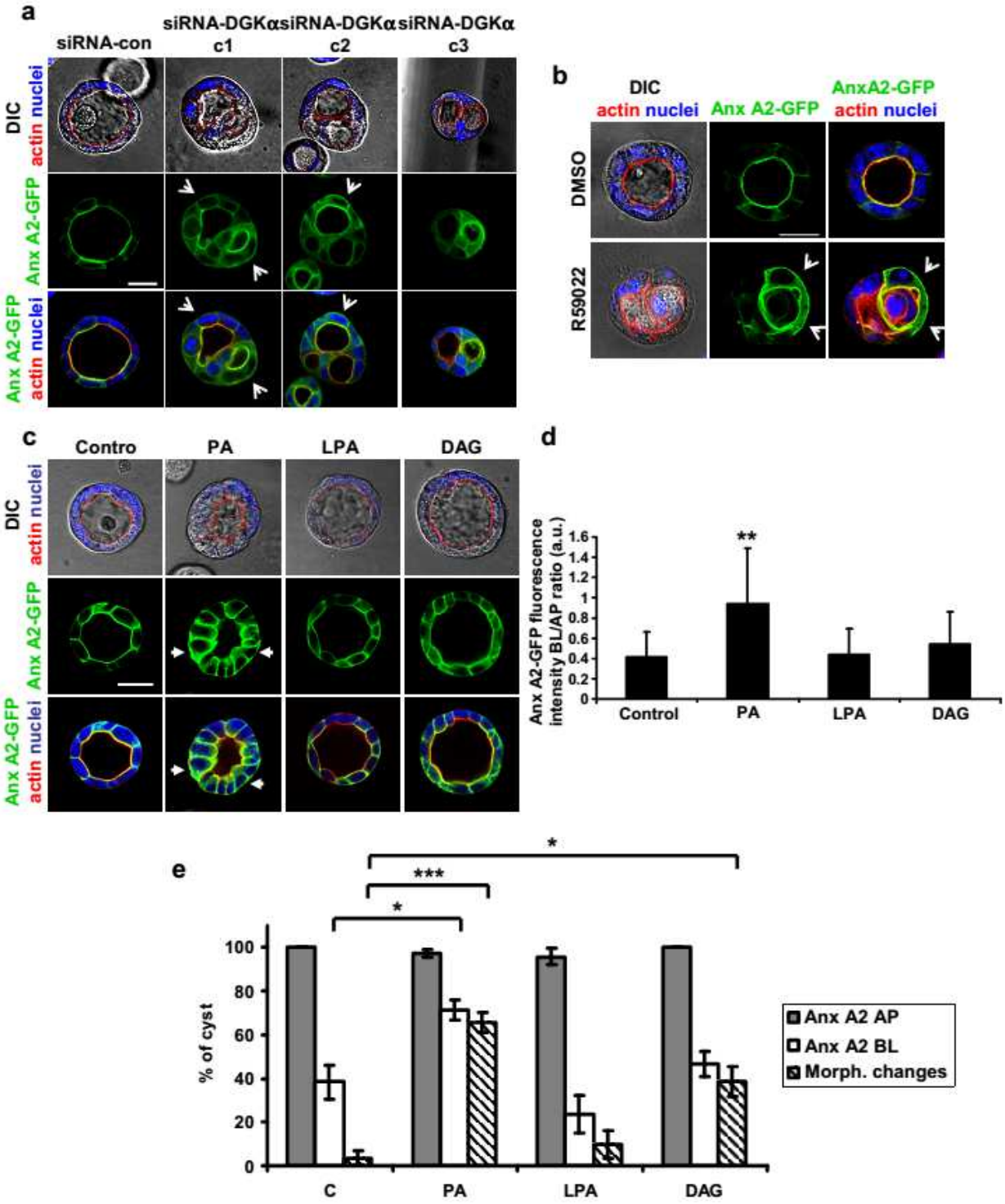

aPKC apical recruitment is independent from DGKα

The previously described data suggest that DGKα regulates Cdc42 apical enrichment acting on the Par complex-mediated pathway. aPKC is a member of the Par polarity complex. Intriguing, in our laboratory it has been previously demonstrated that aPKC intracellular localization is regulated by DGKα (32; 37). Indeed, during HGF-mediated membrane ruffling in MDCK cells, DGKα regulates the localization of the RhoGDI-aPKC-Rac1 complex to the migratory leading edge (32). Thus, we decided to analyze aPKC localization in MDCK cysts. Surprisingly, we found that aPKC apical enrichment is not perturbed upon DGKα silencing (Figure 19a and 19b). Moreover, DGKα silencing or pharmacological inhibition doesn't affect aPKC apical recruitment also at early stages of cystogenesis (Figure 19c, 19d, 19e, 19f). Indeed, a strong apical aPKC enrichment is still present upon DGKα silencing/inhibition, no diffuse or basolateral staining are detectable and there are no remarkably differences among control and DGKα silenced/inhibited cysts respect to aPKC localization both after 2 or 4 days of culture.

These data indicate that upon DGKα silencing/inhibition aPKC is recruited to the apical domain by alternative pathways.

Figure 19: DGKα is not involved in aPKC apical recruitment.

a) DGKα pharmacological inhibition doesn't affect aPKC localization in 4 days old MDCK cysts. MDCK cysts grown in presence or not of DGKα pharmacological inhibitor R59022 at 1μM final concentration for 4 days were fixed and stained for aPKC (green), actin (red) and nuclei (blue). Representative single confocal sections through the middle of the cysts are shown. Scale bar 20μM. **b)** Quantification of aPKC apical and basolateral localization in 4 days old MDCK cysts. Graph showing percentage of cysts with apical or basolateral aPKC localization mean value of 2 independent experiments ± S.V. **c and d)** DGKα silencing/pharmacological inhibition doesn't affect aPKC localization in 2 days old MDCK cysts. MDCK cysts transfected with siRNAs against DGKα (c) or grown in presence or not of DGKα pharmacological inhibitor R59022 at 1μM final concentration (d) for 2 days were fixed and stained for aPKC (green), actin (red) and nuclei (blue). Representative single confocal section through the middle of the cysts are shown. Scale bar 20μM. **e and f)** Quantification of aPKC apical and basolateral localization in 2 days old MDCK cysts. Graph showing percentage of cysts with apical or basolateral aPKC localization mean value of 2 independent experiments ± S.V.

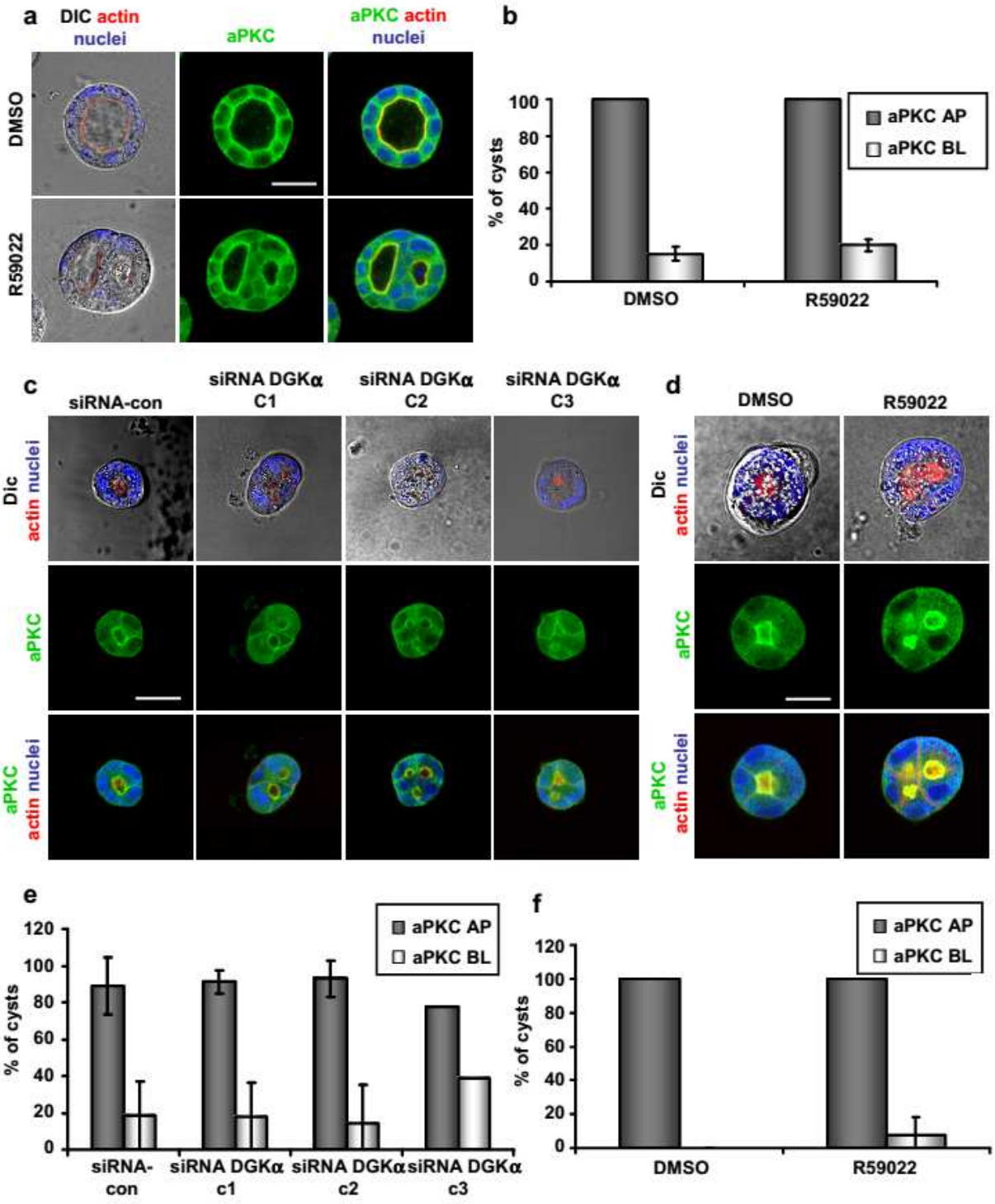

Rab11-mediated vesicular trafficking is independent from DGKα in MDCK cysts

In early phases of cystogenesis, after the first mitosis, the two newly formed cells must recognize their apical domain and direct their vesicular trafficking to form the central lumen. Thus, the formation of the apical membrane initiation site (AMIS) is a crucial step to allow proper cystogenesis. During the first steps of AMIS generation, Rab11 positive vesicles are recruited to the nascent apical domain. These vesicles

contain not only Rab11, but also GP135 – a well define apical marker – Annexin A2 and Cdc42. The recruitment of these proteins induces the basolateral localization of the tight junctions and the maturation of the AMIS to the pre-apical domain (PAD). Then, polarized vesicular trafficking ensures the expansion of the central lumen and the apical-basolateral polarization of lipids and proteins. When this pathway is perturbed also cystogenesis is altered and multiple lumen and other alterations appears. This behaviour can be observed both in the early and later steps of cystogenesis (36).

DGKα is involved in Rab11-RCP-mediated α5β1-Integrin recycling in ovarian cancer cells (42). Moreover, in MDCK cysts endogenous DGKα localizes in vesicle-like structure (Figure 11a) and controls Annexin A2 (Figure 18) and Cdc42 (Figure 13) apical recruitment. These observation suggests that DGKα can regulates Rab11-dependent vesicular trafficking in MDCK cysts, acting to define the AMIS during the early phases of cystogenesis and to maintain the polarized vesicular trafficking during the late phases of cystogenesis.

In order to study Rab11 localization in MDCK cysts, we used an MDCK cell line that stably expresses Rab11-GFP. Looking at its localization, we found that it is not perturbed when DGKα is pharmacologically inhibited (Figure 20a and 20b). Indeed, Rab11 is strongly enriched at the apical domain and is also detectable in vesicle-like structures under the apical plasma membrane both in control than in DGKα inhibited cysts.

These observation suggests that DGKα is not involved in Rab11-dependent vesicular trafficking in MDCK cysts, at least at late stages of cystogenesis. This data enforce the hypothesis that the most important event downstream DGKα silencing/inhibition in MDCK cysts is the mitotic spindle misorientation and that the multiple lumen phenotype of MDCK silenced/inhibited cysts is a direct consequence of mitotic spindle misorientation instead of vesicular trafficking regulation.

Figure 20: Rab11 apical recruitment is DGKα independent.

a) DGKα pharmacological inhibition doesn't affect Rab11-GFP apical localization. MDCK Rab11-GFP cysts grown in presence or not of DGKα pharmacological inhibitor R59022 at 1μM final concentration were fixed and stained for actin (red) and nuclei (blue). Representative single confocal sections through the middle of the cysts are shown. Scale bar 20μM. **b)** Quantification of Rab11-GFP

apical and basolateral localization. Graph showing percentage of cysts with apical or basolateral Rab11-GFP localization mean value of 2 independent experiments ± S.V.

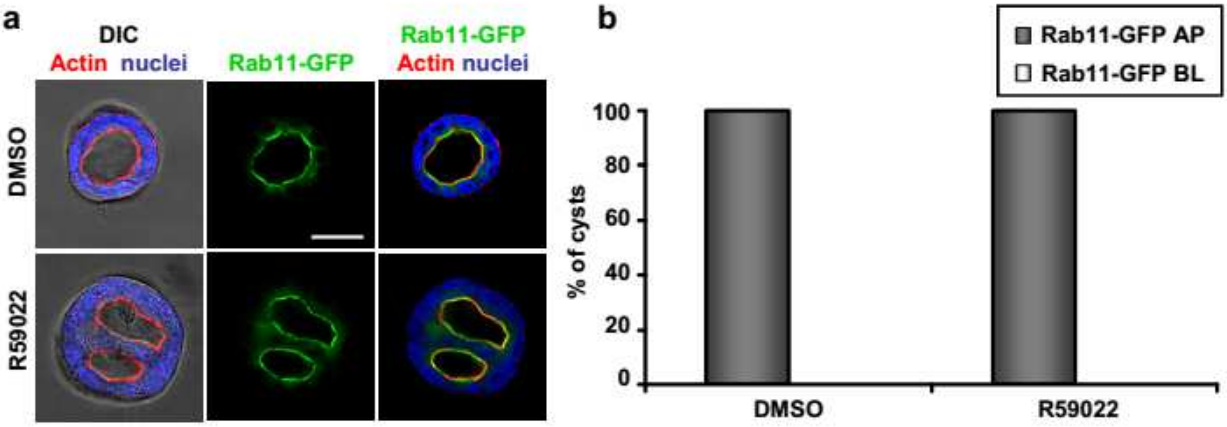

Discussion

One of the main prerequisite for tissues and organs development is to maintain a polarized phenotype. To understand how physiological homeostasis is preserved, is important to define the main molecular mechanisms underlying cell polarization. This will allow us to better understand how diseases that alter the structure of epithelial tissues originate and progress. In USA, more than 85% of adults mortal diseases affect epithelial tissues. Here, lost of the polarized phenotype is a marker of high malignancy. Moreover, acute organs damage is one of the most important cause of death all over the world.

One essential point is that some organs, such as lung and liver, are able to restore their structure and functionalities after acute damage. Then, identify all the mechanisms underlying epithelial cells polarization is fundamental to analyze epithelial tissues response to the damage itself, creating new perspectives for regenerative medicine.

One of the most used model to study epithelial cells polarization are MDCK cysts: when MDCK cells were cultured in extracellular matrix gels, they form polarized, hollow structures known as cysts, which polarization resemble the one that can be found in epithelial tissues *in vivo* (8; 9). DGKα is a key regulator of cystogenesis and of the polarized phenotype of epithelial cells. Indeed, when DGKα is silenced or inhibited in MDCK cysts, large multiple intercellular lumens appear, although the apical-basolateral polarization of the single cells is preserved (Figure 10).

Generation of a single central lumen relies on two main pathways: *i*) apical recruitment of vesicles and proteins and *ii*) mitotic spindle orientation. These two pathways together allow the formation of the single central lumen: oriented mitosis maintain the structure of the cysts, in which cell are in contact only at the basolateral level, and vesicular trafficking is necessary to transport and segregate proteins at specific membrane and cellular domains. MDCK cysts generate their central lumen through the cavitation mechanism. In this setting, the proper orientation of the mitotic spindle parallel to the central lumen is the most important event that ensure the formation of a single central lumen (22; 23; 24). DGKα activity is necessary for proper mitotic spindle orientation and the multiple lumen phenotype observed upon

its inhibition/silencing is a direct consequence of the mitotic spindle misalignment (Figure 12).

Today, some important pathways that regulate mitotic spindle orientation have been described. The most important are astral microtubules anchorage to the cell cortex, Integrins recycling and Cdc42 localization and activation at the mitotic spindle. Astral microtubules contact PI(3,4,5)P_3 enriched area at the midcortex and anchor the mitotic spindle to the cell cortex through +TIPs proteins (18; 37). Integrin $\alpha 3\beta 1$ has been specifically associated whit polarized mitosis through a mechanisms that seems to involve Cdc42 (42). Finally, the small Rho GTPase Cdc42 is a key regulator of mitotic spindle orientation in the polarized context: its inhibition induces mitotic spindle misalignment and Cdc42 is recruited and activated specifically at the mitotic spindle during mitosis (22; 23; 24).

DGKα localizes at the basolateral domain of MDCK cysts (Figure 11). This basolateral localization suggests that the lipid kinase acts at this domain, regulating the interaction with the extracellular matrix and the consequent downstream signalling, leading to mitotic spindle orientation. The PA enrichment at the basolateral domain supports this hypothesis (35). Moreover, DGKα relocalizes at the apical domain when pharmacologically inhibited (Figure 11f and 11d). This observation suggests that DGKα localization depends on its activation status in MDCK cysts. It is not the first evidence of a correlation between DGKα activation status and localization. Indeed, in T-cells DGKα is recruited to DAG rich membranes, where DAG itself acts as a docking molecule (48). Here, DGKα converts DAG into PA and then detach from the membrane as consequence of DAG reduction. Moreover, a kinase dead mutant of DGKα accumulates at DAG rich membranes (49). The same mechanism can be observed in MDCK epithelial cells, where a DGKα kinase dead mutant blocks HGF-induced ruffles formation and accumulates at the leading edge (30). It has also been demonstrated that DGKα translocation to the actin-rich cytoskeleton rely on its Y335 phosphorylation (30; 50) and consequent activation: the DGKα-Y335F mutant is unable to translocate to the plasma membrane upon HGF stimulation and associates with intracellular vesicles (30). In MDCK cysts, the vesicular localization of DGKα suggests that the DGKα-enriched vesicles can be recruited to the apical domain, triggering the vesicular trafficking and the delivery of

apical proteins. Moreover, its transient activation at this domain can modulate DAG signalling.

The vesicular trafficking to the apical domain is indispensable for apical recruitment of proteins. The polarized vesicular trafficking is established during the early phases o cystogenesis, after the first mitosis – the so called two cell stage – and is preserved in time (1;36). Vesicles can cycle from the basolateral domain and from recycling endosomes to different cell compartments. At the two cell stage, vesicular trafficking became polarized along the apical-basolateral axis: Cdc42 and Annexin A2-containing Rab11 positive vesicles are recruited to the nascent apical domain, where they act to induce the basolateral segregation of tight junctions and to define the apical plasma membrane identity (36). In the later stage of cystogenesis, Annexin A2 is involved in the maintenance of the polarized phenotype through a trafficking pathway that involves PTEN and the Par complex (18). Indeed, PTEN-mediated $PI(4,5)P_2$ apical enrichment recruits Annexin A2, Cdc42 and aPKC to the apical domain. Acidic lipids are docking molecules for Annexin A2, that binds them. Thus, also DGKα product, PA, can act as an Annexin A2 docking molecule. Indeed, in MDCK cysts Annexin A2 apical recruitment is DGKα-dependent (Figure 18). Furthermore, exogenous PA administration is sufficient to recruit Annexin A2 to other membrane domains, specially to the basolateral domain where it likely accumulates (Figure 18e). DGKα regulates also Cdc42 apical recruitment (Figure 13), but not aPKC localization at the apical domain (Figure 19). Thus, DGKα regulates the intracellular localization of only some players of the vesicular trafficking responsible for the apical targeting of proteins. This surprising finding can be explained by the involvement of another polarity complex, the Crumbs complex, in the recruitment of proteins at the apical domain. Indeed, Crumbs is able to bind a member of the Par complex, Par-6, and to recruit it to the apical domain. In particular, Crumbs binds to Par-6 in the Par-3 binding region and acts as a binding competitor for Par-3 (47). Thus, Cdc42 and aPKC can be recruited to the apical domain through different pathways: one mediated by apical $PI(4,5)P_2$ and Annexin A2 and one mediated by Crumbs. Upon DGKα silencing or pharmacological inhibition, only the $PI(4,5)P_2$-Annexin A2-mediated pathway is perturbed, leading to Annexin A2 and Cdc42 cytoplasmic and basolateral recruitment. Conversely, the Crumbs-mediated pathway is not perturbed upon DGKα silencing/inhibition and the Par-6-aPKC complex is still recruited only at the apical domain.

During the early phases of cystogenesis, Rab-11-mediated vesicle trafficking is crucial to establish the apical-basolateral polarization (36). In ovarian cancer cells, DGKα is a well established regulator of Rab-11-mediated β1-Integrin recycling (42). Surprisingly, in MDCK cysts DGKα doesn't regulates the recruitment to the apical domain of Rab-11-contayining vesicles (Figure 20). This observation suggests that DGKα is a minor regulator of vesicular trafficking in MDCK cysts. Indeed, the lipid kinase regulates the apical localization of only a few proteins – Annexin A2 and Cdc42 – while almost all the other proteins examined – aPKC, GP135, E-cadherins and Rac1 – are properly localized in MDCK cyst where DGKα is silenced or inhibited. This observation supports the hypothesis that the main phenotype induced downstream DGKα inhibition or silencing in MDCK cysts is mitotic spindle misorientation.

Integrins are some of the most important molecules that localize at the basolateral domain. Their recycling is involved in apical recruitments of vesicles and proteins. Different Integrin isoforms localizes at the basolateral domain, where they work as receptors and bind their ligands, transducing a downstream signal. The best characterized Integrin-mediated basolateral pathway involves β1-Integrin and Rac1. This pathway leads to laminin deposition on the external surface of MDCK cysts and is necessary to maintain the polarized phenotype (39). Moreover, it has been demonstrated that a sustained Rac1 activation leads to mitotic spindle misorientation (38). Although DGKα regulates Rac1 activation (Figure 16c), but not its localization (Figure 16a and 16b), the phenotype observed upon its silencing or inhibition is far away from the one observed upon Rac1 or β1-integrin inhibition. Indeed, no lumen filling or inversion of polarity are observed, which are characteristic phenotypes of Rac1 and β1-integrin inhibition respectively. These observations suggest that the small effect on Rac1 activity is not responsible of the multiple lumen phenotype observed in MDCK cysts lacking DGKα and that the laminin deposition pathway is not affected.

A second integrin-mediated pathway that regulates mitotic spindle has been described and involves α3β1-Integrin and Cdc42 (41). The small Rho GTPase Cdc42 has been strongly linked to mitotic spindle orientation during polarized mitosis (22; 23;24) and its intracellular localization is regulated by DGKα (Figure 13). Despite DGKα do not regulate also its activation (Figure 13g), it is possible that the improper

localization of Cdc42 during mitosis is responsible of the mitotic spindle misalignment. Today, there are no evidences that DGKα regulates the localization of Cdc42 directly at the mitotic spindle, but only at the apical domain (Figure 13). Despite this lacuna, we can not ignore the hypothesis that DGKα can regulate the mitotic spindle orientation through Cdc42, considering that DGKα regulates the small GTPase localization not only in MDCK cysts but also in other cellular models (37).

Basolateral DGKα localization and PA enrichment suggest also another possible pathway that can lead to mitotic spindle orientation. Recently, Martin-Belmonte and coworkers have demonstrated that +Tips proteins can interact with the EGF receptor (EGFR) in absence of its extracellular ligand, anchoring astral microtubules to the cell cortex (51). In particular, this mechanisms involve NuMA, which is a member of the Gαi-LGN-NuMA complex responsible for microtubules anchorage to the cell cortex (21). In the pathway proposed by Martin-Belmonte and coworkers, IQGAP1 binds to both EGFR and NuMA – acting as an alternative partner for NuMA instead of LGN – recruiting microtubules at the cell cortex where EGFR localizes. When EGFR binds to its ligand, it is internalized and no more able to bind NuMA, leading to the loss of microtubules anchorage and to the consequent spindle misorientation and multiple lumen phenotype (Figure 21).

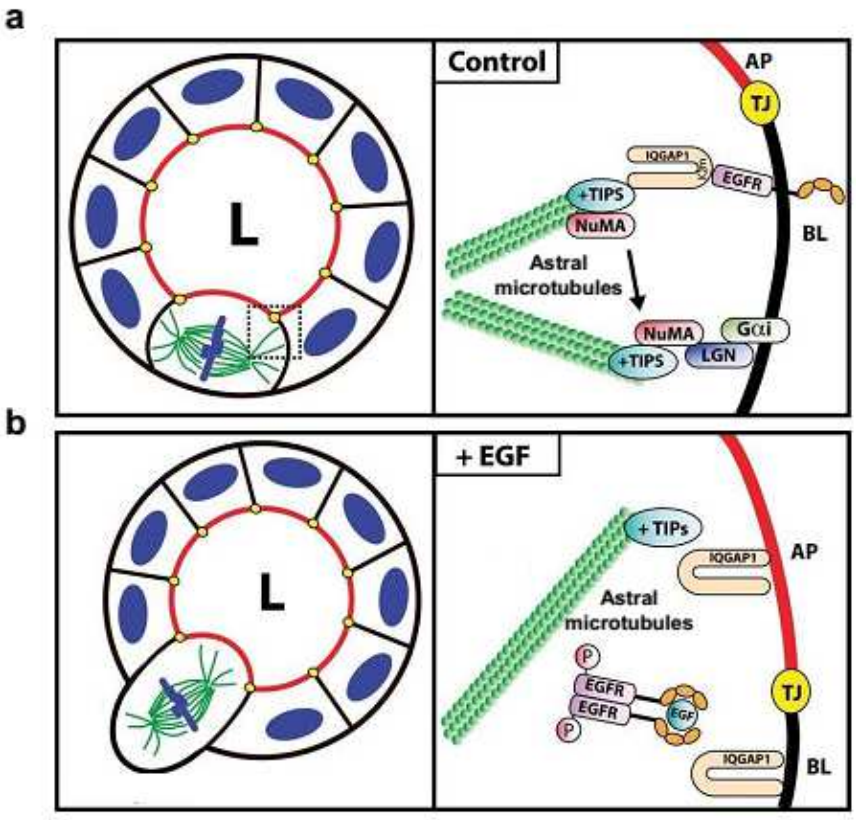

Figure 21: Proposed model for EGFR and NuMa interaction.

a) In basal state, NuMA is associated to astral microtubules and is recruited to the membrane by both EGFR and Gαi-LGN complex. This allow astral microtubule anchorage to the cell cortex and proper mitotic spindle orientation. **b)** Upon EGF stimulation, EGFR is internalized and NuMA can't bind it, leading to mitotic spindle misorientation. (Adapted from 51).

One of the most intriguing finding is that phorbol myristate acetate (PMA) administration induces EGFR internalization, dampening EGFR interaction with IQGAP1 and inducing the consequent spindle misorientation (51). PMA is the most commonly used phorbol ester and is a well known activator of PKCs and other DAG regulated proteins (52). Thus, PMA administration can mime an high DAG concentration in the plasma membrane. DGKα can regulate both DAG and PA concentration: its inhibition induces a decrease PA production and the consequent increase in DAG concentration. As DAG concentration rise up, EGFR is phosphorylated and internalized: astral microtubules are less anchored to the membrane and mitotic spindle will not be proper oriented. In this pathway there is a synergic action between high DAG levels, due to the loss of DGKα catalytic activity, and the PA product by PLDs. Indeed, inhibiting both DGKα and PLDs we are able to restore the normal-single lumen phenotype in MDCK cists (Figure 17).

In MDCK cysts, PLDs are involved in an ARF-6-mediated pathway necessary for correct cystogenesis (53). ARF-6 is a member of the ARF family of Ras-related GTPases and controls endocytic trafficking and actin remodelling (54). MDCK cysts expressing a constitutively-active form of ARF-6 (ARF-6Q67L) present two major phenotypes: filled lumen and multiple lumen. The ones whit multiple lumen show a proper single cell polarization, whit GP135 localized at the apical domain and β-catenin localized at the basolateral domain. The same behaviour is observed upon DGKα silencing or inhibition (Figure 10b, 10c, 10e and 10f). In ARF-6Q67L expressing cysts, PLDs inhibition by 1-butanol administration restores the normal-single lumen phenotype acting on a pathway involving ARF-6, PLDs and ERK activation (53). PLDs inhibition restores the single lumen phenotype also in cysts where DGKα is inhibited (Figure 17). The involvement of PLDs in the endocytic traffic regulator ARF-6-mediated pathway suggests that when DGKα is not catalytically active, the PA product by PLDs is responsible for EGFR internalization in concert whit the high DAG levels due to the loss of DGKα activity. PLDs inhibition alone has

no effect on cystogenesis (Figure 17a and 17b), indicating that PA product by PLDs is not sufficient to perturb the normal cystogenesis. Inhibiting both DGKα and PLDs we can revert the multiple lumen phenotype due to DGKα inhibition/silencing blocking the EGFR internalization and the consequent mitotic spindle misorientation. Moreover, IQGAP1 is a regulator of Rac1 activation, because RacGAP1 is one of its binding partners (55). As any other GAP protein, RacGAP1 can activate the GTPase activity of Rac1, leading to GTP hydrolysis and Rac1 inactivation. Thus, IQGAP1 displacement from the plasma membrane due to EGFR internalization can also affect Rac1 activation at the basolateral domain actin on RacGAP1. In this context, IQGAP1 is more available and interacts with RacGAP1, regulating Rac1 activation. This hypothesis can explain the reduced Rac1-GTP levels observed upon DGKα inhibition (Figure 16c).

Together, these hypothesis suggest that DGKα could act both on the EGFR and the Gαi-LGN-NuMa complex and on the PI(3,4,5)P_3 enrichment at the basolateral domain – that is lost upon DGKα inhibition/silencing (Figure 15a and 15b) – regulating the anchorage of astral microtubules to the cell cortex and the mitotic spindle orientation as final outcome.

Taken together, DGKα is emerging as a new key regulator of epithelial apical-basolateral polarization and of the mitotic spindle orientation. In the past few years, the importance of proper mitotic spindle orientation in different contexts has been demonstrated. In particular, it is involved in symmetric and asymmetric cell division in stem and cancer cells and its lost due to pathological outcomes and cancer progression. We found that DGKα is a strong regulator of mitotic spindle orientation in MDCK cysts and we hypothesized that DGKα regulates multiple pathways, mediating both Integrin-mediated signalling/vesicular trafficking and mitotic spindle orientation, likely independently from one each other. We also proposed some models for DGKα involvement in these processes, but they need to be further explored.

Abbreviation list

Abbreviation	Extended form
+Tips	Plus-end-tracking proteins
Anx A2	Annexin A2
APC	Adenomatous Polyposis Coli
Apical domain	AP
Atypical protein kinase C	aPKC
Basolateral domain	BL
CBD	CRIB domain of WASP
CLASPs	CLIP associating proteins
Crb	Crumbs
DAG	Diacylglycerol
DGKα	Diacylglycerol kinase alpha
DGKs	Diacylglycerol kinases
Discs large	Dlg
EGFR	Epidermal growth factor receptor
EMT	Epithelial to mesenchymal transition
GAPs	GTPase activating proteins
GDI	GTPase dissociation inhibitors
GEFs	GTPase exchange factors
HGF	Hepatocyte growth factor
Lgl	Lethal giant larvae
LPA	Lysophosphatidic acid
MDCK	Madin-Darby canine kidney
MET	Mesenchymal to epithelial transition
PA	Phosphatidic acid
$PI(3,4)P_2$	phosphatidylinositol-3,4-biphosphate
$PI(3,4,5)P_3$	phosphatidylinositol-3,4,5-triphosphate
$PI(4,5)P_2$	phosphatidylinositol-4,5-biphosphate
PLD	Phospholipase D
PMA	phorbol myristate acetate
PtdIns	Phosphoinositides
SCRIB	Scribble
VEGF	Vascular endothelial growth factor

References

1. Bryant D.M. and Mostov K.E. (2008) *Nature Rev*. **9**: 887-901.
2. Lamouille S., Xu J., Derynck R. (2014) *Nat. Rev. Mol. Cell Biol.* **15(3)**: 178-196
3. Nieto M.A. (2013) *Science* **342(6159)**: 1234850
4. Thiery J.P., Acloque H., Huang R.Y., Nieto M.A. (2009) *Cell* **139(5)**: 871-890.
5. Galichon P., Finianos S., Hertig A. (2013) *Cancer Letters* **341**: 24-29.
6. Yamanda S. and Nelson W.J. (2007) *Annu. Rev. Biochem*. **76**: 267-294.
7. Iglesias P.A. and Devreotes P.N. (2008) *Curr. Opin. Cell. Biol*. **20**: 35-40.
8. Birchmeier, C. and Gherardi, E. (1998) *Trends Cell Biol*. **8**: 404–410.
9. Montesano R., Schaller G., Orci L. (1991) *Cell* **66**: 697–711.
10. Zegers M.M., O'Brien L.E., Yu W., Datta A., Mostov K.E. (2003) *Trends Cell Biol*. **13(4)**: 169-76
11. Rose L.S. and Kemphues K.J. (1998) *Annu. Rev. Genet.* **32**: 521-45
12. Noda Y., Takeya R., Ohno S., Naito S., Ito T., Sumimoto H. (2001) *Genes Cells.* **2**:107-19.
13. Bulgakova N.A. and Knust E. (2009) *J. Cell Sci*. **122**: 2587-96.
14. Benton R. and St Johnston D. (2003) *Cell* **115(6)**: 691-704.
15. Yamanaka T., Horikoshi Y., Sugiyama Y., Ishiyama C., Suzuki A., Hirose T., Iwamatsu A., Shinohara A., Ohno S. (2003) *Curr. Biol.* **13(9)**: 734-43.
16. Laprise P., Viel A., Rivard N. (2004) *J. Biol. Chem.* **279(11)**: 10157-66
17. Royal I., Lamarche-Vane N., Lamorte L., Kaibuchi K., Park M. (2000) *Molecular Biology of the Cell*. **11**: 1709-1725.
18. Martin-Belmonte F., Gassama A., Datta A., Yu W., Rescher U., Gerke V., Mostov K. (2007) *Cell* **128(2)**: 383-97.
19. Toyoshima F., Matsumura S., Morimoto H., Mitsushima M., Nishida E. (2007) Dev. Cell 13(6): 796-811.
20. Tall G.G. and Gilman A.G. (2005) *PNAS* **102(46)**: 16584-9
21. Merdes A., Heald R., Samejima K., Earnshaw W.C., Cleveland D.W. (2000) J. Cell Biol. 149(4): 851-62
22. Durgan J., Kaji N., Hall A. (2011) *J. Biol. Chem.* **286(14)**: 12461-74.
23. Rodriguez-Fraticelli A.E., Vergarajauregui S., Eastburn D.J., Datta A., Alonso M.A., Mostov K., Martin-Belmonte F. (2010) *J. Cell Biol.* **189(4)**: 725-38.

24. Jaffe A.B., kaji N., Durgan J., Hall A. (2008) *J. Cell Biol.* **183(4)**: 625-33.
25. Topham M.K., Epand R.M. (2009) *Biochim. Biophys Acta* **1790**: 416-424.
26. Zhao C., Du G., Skowonek K., Frohman M.A., Bar-Sagi D. (2007) *Nat. Cell Biol.* **9(6)**: 706-712.
27. Merida I., Avila-Flores A., Merino E. (2008) *Biochem J.* **409(1)**: 1-18
28. Cutrupi S., Baldanzi G., Gramaglia D., Maffè A., Schaap D. Giraudo E., van Blitterswijk W., Bussolino F., Comoglio P.M., Graziani A. (2000) *EMBO J.* **19(17)** : 4614-4622.
29. Baldanzi G., Mitola S., Cutrupi S., Filigheddu N., van Blitterswijk W., Sinigaglia F., Bussolino F., Graziani A. (2004) *Oncogene* **23(28)**: 4828-4838.
30. Baldanzi G., Cutrupi S., Chianale F., Gnocchi V., Rainero E., Porporato P., Filigheddu N., van Blitterswijk W., Parolini O., Bussolino F., Sinigaglia F., Graziani A. (2008) *Oncogene* **27(7)**: 942-956.
31. Chianale F., Cutrupi S., Rainero E., baldanzi G., Porporato P., Traini S., Filigheddu N., Gnocchi V., Santoro M., Parolini O., van Blitterswijk W., Sinigaglia F., Graziani A. (2007) *Mol. Biol. Cell* **18(12)**: 4859-71.
32. Chianale F., Rainero E., Cianflone C., Bettio V., Pighini A., Porporato P., Filigheddu N., Serini G., Sinigaglia F., Balzandi G., Graziani G. (2010) *PNAS* **107(9)**: 4182-4187.
33. Sato M., Liu K., Sasaki S., Kunji N., Sakai H., Mizuno H., Saga H., Sakane F. (2013*) Parmacology* **92(1-2)**: 99-107
34. Nakamura N., Rabouille C., Watson R., Nilsson T., Hui N., Slusarewicz P., Kreis T.E., Warren G. (1995) *J. Cell Biol.* **131(6 Pt 2)**: 1715-26.
35. Gerl M.J., Sampaio J.L., Urban S., Kalvodova L., Verbavatz J.M., Binnington B., Lindemann D., Lingwood C.A., Shevchenko A., Schroeder C., Simons K. (2012) *J. Cell Biol.* **196(2)**: 213-21.
36. Bryant D.M., Datta A., Rodriguez-Fraticelli A.E., Peränen J., Martin-Belmonte F., Mostov K. (2010) *Nat. Cell Biol.* **12(11)**: 1035-45.
37. Rainero E., Cianflone C., Porporato P., Chianale F., Malacarne V., Bettio V., Ruffo E., Ferrara M., Benecchia F., Capello D., Paster W., Locatelli I., Bertoni A., Filigheddu N., Sinigaglia F., Norman J.C., Baldanzi G., Graziani A. (2014) *PLos One* **9(6)**: e97144.
38. Matsumura S., Toyoshima F. (2012) *Cell Struct. Funct.* **37(2)**: 81-7.

39. Yu W., Datta A., Laroy P., O'Brien L.E., Mark G., Jou T.S., Matlin K.S., Mostov K., Zegers M.M. (2005) *Mol. Biol. Cell* **16(2**): 433-45.
40. Yagi S., Matsuda M., Kiyokawa E. (2012) *EMBO rep.* **13(3)**: 237-43.
41. Myllymäki S.M., Teräyäinen T.P., Manninen A. (2011) *PLoS One* **6(5)**:e19453.
42. Rainero E., Caswell P.T., Muller P.A., Grindlay J., McCaffrey M.W., Zhang Q., Wakelam M.J., Vousden K.H., Graziani A., Norman J.C. (2012) *J. Cell Biol.* **196(2)**: 277-95.
43. Zhang Y., Du G. (2009) *BBA* **1791(9)**:850-5.
44. Gomez-Cambronero J. (2014) *Adv. Biol. Regul.* **54C**: 197-206.
45. Gomez-Cambronero J., Di Fulvio M., Knapek K. (2007) *J. Leukoc. Biol.* **82(2)**: 272-8.
46. Gloerich M., ten Klooster J.P., Vliem M.J., Koorman T., Zwartkruis F.J., Clevers H., Bos J.L. (2012) *Nat. Cell Biol*. **14(8)**: 793-801.
47. Horikoshi Y., Suzuki A., Yamanaka T., Sasaki K., Mizuno K., Sawada H., Yonemura S., Ohno S. (2009) *J. Cell Sci.* **122(10)**: 1595-1606.
48. Baldanzi G., Pighini A., Bettio V., Rainero E., Traini S., Chianale F., Porporato P., Filigheddu N., Mesturini R., Song S., Schweighoffer T., Patrussi L., Baldari C.T., Zhong X.P., van Blitterswijk W., Sinigaglia F., Nichols K.E., Rubio I., Parolini O., Graziani A. (2011) *J. Immunol.* **187(11)**: 5941-51.
49. Sanjuan M.A., Pradet-Balade B., Jones D.R., Martinez A.C., Stone J.C., Garcia-Sanz J.A., Merida I. (2003) *J. Immunol*. **170(6)**: 2877-83.
50. Merino E., Avila-Flores A., Shirai Y., Moraga I., Saito N., Merida I. (2008) *J. Immunol.* **180(9)**: 5805-15.
51. Bañón-Rodriguez I., Gálvez-Santisteban M., Vergarajauregui S., Bosch M., Borregueri-Pascual A., Martin-Belmonte F. (2014) *EMBO J.* **33(2)**: 129-45.
52. Liu W.S. and Heckman C.A. (1998) *Cell Signal.* **10(8)**:529-42.
53. Tushir J.S., Clancy J., Warren A., Wrobel C., Brugge J.S., D'Souza-Schorey C. (2010) *Mol. Biol. Cell* **21(13)**: 2355-2366.
54. D'Souza-Schorey C., Chavrier P. (2006) *Nat. Rev. Mol. Cell Biol.* **7(5)**: 347-358.
55. Jacquement G., Morgan M.R., Bryon A., Humphries J.D., Choi C.K., Chen C.S., Caswell P.T., Humphries M.J. (2013) *J. Cell Sci.* **126**:4121-35.
56. Matsumura S., Toyoshima F. (2012) *Cell Struct. Funct.* **37(2)**: 81-87.

Annexed papers

Diacylglycerol kinase α mediates HGF-induced Rac activation and membrane ruffling by regulating atypical PKC and RhoGDI

Federica Chianale[a,1], Elena Rainero[a,1], Cristina Cianflone[a], Valentina Bettio[a], Andrea Pighini[a], Paolo E. Porporato[a], Nicoletta Filigheddu[a], Guido Serini[b,c], Fabiola Sinigaglia[a], Gianluca Baldanzi[a], and Andrea Graziani[a,2]

[a]Department of Clinical and Experimental Medicine and Biotecnologie per la Ricerca Medica Applicata, University Amedeo Avogadro of Piemonte Orientale, 28100 Novara, Italy; [b]Department of Oncological Sciences and Division of Molecular Angiogenesis, Istituto per la Ricerca e la Cura del Cancro, Institute for Cancer Research and Treatment, University of Torino School of Medicine, 10060 Candiolo, Italy; and [c]Center for Complex Systems in Molecular Biology and Medicine, University of Torino, 10100 Torino, Italy

Edited* by Lewis Clayton Cantley, Harvard Medical School, Boston, MA, and approved December 14, 2009 (received for review July 29, 2009)

Diacylglycerol kinases (DGKs) convert diacylglycerol (DAG) into phosphatidic acid (PA), acting as molecular switches between DAG- and PA-mediated signaling. We previously showed that Src-dependent activation and plasma membrane recruitment of DGKα are required for growth-factor-induced cell migration and ruffling, through the control of Rac small-GTPase activation and plasma membrane localization. Herein we unveil a signaling pathway through which DGKα coordinates the localization of Rac. We show that upon hepatocyte growth-factor stimulation, DGKα, by producing PA, provides a key signal to recruit atypical PKCζ/ι (aPKCζ/ι) in complex with RhoGDI and Rac at ruffling sites of colony-growing epithelial cells. Then, DGKα-dependent activation of aPKCζ/ι mediates the release of Rac from the inhibitory complex with RhoGDI, allowing its activation and leading to formation of membrane ruffles, which constitute essential requirements for cell migration. These findings highlight DGKα as the central element of a lipid signaling pathway linking tyrosine kinase growth-factor receptors to regulation of aPKCs and RhoGDI, and providing a positional signal regulating Rac association to the plasma membrane.

cell migration | growth factors | phosphatidic acid

Cell migration, central to many biological and pathological processes such as cancer metastatic progression, is a multistep cycle involving extension of protrusions and formation of stable attachments near the leading edge, followed by translocation of the cell body forward (1). The protrusive activity occurring at the leading edge depends on the spatial and temporal coordination between cell substrate adhesion and actin reorganization. Rho-family small GTPases coordinate the recruitment at the leading edge of downstream effectors, thereby mediating the formation of ruffles and lamellipodia. Their GTP-bound state is tightly regulated by both guanine nucleotide exchange factors (GEFs), which stimulate GTP loading, and GTPase activating proteins (GAPs), which catalyze GTP hydrolysis. Moreover, Rho-family GTPases are regulated by guanine nucleotide dissociation inhibitors (GDIs), which antagonize both GEFs and GAPs and mediate the cycling of Rho proteins between the cytosol and the membrane (2, 3).

Atypical protein kinase C ζ and ι (aPKCζ/ι), unlike classical and novel PKCs, feature a C1-like domain which does not bind to either diacylglycerol or phorbol esters, and have recently been proposed as key transducers for establishment of cell polarity and migration (4).

Diacylglycerol kinases (DGKs), which convert diacylglycerol (DAG) to phosphatidic acid (PA), comprise a family of 10 distinct enzymes grouped into five classes, each featuring distinct regulatory domains and a highly conserved catalytic domain preceded by two cysteine-rich C1-like domains. An increasing body of evidence indicates that DGKs, by acting as terminators of diacylglycerol-triggered signaling, contribute to regulating C1 domain-containing proteins, such as classical and novel PKCs and the Rac-GAP β-chimaerin (5). Conversely, by generating PA, DGKs regulate several signaling proteins, including serine kinases, small-GTPase-regulating proteins, and lipid-metabolizing enzymes (reviewed in refs. 6 and 7). Thus, by regulating in a reciprocal manner the level of both DAG and PA lipid second messengers, DGK enzymes may act as terminators of DAG-mediated signals as well as activators of PA-mediated ones. We previously showed that DGKα is activated by growth factors on recruitment to the plasma membrane through its Src-mediated phosphorylation on Tyr^{335}. Activation of DGKα mediates growth-factor-induced cell migration and proliferation in epithelial, endothelial, and lymphoma cells (8–12). Moreover, we demonstrated that in epithelial cells, DGKα is required for hepatocyte growth factor (HGF) -induced membrane ruffling by regulating Rac membrane targeting and activation (13). However, the molecular mechanisms by which DGKα regulates Rac function still remain to be elucidated.

Here we unveil a previously undescribed signaling pathway linking HGF receptor to Rac activation and targeting at the plasma membrane of epithelial cells, where it drives the formation of membrane protrusions. Our data highlight that upon HGF-induced plasma membrane recruitment and activation of DGKα, PA recruits at the plasma membrane and activates aPKCζ/ι, in complex with RhoGDI and Rac. Then, Rac is released from the inhibitory complex with RhoGDI, allowing its activation and formation of membrane ruffles.

Results

DGKα Regulates Rac by Directing Its Recruitment to the Plasma Membrane. MDCK epithelial cells grow in discrete colonies and on HGF stimulation undergo scatter, involving cell spreading, dissolution of intercellular adhesions, and migration of cells away from one another. At early time points from HGF stimulation, cells at the periphery of a colony reorganize the actin cytoskeleton and form dynamic protrusions of the outer plasma membrane known as ruffles, mediated by membrane targeting and activation of Rac (14, 15). We previously showed that down-regulation of DGKα affected both HGF-induced membrane ruffling and recruitment of Rac to the plasma membrane (13). Here, by live-cell imaging, we report that HGF-induced rapid and transient recruitment of EGFP-Rac at sites of intense ruf-

Author contributions: F.C., E.R., F.S., G.B., and A.G. designed research; F.C., E.R., C.C., V.B., A.P., G.S., and G.B. performed research; F.C., E.R., C.C., V.B., A.P., P.E.P., N.F., G.S., G.B., and A.G. analyzed data; G.S. contributed new reagents/analytic tools; and F.C., E.R., and A.G. wrote the paper.

The authors declare no conflict of interest.

*This Direct Submission article had a prearranged editor.

[1]F.C. and E.R. contributed equally to this work.

[2]To whom correspondence should be addressed. E-mail: graziani@med.uniupo.it.

This article contains supporting information online at www.pnas.org/cgi/content/full/0908326107/DCSupplemental.

www.pnas.org/cgi/doi/10.1073/pnas.0908326107

fling was impaired upon DGK inhibition (Fig. S1 and Movies S1 and S2), achieved by cell treatment with 1 μM R59949. R59949 is a DGK-specific inhibitor interacting with the catalytic domain, endowed with a strong preference for α, β, and δ isoforms (16, 17). We previously showed that overexpression of DGKα reverted R59949-mediated inhibition of HGF signaling (8).

Thus, we investigated the mechanisms by which DGKα might regulate Rac-specific localization. In the absence of growth-factor stimulation, constitutively active RacV12 mutant localized mainly in the cytoplasm and at cell-cell adhesions, whereas its expression was not sufficient to induce ruffling at the leading edge of cells at the periphery of a colony, according to previous observations (15). HGF cell treatment increased the percentage of cells featuring concomitant membrane ruffles and RacV12 at the outer plasma membrane in a DGK-dependent manner (Fig. S2). In addition, we compared endogenous Rac localization in MDCK cells transiently transfected with either DGKα wild type (DGKαWT) or a constitutively active membrane-bound DGKα mutant (myr-DGKα). Indeed, the expression of myr-DGKα, but not of DGKαWT, promoted a 2.5-fold increase of the percentage of cells displaying membrane ruffles, along with Rac recruitment to the plasma membrane at ruffling sites (Fig. 1). Overall, these data indicate that DGKα activation provides a crucial signal which is both necessary and sufficient to direct Rac membrane localization at the leading edge, regardless of its GTP loading, thereby promoting ruffle formation.

DGKα Regulates RhoGDI Membrane Recruitment. An increasing body of evidence indicates that RhoGDI, which in unstimulated cells associates with GDP-bound Rac in a cytosolic complex, regulates Rac targeting to specific adhesion sites at the plasma membrane through largely unidentified mechanisms (2). Once at the plasma membrane, Rac is released from the inhibitory complex with RhoGDI and is eventually activated by a Rac-GEF (2, 18). To verify whether growth factors trigger Rac localization at the plasma membrane through interaction with RhoGDI, we transiently transfected MDCK cells with a Rac mutant, RacR66E, unable to bind to RhoGDI (19). Indeed, RacR66E failed to be recruited at ruffling sites upon HGF cell treatment whereas HGF-induced membrane ruffle formation was not impaired, indicating that endogenous Rac is properly activated (Fig. 2). These data demonstrate that RhoGDI physical interaction with Rac mediates growth-factor-induced Rac targeting at ruffling sites.

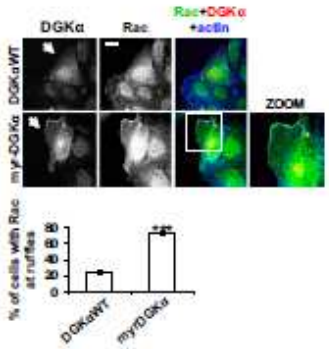

Fig. 1. DGKα provides the signal directing Rac to the nascent ruffle. MDCK cells, transfected with either DGKαWT or myr-DGKα, were cultured overnight in the absence of serum, fixed, and stained for Rac (green), myc tag (red), and actin (blue). Arrows indicate DGKαWT- or myr-DGKα-transfected cells. (Scale bar, 10 μm.) C, 30 transfected cells, scored for the presence of Rac at ruffling sites. $n = 6$, with SEM; $^{***}P = 0.0002$.

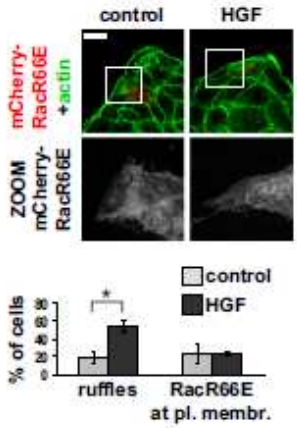

Fig. 2. Rac plasma membrane targeting requires Rac/RhoGDI interaction. MDCK cells were transiently transfected with mCherry-RacR66E, treated with 10 ng/mL HGF for 15 min, fixed, and stained for actin (green). (Scale bar, 24 μm.) C, 30 transfected cells, scored for the presence of ruffles or RacR66E plasma membrane localization. $n = 3$, with SEM; $^{*}P = 0.0057$.

Thus, we investigated whether HGF, although inducing membrane ruffles, was able to recruit RhoGDI to the leading edge and whether this process required DGKα activity. We show that HGF increased the percentage of cells displaying RhoGDI at ruffling sites, which was impaired by both pharmacological inhibition (Fig. 3*A*) and siRNA-mediated silencing of DGKα (Fig. S3*A*). In addition, in time-lapse experiments, HGF-induced rapid and transient recruitment of RhoGDI to ruffling sites required DGK activity (Fig. S4 and Movies S3 and S4).

Moreover, we investigated whether DGKα constitutive activation at the plasma membrane was sufficient to recruit RhoGDI. Thus, the expression of myr-DGKα, but not of DGKαWT, was sufficient to recruit RhoGDI at ruffling sites in almost 80% of transfected cells (Fig. 3*B* and Fig. S3*B*). Altogether, these findings demonstrate that stimulation of DGKα enzymatic activity provides a crucial signal which is necessary and sufficient to direct the recruitment of RhoGDI, which in turn is required for Rac targeting at protrusion sites and ruffle formation.

DGKα Regulates Membrane Ruffling by Modulating aPKCζ/ι Function. The molecular mechanisms regulating RhoGDI localization are still largely unknown, as it lacks membrane-interacting domains. PKCζ, reported to be regulated by direct binding to PA but not to DAG (20), associates with and phosphorylates RhoGDI, thereby allowing its dissociation from Rac (21). Indeed, in MDCK cells, a small amount of the whole cellular aPKCζ/ι was constitutively associated with RhoGDI (see below, Fig. 6). Thus, we raised the hypothesis that DGKα might control RhoGDI by providing the lipid-regulating aPKCζ/ι.

To obtain an appreciable down-regulation of cellular aPKCs, we silenced both PKCζ and PKCι by different combinations of their respective specific siRNAs (Fig. 4*A*). We observed that aPKCζ/ι silencing impaired HGF-induced membrane ruffle formation, as well as both RhoGDI and Rac recruitment to the outer plasma membrane (Fig. 4*B*). The aPKCζ/ι catalytic activity was actually required, as aPKCζ/ι inhibition by cell treatment with PKCζ/ι pseudosubstrate peptide impaired HGF-induced membrane ruffle formation and Rac plasma membrane translocation (Fig. S5*A*). Similarly, inhibition of PKCζ by expression of PKCζ dominant-negative mutant (PKCζKW) impaired HGF-induced RhoGDI translocation to the outer plasma membrane

CELL BIOLOGY

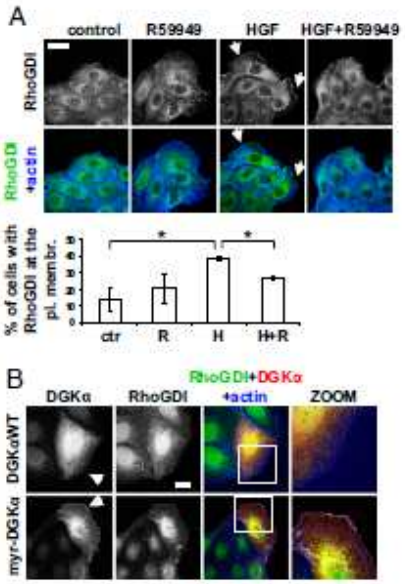

Fig. 3. DGKα regulates RhoGDI targeting to the plasma membrane. (*A*) MDCK cells were stimulated with 10 ng/mL HGF for 5 min in the presence or absence of 1 μM R59949, fixed, and stained for RhoGDI (green) and actin (blue). Arrows indicate RhoGDI at membrane ruffles. (Scale bar, 24 μm.) *C*, 70 cells, scored for RhoGDI localization at ruffling sites. $n = 3$, with SEM; $^{*}P < 0.05$. (*B*) MDCK cells, transfected with either DGKαWT or myr-DGKα, were cultured overnight in the absence of serum, fixed, and stained for RhoGDI (green), myc tag (red), and actin (blue). Arrowheads indicate transfected cells. (Scale bar, 10 μm.)

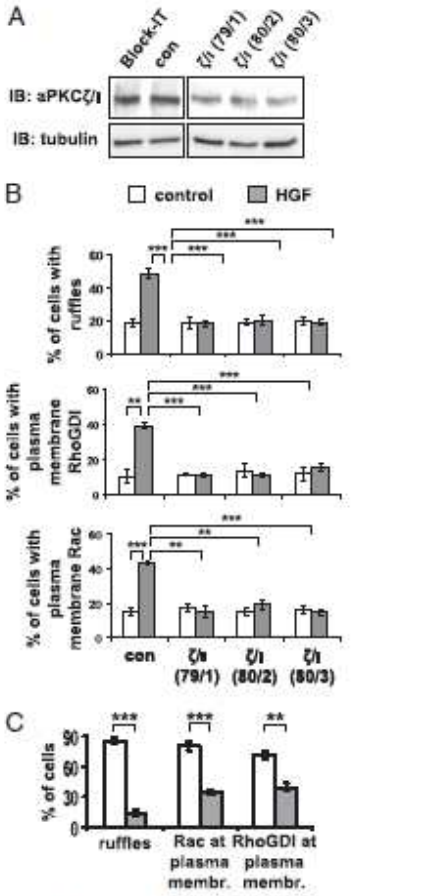

Fig. 4. aPKCζ/ι mediates both HGF- and myr-DGKα-induced extension of membrane protrusions. (*A*) MDCK cells were transfected with three combinations of PKCζ (79, 80) and PKCι (1–3) specific siRNAs. Whole-cell lysates were analyzed for levels of aPKCζ/ι expression by western blot. (*B*) MDCK cells were transfected as in *A*, treated with 10 ng/mL HGF for 15 min, fixed, and stained for Rac or RhoGDI and actin. *C*, 110 cells, analyzed for the presence of ruffles and Rac or RhoGDI at the plasma membrane. $n = 4$ (Rac and RhoGDI), $n = 8$ (ruffles), with SEM; $^{**}P < 0.005$, $^{***}P < 0.0005$. (*C*) MDCK cells were transiently transfected either with myr-DGKα alone or cotransfected with myr-DGKα and PKCζKW, cultured overnight in the absence of serum, fixed, and stained for myc and flag tags, actin, and Rac or RhoGDI. *C*, 20 transfected cells, scored for the presence of ruffles and Rac or RhoGDI at protrusion sites. $n = 4$, with SEM; $^{**}P < 0.001$, $^{***}P < 0.0001$.

(Fig. S5*B*). Moreover, aPKCζ/ι was also required for myr-DGKα-induced membrane ruffle formation and Rac and RhoGDI targeting to the outer plasma membrane (Fig. 4*C* and Fig. S5*C*). Together these data indicate that, upon HGF stimulation or myr-DGKα expression, aPKCζ/ι mediates membrane ruffle formation and recruitment of the molecular machinery necessary for polarized extension of plasma membrane protrusions.

We then investigated whether DGKα was involved in the regulation of aPKCζ/ι downstream of HGF signaling. Indeed, we observed that HGF induced the recruitment of aPKCζ/ι to membrane ruffles in a DGKα-dependent manner. In fact, both specific down-regulation of DGKα by two different siRNAs (Fig. 5*A* and Fig. S6*A*) and its pharmacological inhibition by R59949 cell treatment (Fig. S6*B*) completely abolished HGF-induced recruitment of aPKCζ/ι to the outer plasma membrane, indicating that enzymatic activity of DGKa was required.

Moreover, expression of myr-DGKα was sufficient to recruit aPKCζ/ι to ruffling sites, as the percentage of cells displaying this localization of aPKCζ/ι increased 3-fold in myr-DGKα-expressing cells compared to DGKαWT-expressing ones (Fig. 5*B* and Fig. S6*C*). Accordingly, cell treatment with PA but not with lysophosphatidic acid (LPA) or DAG was sufficient to promote concurrent cortical actin rearrangements and plasma membrane translocation of aPKCζ/ι, Rac, and RhoGDI (Fig. 5*C* and Fig. S7). Moreover, cell treatment with exogenous PA, but not with DAG, induced aPKCζ/ι activation, as revealed by the increase in phosphorylation of the catalytic domain Thr410 (Fig. 5*D*). Together, these data strongly support the idea that the generation of PA by DGKα is a crucial signal driving the recruitment and activation of the molecular machinery necessary for extension of membrane protrusions.

As accumulating evidence suggests that the small GTPase Cdc42 acts upstream of PKCζ and regulates it through the Par3/Par6 complex, thus driving cell polarity and directional migration (22), we further verified whether DGKα might regulate aPKCζ/ι via Cdc42. Indeed, the expression of Cdc42N17, although impairing membrane ruffles induced by myr-DGKα, did not affect aPKCζ/ι plasma membrane recruitment (Fig. S8). Thus, although Cdc42 is required for ruffle formation induced by constitutive generation of PA at the plasma membrane, it is not required for the recruitment of aPKCζ/ι. Overall, these data indicate that DGKα acts upstream of aPKCζ/ι, in a Cdc42-independent manner, by regulating its recruitment to ruffling sites through production of PA.

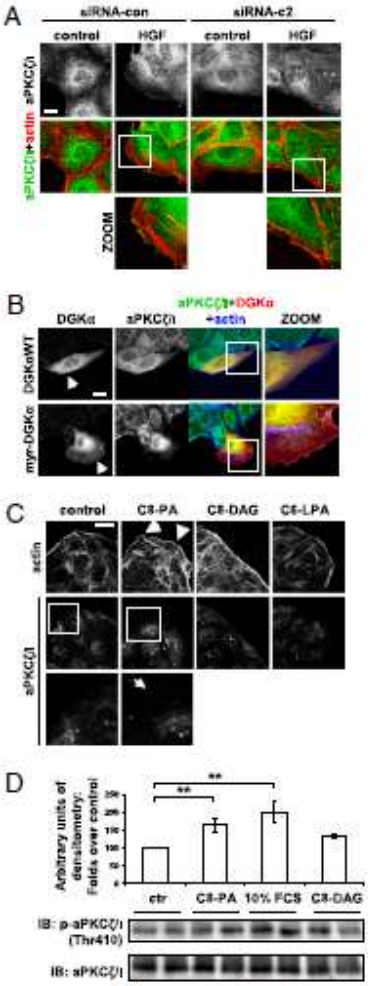

Fig. 5. DGKα regulates aPKCζ/ι function. (*A*) MDCK cells were transfected either with control siRNA or DGKα siRNA c1 and c2, treated with 10 ng/mL HGF for 15 min, fixed, and stained for aPKCζ/ι (green) and actin (red). (Scale bar, 10 μm.) (*B*) MDCK cells, transfected either with DGKαWT or myr-DGKα, were cultured overnight in the absence of serum, fixed, and stained for aPKCζ/ι (green), myc tag (red), and actin (blue). Arrowheads indicate transfected cells. (Scale bar, 10 μm.) (*C*) MDCK cells were stimulated with either 250 μM C8-PA, C8-DAG, or C6-LPA or left untreated, and fixed and stained for actin (red) and aPKCζ/ι (green). Arrowheads indicate cortical actin rearrangements, while the arrow indicates aPKCζ/ι membrane localization. (Scale bar, 19 μm.) (*D*) MDCK cells were stimulated with either 250 μM C8-PA, 10% FCS medium (as positive control), 250 μM C8-DAG, or left untreated. Whole-cell lysates were analyzed by western blot and the intensity of phospho-aPKCζ/ι bands was quantified by densitometry. For each condition, nine replicate points were performed in four independent experiments. The densitometry of each band was normalized as the percentage of the densitometry mean of control points in the same experiment, and is shown in the histogram, with SEM; $^{**}P < 0.005$. A representative picture is shown.

We then investigated whether, by regulating the function of aPKCζ/ι, DGKα might control the dissociation of Rac/RhoGDI complex. We immunoprecipitated RhoGDI from MDCK cells stably expressing either the control vector (MDCK/empty vector) or a kinase-defective dominant-negative mutant of DGKα (DGKαDN). Rac coimmunoprecipitated with RhoGDI both in MDCK/empty vector and in MDCK/DGKαDN unstimulated cells. Upon HGF stimulation, Rac was released from the complex with RhoGDI in MDCK/empty vector cells, whereas expression of DGKαDN prevented both dissociation of the complex (Fig. 6 and Fig. S9) and Rac activation (13). Collectively, the data presented above identify DGKα as an upstream regulator of aPKCζ/ι. DGKα, by producing PA, provides the crucial signal for the recruitment at the plasma membrane and activation of aPKCζ/ι, in complex with RhoGDI and Rac, which finally dissociates in a DGKα-dependent manner, thereby allowing Rac activation.

Finally, we tested the hypothesis that DGKα mediates the formation of membrane ruffles by regulating aPKCζ/ι. Thus, we verified whether transient expression of membrane-bound constitutively active myr-PKCζ could overcome DGKα inhibition, as expected for a downstream effector. Indeed, myr-PKCζ-expressing cells featured an altered morphology with membrane protrusions and ruffles, even in the absence of stimulation, and in 60% of them RhoGDI was localized at the outer plasma membrane. Prolonged (1-h) pharmacological inhibition of DGK activity by R59949 did not affect either formation of membrane protrusions or RhoGDI localization to the outer plasma membrane (Fig. 7), confirming that aPKCζ/ι is responsible, downstream of DGKα, for the recruitment of RhoGDI at the leading edge and consequent activation of the molecular machinery necessary for extension of membrane ruffles.

Overall, our findings highlight that DGKα, by producing PA, provides a crucial signal to recruit aPKCζ/ι and RhoGDI/Rac complex and to activate aPKCζ/ι, thereby allowing Rac membrane targeting and activation and consequent actin cytoskeleton remodeling preliminary to cell migration.

Discussion

Epithelial cells at the periphery of a colony initiate migration by extending membrane protrusions whose formation relies on recruitment and activation of Rac to their tips, to harness and localize actin polymerization (23). Spatially restricted activation of Rac at nascent ruffles is triggered by coordinated signals provided by both growth factors and adhesion receptors. Moreover, the observation that in epithelial cells the expression of a constitutively active form of Rac is not per se sufficient to promote ruffle formation (15, 24) strongly indicates that a further localization signal,

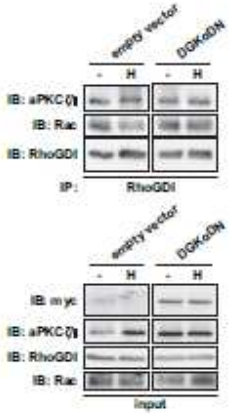

Fig. 6. DGKα regulates Rac/RhoGDI complex dissociation. MDCK/empty vector or MDCK/DGKα-DN cells were stimulated with 50 ng/mL HGF for 15 min. Cell lysates were immunoprecipitated for RhoGDI and analyzed by western blot.

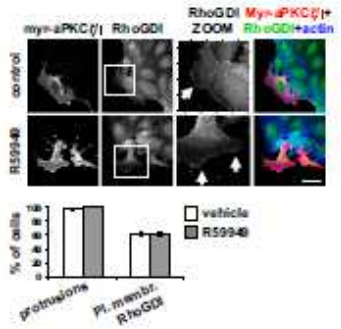

Fig. 7. DGKα does not affect myr-PKCζ-induced events. MDCK cells were transiently transfected with myr-PKCζ, grown overnight in the absence of serum, and treated with 1 μM R59949 for 1 h. Cells were fixed and stained for flag tag (red), RhoGDI (green), and actin (blue). Arrows indicate RhoGDI staining at protrusion sites. (Scale bar, 24 μm.) C, 30 transfected cells, scored for the presence of protrusions and RhoGDI at protrusion sites. $n = 3$, with SEM.

provided by growth factors, is required to generate RacGTP accumulation at protrusion sites. Starting from our initial observation that DGKα is required for HGF-induced RacV12 membrane targeting, we unveil a signaling pathway by which HGF regulates Rac localization to nascent ruffles through membrane recruitment of DGKα, aPKCζ/ι, and RhoGDI.

We previously showed that, upon HGF stimulation, activation and membrane recruitment of Rac, as well as ruffle formation, are fully dependent on DGKα (13). Our finding that expression of a myristoylated mutant of DGKα promoted ruffle formation and Rac recruitment at protrusion sites, in the absence of growth factor, strongly suggests that activation of DGKα at the plasma membrane provides a crucial signal to regulate Rac function.

Previous evidence underscored the role of RhoGDI in regulating the dynamics of Rac targeting to the plasma membrane, where Rac dissociates from the inhibitory complex with RhoGDI to interact with its downstream effectors (2, 18). Our observation that in HGF-treated cells RhoGDI is recruited to nascent ruffles, and that a Rac mutant unable to bind to RhoGDI is not, provides further support to the claim that the interaction between Rac and RhoGDI is necessary for Rac membrane targeting. Moreover, the present data demonstrate that growth factors promote Rac membrane localization by regulating RhoGDI targeting. We show that DGKα at the plasma membrane provides a key lipid signal necessary and sufficient to recruit RhoGDI. Furthermore, the failure to detect DGKα in a complex with RhoGDI and Rac suggests that DGKα, rather than acting as a scaffolding protein, may recruit RhoGDI through its enzymatic activity. However, RhoGDI does not feature any clear domain responsible for membrane binding, suggesting that the lipid signal generated by DGKα may recruit RhoGDI through an interacting lipid-binding protein.

Recent evidence indicates that PKCζ associates with RhoGDI and regulates the dissociation of Rac/RhoGDI complex, thereby allowing Rac activation (21). Moreover, PKCι regulates invasive behavior by activating Rac in lung cancer cells (25). Interestingly, PA, the lipid product of DGKα activity, has been reported to bind directly to PKCζ and to stimulate its enzymatic activity (20), whereas it was recently shown that DGKα enhances PKCζ-mediated phosphorylation of p65/Rel (26). Here we show that upon HGF stimulation, DGKα-generated PA is a necessary and sufficient signal to recruit aPKCζ/ι at protrusion sites and activate it, thereby promoting Rac and RhoGDI membrane targeting.

Kuribayashi et al. showed that PKCζ, associated in a complex with RhoGDI, mediates its phosphorylation on threonine, thereby allowing Rac release (21). Based on this observation and on our data, we expected that Rac release from the complex with RhoGDI depended on DGKα activity. Consistently, in the present report, we show that DGKα enzymatic activity mediated HGF-induced Rac release from RhoGDI, although we could not detect any threonine phosphorylation of endogenous RhoGDI. Finally, these results suggest the following working model: Upon HGF stimulation, Src-mediated activation of DGKα, once targeted to the plasma membrane, results in accumulation of PA, which directs the recruitment of aPKC/RhoGDI/Rac complex at protrusion sites, likely through the interaction of DGKα-produced PA with the C1-like domain of aPKCζ/ι, which is finally activated. Thus, aPKCζ/ι is identified as the direct downstream effector of DGKα. Once at the plasma membrane, aPKCζ/ι may allow Rac release from RhoGDI, likely through RhoGDI phosphorylation. This model is confirmed by the finding that expression of myr-PKCζ, in the absence of growth factors, recapitulates both RhoGDI recruitment and protrusion formation in a DGKα-independent manner, providing further support to the tenet that DGKα regulates RhoGDI and Rac by acting upstream of aPKCζ/ι (Fig. 8).

aPKC is recruited to the plasma membrane through binding to active Cdc42 (27) or by directed interaction with ceramide in a Cdc42-independent manner (28). Our finding that Cdc42 is dispensable for aPKCζ/ι recruitment induced by myr-DGKα suggests that Cdc42 function is not required for lipid-mediated aPKCζ/ι membrane targeting, albeit necessary for ruffle formation downstream of DGKα.

As RhoGDI also controls Cdc42, we may speculate that activation of DGKα provides a localization signal driving plasma membrane recruitment of aPKCs in complex with RhoGDI and Rac or Cdc42, eventually leading to the activation of Cdc42 and Rac, which may further recruit aPKCs in a Cdc42-dependent manner. This might establish a feed-forward mechanism that allows the full activation of the molecular machinery driving actin polymerization and consequent formation of membrane protrusions.

PAK1-mediated serine phosphorylation of RhoGDI promotes the selective release of Rac downstream of Cdc42 activation (29). Recently, DGKζ was shown to regulate PAK1-mediated phosphorylation of RhoGDI, leading to selective activation of Rac but not of Cdc42 (30). Conversely, PKCζ-dependent phosphorylation of RhoGDI promotes the release of both Rac and Cdc42 (21). Thus, it seems that DGKα and DGKζ, by regulating, respectively, aPKCζ/ι and PAK1, are involved in two

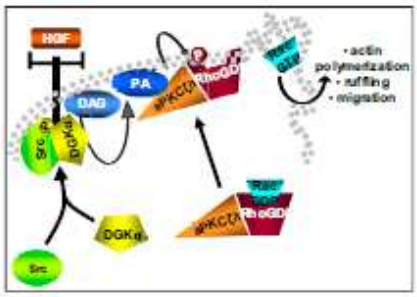

Fig. 8. Model proposed for Rac-localized activation at the leading edge upon growth-factor stimulation. Upon growth-factor stimulation, DGKα is activated in a Src-dependent manner and recruited to the plasma membrane. The production of PA is the crucial signal to direct the recruitment of aPKCζ/ι, in complex with RhoGDI and Rac. PKCζ/ι, in turn, mediates the dissociation of Rac from the inhibitory complex with RhoGDI, which may become prone to activation by a RacGEF.

distinct molecular mechanisms leading to the control of small-GTPase function.

In conclusion, our findings constitute a coherent demonstration that DGKα, upon Src-mediated activation, acts as a positive transducer of growth-factor signaling by producing PA rather than removing DAG. Here we unveil a PA-mediated signaling pathway linking tyrosine kinase receptors to Rac activation, membrane ruffling, and cell migration. In particular, we highlight a pivotal role for a DGKα-aPKCζ/λ-RhoGDI axis in the regulation of the initial events leading to activation of Rac at the leading edge of migrating cells.

Materials and Methods

Cell Stimulation. Before any treatment, cells were cultured overnight in the absence of serum. In the case of R59949 cell treatment, a 15-min pretreatment with R59949, or vehicle alone, was performed.

Immunofluorescence. Culturing, fixing, and staining detailed procedures are described in *SI Materials and Methods* and ref. 13. Representative pictures are shown in the figures.

Statistical Analysis. In experiments involving counting of cells displaying ruffles, membrane protrusions, or localization of proteins at the outer plasma membrane (not at cell-cell contacts), only colony-edge cells were considered. The average number of cells scored for each condition in each experiment is indicated in figure legends by "C." Statistical analysis was performed considering *n* independent experiments (indicated in the figure legends). The *P* values were calculated by one-tailed Standard *t* test.

Further details are provided in *SI Materials and Methods*.

ACKNOWLEDGMENTS. This work was supported by Associazione Italiana per la Ricerca sul Cancro, Ministero dell'Istruzione, dell'Università e della Ricerca, PRIN Program 2007, and Regione Piemonte (Ricerca Sanitaria Finalizzata). F.C. is funded by Regione Piemonte (L.R. 4/2006 for brain drain containment, D.R. 392-2007). We thank Paola Chiarugi, Celine DerMardirossian, Louise Hodgson, Giorgio Scita, and Alex Toker for providing reagents.

1. Webb D-J, Parsons J-T, Horwitz A-F (2002) Adhesion assembly, disassembly and turnover in migrating cells: over and over and over again. *Nat Cell Biol* 4:97–100.
2. Del Pozo M-A, et al. (2002) Integrins regulate GTP-Rac localized effector interactions through dissociation of Rho-GDI. *Nat Cell Biol* 4:232–239.
3. Del Pozo M-A, Schwartz M-A (2007) Rac, membrane heterogeneity, caveolin and regulation of growth by integrins. *Trends Cell Biol* 17:246–250.
4. Nishimura T, Yamaguchi T, Kato K, Yoshizawa M, Nabeshima Y, Ohno S, Hoshino M, Kaibuchi K (2005) PAR-6-PAR-3 mediates Cdc42-induced Rac activation through the Rac GEFs STEF/Tiam1. *Nat Cell Biol* 7:270–27.
5. Carrasco S, Merida I (2006) Diacylglycerol, when simplicity becomes complex. *Trends Biochem Sci* 32:27–36.
6. Sakane F, Imai S, Kai M, Yasuda S, Kanoh H (2007) Diacylglycerol kinases: why so many of them? *Biochim. Biophys Acta* 1771:793–806.
7. Mérida I, Avila-Flores A, Merino E (2008) Diacylglycerol kinases: at the hub of cell signalling. *Biochem J* 409:1–18.
8. Cutrupi S, et al. (2000) Src-mediated activation of alpha-diacylglycerol kinase is required for hepatocyte growth factor-induced cell motility. *EMBO J* 19:4614–4622.
9. Baldanzi G, et al. (2004) Activation of diacylglycerol kinase alpha is required for VEGF-induced angiogenic signaling in vitro. *Oncogene* 23:4828–4838.
10. Bacchiocchi R, et al. (2005) Activation of alpha-diacylglycerol kinase is critical for the mitogenic properties of anaplastic lymphoma kinase. *Blood* 106:2175–2182.
11. Baldanzi G, et al. (2008) Diacylglycerol kinase-alpha phosphorylation by Src on Y335 is required for activation, membrane recruitment and HGF-induced cell motility. *Oncogene* 27:942–956.
12. Filigheddu N, et al. (2007) Diacylglycerol kinase is required for HGF-induced invasiveness and anchorage-independent growth of MDA-MB-231 breast cancer cells. *Anticancer Research* 27:1489–1492.
13. Chianale F, et al. (2007) Diacylglycerol kinase-alpha mediates hepatocyte growth factor-induced epithelial cell scatter by regulating Rac activation and membrane ruffling. *Mol Biol Cell* 18:4859–4871.
14. Royal I, Lamarche-Vane N, Lamorte L, Kaibuchi K, Park M (2000) Activation of cdc42, rac, PAK, and rho-kinase in response to hepatocyte growth factor differentially regulates epithelial cell colony spreading and dissociation. *Mol Biol Cell* 11:1709–1725.
15. Ridley A-J, Comoglio P-M, Hall A (1995) Regulation of scatter factor/hepatocyte growth factor responses by Ras, Rac, and Rho in MDCK cells. *Mol Cell Biol* 15:1110–1122.
16. Jiang Y, Sakane F, Kanoh H, Walsh JP (2000) Selectivity of the diacylglycerol kinase inhibitor 3-[2-(4-[bis-(4-fluorophenyl)methylene]-1-piperidinyl)ethyl]-2,3-dihydro-2-thioxo-4(1H)quinazolinone (R59949) among diacylglycerol kinase subtypes. *Biochem Pharmacol* 59:763–772.
17. Mistafa O, et al. (2007) Glucose regulates diacylglycerol intracellular levels and protein kinase C activity by modulating diacylglycerol kinase subcellular localization. *J Biol Chem* 282:31835–31843.
18. Moissoglu K, Slepchenko B-M, Meller N, Horwitz A-F, Schwartz M-A (2006) In vivo dynamics of Rac-membrane interactions. *Mol Biol Cell* 17:2770–2779.
19. Gandhi P-N, et al. (2004) An activating mutant of Rac1 that fails to interact with Rho GDP-dissociation inhibitor stimulates membrane ruffling in mammalian cells. *Biochem J* 378:409–419.
20. Limatola C, Schaap D, Moolenaar W-H, van Blitterswijk W-J (1994) Phosphatidic acid activation of protein kinase C-zeta overexpressed in COS cells: comparison with other protein kinase C isotypes and other acidic lipids. *Biochem J* 304:1001–1008.
21. Kurihayashi K, et al. (2007) Essential role of protein kinase C zeta in transducing a motility signal induced by superoxide and a chemotactic peptide, fMLP. *J Cell Biol* 176:1049–1060.
22. Henrique D, Schweisguth F (2003) Cell polarity: the ups and downs of the Par6/aPKC complex. *Curr Opin Genet Dev* 13:341–350.
23. Small J-V, Stradal T, Vignal E, Rottner K (2002) The lamellipodium: where motility begins. *Trends Cell Biol* 12:112–120.
24. Kurokawa K, Itoh R-E, Yoshizaki H, Nakamura Y-O, Matsuda M (2004) Coactivation of Rac1 and Cdc42 at lamellipodia and membrane ruffles induced by epidermal growth factor. *Mol Biol Cell* 15:1003–1010.
25. Frederick, et al. (2008) Matrix metalloproteinase-10 is a critical effector of protein kinase Ciota-Par6alpha-mediated lung cancer. *Oncogene* 27:4841–4853.
26. Kai M, et al. (2009) Diacylglycerol kinase alpha enhances protein kinase Czeta-dependent phosphorylation at Ser311 of p65/RelA subunit of nuclear factor-kappaB. *FEBS Lett* 583:3265–3268.
27. Etienne-Manneville S (2008) Polarity proteins in migration and invasion. *Oncogene* 27:6970–6980.
28. Krishnamurthy K, Wang G, Silva J, Condie B-G, Bieberich E (2007) Ceramide regulates atypical PKCzeta/lambda-mediated cell polarity in primitive ectoderm cells. A novel function of sphingolipids in morphogenesis. *J Biol Chem* 282:3379–3390.
29. DerMardirossian C, Schnelzer A, Bokoch G-M (2004) Phosphorylation of RhoGDI by Pak1 mediates dissociation of Rac GTPase. *Mol Cell* 15:117–127.
30. Abramovici H, et al. (2009) Diacylglycerol Kinase {eta} Regulates Actin Cytoskeleton Reorganization through Dissociation of Rac1 from RhoGDI. *Mol Biol Cell*, 10.1091/mbc.E07-12-1248.

SAP-Mediated Inhibition of Diacylglycerol Kinase α Regulates TCR-Induced Diacylglycerol Signaling

Gianluca Baldanzi,*,[1] Andrea Pighini,*[1] Valentina Bettio,* Elena Rainero,*,[2] Sara Traini,* Federica Chianale,* Paolo E. Porporato,*,[3] Nicoletta Filigheddu,* Riccardo Mesturini,[†] Shuping Song,[‡] Tamas Schweighoffer,[§] Laura Patrussi,[¶] Cosima T. Baldari,[¶] Xiao-Ping Zhong,[‖,#] Wim J. van Blitterswijk,** Fabiola Sinigaglia,* Kim E. Nichols,[††] Ignacio Rubio,[‡] Ornella Parolini,[‡‡] and Andrea Graziani*

Diacylglycerol kinases (DGKs) metabolize diacylglycerol to phosphatidic acid. In T lymphocytes, DGKα acts as a negative regulator of TCR signaling by decreasing diacylglycerol levels and inducing anergy. In this study, we show that upon costimulation of the TCR with CD28 or signaling lymphocyte activation molecule (SLAM), DGKα, but not DGKζ, exits from the nucleus and undergoes rapid negative regulation of its enzymatic activity. Inhibition of DGKα is dependent on the expression of SAP, an adaptor protein mutated in X-linked lymphoproliferative disease, which is essential for SLAM-mediated signaling and contributes to TCR/CD28-induced signaling and T cell activation. Accordingly, overexpression of SAP is sufficient to inhibit DGKα, whereas SAP mutants unable to bind either phospho-tyrosine residues or SH3 domain are ineffective. Moreover, phospholipase C activity and calcium, but not Src-family tyrosine kinases, are also required for negative regulation of DGKα. Finally, inhibition of DGKα in SAP-deficient cells partially rescues defective TCR/CD28 signaling, including Ras and ERK1/2 activation, protein kinase Cθ membrane recruitment, induction of NF-AT transcriptional activity, and IL-2 production. Thus SAP-mediated inhibition of DGKα sustains diacylglycerol signaling, thereby regulating T cell activation, and it may represent a novel pharmacological strategy for X-linked lymphoproliferative disease treatment. *The Journal of Immunology*, **2011, 187: 5941–5951.**

In T lymphocytes, engagement of the TCR by specific Ags, along with stimulation by costimulatory receptors such as CD28, leads to T cell activation, cytokine production, and differentiation. Moreover, several other receptors influence cell activation by quantitatively or qualitatively modifying immunoreceptor-derived signals. Conversely, stimulation via the TCR alone, although partially activating intracellular signaling pathways, is not sufficient to induce effector functions such as cytokine production and proliferation (1).

Signaling lymphocyte activation molecule (SLAM; CD150) is a homotypic transmembrane receptor expressed in T and B lymphocytes, dendritic cells, and monocytes (2). Upon engagement, SLAM undergoes a conformational change leading to Fyn-mediated tyrosine phosphorylation and activation of several signaling pathways that modulate TCR-induced responses (2). Fyn recruitment to the activated SLAM is mediated by SAP, an adaptor protein comprising a single SH2 domain and a SH3 domain-binding sequence (3). In humans, SAP loss-of-function mutations cause X-linked lymphoproliferative disease (XLP), an immune disorder characterized by a deregulated immune response to EBV, susceptibility to lymphoma and defective Ab production (4). Interestingly, SAP-deficient T lymphocytes from either XLP patients or SAP knockout mice exhibit defective responses to TCR/CD28 costimulation in vitro: 1) T cells from XLP patients feature reduced ERK1/2 and NF-κB activation, decreased IL-2 production, and impaired proliferation (5); 2) $CD4^+$ T cells from XLP patients exhibit reduced ICOS expression and IL-10 production (6); and 3) T cells from SAP knockout mice feature reduced protein kinase C (PKC)θ membrane recruitment, Bcl-10 phosphorylation, and NF-κB activation, which are associated with defective IL-4 secretion and enhanced INF-γ production (7).

Ag-mediated activation of the TCR in the presence of other co-activating molecules triggers a complex signaling network leading

*Department of Clinical and Experimental Medicine, University A. Avogadro of Piemonte Orientale, 28100 Novara, Italy; [†]Department of Medical Sciences, University A. Avogadro of Piemonte Orientale, 28100 Novara, Italy; [‡]Institute of Molecular Cell Biology, Center for Molecular Biomedicine, Friedrich Schiller University, D-07745 Jena, Germany; [§]Novartis Institutes for BioMedical Research, CH-4056 Basel, Switzerland; [¶]Department of Evolutionary Biology, University of Siena, 53100 Siena, Italy; [‖]Department of Pediatrics, Duke University Medical Center, Durham, NC 27710; [#]Department of Immunology, Duke University Medical Center, Durham, NC 27710; **Division of Cellular Biochemistry, The Netherlands Cancer Institute, 1066 CX Amsterdam, The Netherlands; [††]Division of Oncology, Children's Hospital of Philadelphia, Philadelphia, PA 19104; and [‡‡]Centro Di Ricerca E. Menni, Fondazione Poliambulanza-Istituto Ospedaliero, 25124 Brescia, Italy

[1]G.B. and A.P. contributed equally to this work.

[2]Current address: Beatson Institute for Cancer Research, Bearsden, Glasgow, United Kingdom.

[3]Current address: Unit of Pharmacology and Therapeutics, Catholic University of Louvain, Brussels, Belgium.

Received for publication July 22, 2010. Accepted for publication September 28, 2011.

This work was supported by Telethon Grant GGP10034 (to A.G.), Ricerca Sanitaria Finalizzata Regione Piemonte (to A.G.), Italian Ministry for University and Research Grants PRIN 2007 (to A.G.) and FIRB 2001 RBNE019J9W_003 (to O.P.), Grant XRT003 from the XLP Research Trust, and National Institutes of Health Grant R01HL089745 (to K.N.).

Address correspondence and reprint requests to Dr. Gianluca Baldanzi, Dipartimento di Medicina Clinica e Sperimentale, Università del Piemonte Orientale, Via Solaroli 17, 28100 Novara, Italy. E-mail address: baldanzi@med.unipmn.it

The online version of this article contains supplemental material.

Abbreviations used in this article: DAG, diacylglycerol; DGK, diacylglycerol kinase; LAT, linker for activation of T cells; PA, phosphatidic acid; PKC, protein kinase C; PLC, phospholipase C; RCF, relative centrifugal force; SAP, signaling lymphocyte activation molecule-associated protein; SFK, Src family tyrosine kinase; shRNA, short hairpin RNA; siRNA, small interfering RNA; SLAM, signaling lymphocyte activation molecule; TAC, anti–IL-2α receptor Ab; XLP, X-linked lymphoproliferative disease; YFP, yellow fluorescent protein.

www.jimmunol.org/cgi/doi/10.4049/jimmunol.1002476

to transcriptional activation of specific genes whose expression mediates T cell proliferation and differentiation. Activation of Ras and PKCθ triggers key signaling pathways, leading, among others, to the activation of NF-AT and NF-κB and contributing to transcription of the IL-2 gene (8, 9). In T cells, activation of Ras and PKCθ is dependent on the generation of diacylglycerol (DAG) through phospholipase C (PLC)-mediated hydrolysis of phosphatidylinositol-4,5-bis-phosphate. DAG recruits RasGRP, the RasGEF mainly responsible for TCR-induced Ras activation, and PKCθ to the plasma membrane (10, 11). Notably, engagement of TCR in the absence of costimulation results in a weak and transient activation of both Ras and PKCθ, which drives T cells into anergy, a hyporesponsive status characterized by the inability to produce IL-2 and proliferate (12, 13).

DAG generated upon T cell activation is rapidly metabolized by DAG kinases (DGKs), a multigenic family of enzymes responsible for phosphorylation of DAG to phosphatidic acid (PA). Consistently with the crucial role of DAG signaling in T cell activation, several pieces of evidence indicate that the DGKα and DGKζ isoforms, which are highly expressed in thymus and T cells, act as negative regulators of TCR signaling and immune cell function (14). Specifically, 1) genetic deletion of DGKα and DGKζ in T cells enhances TCR-induced activation of ERK1/2, resulting in defective induction of anergy (15, 16); 2) DGKα is strongly induced in anergic T cells (13); 3) overexpression of either DGKα or DGKζ impairs CD3/CD28-induced activation of Ras signaling (17–19); 4) pharmacological inhibition of DGKs reverses the inability of anergic cells to produce IL-2 in response to TCR stimulation (13); and 5) DGKα expression is downregulated within a few hours from T cell activation (19). Collectively, these data support the concept that second messengers signaling is highly dependent on the fine tuning of DAG synthesis and degradation rates. Although there is no evidence for regulation of DGKζ upon T cell activation, TCR/CD28 costimulation of T cells results in rapid and sustained recruitment of DGKα to the plasma membrane (19), an event mediated by both Lck-dependent phosphorylation of tyrosine 335 and calcium binding to the EF hand domain of DGKα (20, 21).

Based on the role of DGKα as a negative regulator of T cell responses, we investigated the hypothesis that, upon T cell stimulation, DGKα activity might undergo negative regulation. In this study, we show indeed that the enzymatic activity of DGKα is inhibited upon costimulation of TCR and CD28 through a SAP-mediated mechanism. Moreover, we found that, in SAP-deficient cells, defective TCR/CD28 signaling and T cell activation can be partially rescued by inhibition of DGKα.

Materials and Methods

Cell culture

Jurkat A3 cells (LGC Standards) and 293FT cells (Life Technologies) were cultured, respectively, in RPMI 1640 GlutaMAX medium or DMEM GlutaMAX high glucose (Life Technologies), supplemented with 10% FBS (Life Technologies) and antibiotic-antimycotic solution (Sigma-Aldrich) in humidified atmosphere with 5% CO_2. PBMCs (PBLs) were isolated by Lymphoprep gradient (Axis-Shield) of ACD (130 mM citric acid, 152 mM sodium citrate, and 112 mM glucose)-treated venous blood obtained from healthy volunteers after informed consent. Briefly, blood was layered onto Ficoll-Hypaque separating media and, after 20 min centrifugation at 300 relative centrifugal force (RCF), cells were collected, washed, and suspended in RPMI 1640 GlutaMAX medium supplemented with 10% heat-inactivated FBS and antibiotic-antimycotic solution. Monocytes were depleted by plastic adherence at 37°C for 1 h, and the remaining PBLs were maintained for 18 h in a humidified atmosphere with 5% CO_2 before further stimulation. BI-141 TTS-SAP cells were a gift of A. Veillette (Montréal, QC, Canada).

Jurkat/SAP-short hairpin RNA (shRNA) cells were obtained by infection of Jurkat cells with lentiviruses encoding SAP-specific shRNA in pLKO.1-Puro vector (clone ID TRCN00000 82712 RNAi Consortium through Sigma-Genosys), sequence: 5′-CCGGCACAAGGTACTACAGGGATAA-CTCGAGTTATCCCTGTAGTACCTTGTGTTTTTG-3′.

Jurkat/control-shRNA cells were obtained by infection with lentiviruses encoding a shRNA specific for murine DGKα in pLKO.1-Puro vector (clone ID TRCN00000 24825 RNAi Consortium through Sigma-Genosys), sequence: 5′-CCGGGAGCTAAGTAAGGTGGTATATCTCGAGATATAC-CACCTTACTTACTTAGCTCTTTTT-3′.

Lentivirus production and Jurkat infection were carried out according to the manufacturer's instructions. Infected Jurkat cells were selected for 14 d in puromycin (1 μg/ml) and used as a bulk population in all experiments.

Reagents

The Abs used recognize the following proteins: pan-Ras (Ab-4; Merck), H-Ras (F235; Cell Signaling Technology), linker for activation of T cells (LAT; Santa Cruz Biotechnology), anti–IL-2α receptor Ab (TAC; Abcam), CD3 agonist (OKT3; provided by U. Dianzani, Novara, Italy), CD28 agonist (ANC28.1/5D10; Ancell) (except for Fig. 4*D*, where anti-CD28 was from BD Pharmingen), SLAM agonistic Ab (A12; BioLegend), anti-DGKζ Abs (gift of M. Topham, Salt Lake City, UT), mixture of DGKα Abs used for immunoprecipitation (22), DGKα (C-20) and PKCθ (Santa Cruz Biotechnology) used for immunofluorescence, ERK1/2 and phospho-ERK1/2 from Cell Signaling Technology for Supplemental Fig. 2 and from Transduction Laboratories for Fig. 5*C*, SAP (FL-128; Upstate Biotechnology), α-tubulin (Sigma-Aldrich), secondary HRP-conjugated Abs (PerkinElmer), secondary FITC-conjugated Ab (Dako), and Alexa Fluor 546-phalloidin (Life Technologies). In all experiments involving stimulation with Abs, species-matched preimmune serum (Santa Cruz Biotechnology) was used for controls in equal amounts.

Inhibitors used were from Sigma-Aldrich: R59949, DGKs inhibitor; PP2, Src family inhibitor; U73122, PLC inhibitor; BAPTA-AM, cell-permeable calcium chelator; wortmannin, PI3Ks inhibitor; and IPA-3, PAK-specific inhibitor. BAPTA-AM was dissolved in water; others inhibitors were dissolved in DMSO. DMSO was always used in control samples at the same dilution as the inhibitor tested.

Expression vectors and transfections

GFP-SAP-wild type, GFP-SAP-R78A, and GFP-SAP-R55L were a gift of P. Schwartzberg (National Institutes of Health, Bethesda, MD). N-terminal yellow fluorescent protein (YFP)-DGKα was obtained by cloning DGKα in pYFP-N-DEST (Life Technologies) using the Gateway kit (Life Technologies) according to the manufacturer's instructions. pNF-AT-TA-luciferase reporter vector and pRL-TK normalization vector were from Clontech. Small interfering RNA (siRNA) and negative control siRNA were from Ambion/Life Technologies: DGKα siRNA (23) sense, 5′-GGUCA-GUGAUGUCCUAAAGTT-3′, antisense, 5′-CUUUAGGACAUCACUG-ACCTT-3′.

Transient transfections in Fig. 5*D* and 5*E* were performed using Lipofectamine 2000 reagent (Life Technologies) according to the manufacturer's instructions. Microporation of Jurkat cells for imaging experiments was performed according to the manufacturers' instructions with the Microporator MP-100 system from Digital Bio Technology (Fig. 2, Supplemental Fig. 3*B*) or with the Gene Pulser II from Bio-Rad (Fig. 5*B*).

Cell stimulation, preparation of cell lysates and homogenates, immunoprecipitation, Western blotting, and DGK assay

Cells (3×10^7/ml) were resuspended in RPMI 1640 and incubated for the indicated time with agonist Abs or control species-matched preimmune serum at 37°C. For immunoprecipitation, 3×10^7 cells were lysed in 1 ml lysis buffer A (25 mM HEPES [pH 8], 1% Nonidet P-40, 10% glycerol, 150 mM NaCl, 5 mM EDTA, 2 mM EGTA, 1 mM $ZnCl_2$, 50 mM ammonium molybdate, 10 mM NaF, 1 mM sodium orthovanadate, and protease inhibitor mixture from Sigma-Aldrich). An aliquot of cell lysate was retained for Western blot analysis, and the remainder was immunoprecipitated with a mixture of anti-DGKα Abs as previously described (24). Whole-cell homogenates were prepared by homogenizing 3×10^7 cells in 1 ml cold buffer B (buffer A without detergent) by 20 passages in a 23-gauge syringe. Protein concentration was determined by BCA (Pierce), and equal amounts of proteins were loaded in each lane. SDS-PAGE and Western blots were performed as described previously (25). Western blot results were acquired with a VersaDoc system and quantified using Quantity One software (Bio-Rad).

DGKα activity in cell homogenates (25 μl) and anti-DGKα immunoprecipitates were assayed by measuring initial velocities (5 min at 30°C) as previously described (24). Radioactive signals were detected and quantified by GS-250 Molecular Imager and Phosphor Analyst software (Bio-Rad).

Immunofluorescence

For immunofluorescence on fixed cells with Ab stimulation, cells were seeded on poly-L-lysine-coated glass coverslips (Marienfeld) in 24-well plates for 1 h and then stimulated with 10 μg/ml agonist Abs for 1 h in the presence or absence of the indicated inhibitors. Cells were then fixed with formaldehyde and stained as previously described (26). Confocal images were acquired with a Leica confocal microscope TSP2 (objective, ×63; numerical aperture, 1.32) and analyzed with LCS confocal software (Leica).

For the immunological synapse experiments, Raji cells (used as APCs) were incubated for 2 h with 10 μg/ml staphylococcal enterotoxin E. Raji cells were washed, mixed with Jurkat control-shRNA or Jurkat SAP-shRNA (1:1) for 15 min, and plated on polylysine-coated wells of diagnostic microscope slides (Erie Scientific). Cells were allowed to adhere for 15 min and then fixed in methanol at −20°C for 10 min. Samples were then washed for 5 min in PBS and incubated with anti-PKCθ Ab overnight at 4°C. After washing in PBS, samples were incubated for 1 h at room temperature with FITC-labeled anti-goat Ab. Images were taken using an Axio Imager Z1 microscope equipped with an HBO 50-W mercury lamp for epifluorescence and with an AxioCam HR cooled charge-coupled camera (Carl Zeiss).

For live cell imaging experiments, Jurkat A3 cells, Jurkat control-shRNA, and Jurkat SAP-shRNA were microporated and serum starved in RPMI 1640 plus 0.2% BSA plus 50 mM HEPES for 2 h. Cells were seeded on glass-bottom dishes coated with poly-L-lysine or with the agonistic Ab anti-CD3, anti-CD3 plus anti-SLAM, or anti-CD3 plus anti-CD28 at the final concentration of 10 μg/ml. Confocal images were acquired at the indicated times with a Zeiss LSM 510 inverted laser scanning microscope using a C-Apochromat ×63 water immersion objective lens (Carl Zeiss). Laser scanning microscope image files were processed using the Zeiss ZEN laser scanning microscope image browser software. When comparisons among images were to be made, the images were taken in identical conditions and equally manipulated using Adobe Photoshop 7.0 software (Adobe Systems).

Cell fractionation

Cells (3×10^7/ml) were resuspended in RPMI 1640 and incubated for the indicated time with agonist Abs or control species-matched preimmune serum at 37°C. Whole-cell homogenates were prepared by homogenizing 3×10^7 cells as described above and sonicating the homogenates for 1 min. Postnuclear and postmitochondrial fractions (obtained by 10 min centrifugation at 10,000 RCF) were further separated by ultracentrifugation (30 min at 10,0000 RCF). Supernatants (soluble cytoplasmic fraction) and pellets (insoluble membrane fraction) were collected and SDS-PAGE and Western blots were performed as described previously (25) using anti-DGKα and anti-LAT Abs.

Biochemical Ras activation assays

Recombinant GST-c-Raf-RBD protein was produced in *Escherichia coli* as described (27). Jurkat cells were serum deprived (2 h in RPMI 1640 supplemented with 0.2% fatty acid-free/endotoxin-low BSA and 50 mM HEPES [pH 7.5]). After stimulation, 1 ml cell suspension (10^7 cells) was lysed in 1 ml ice-cold lysis buffer (50 mM HEPES [pH 7.5], 140 mM NaCl, 5 mM $MgCl_2$, 1 mM DTT, 1% Nonidet-40, protease inhibitors) supplemented with 25 μg GST-RBD protein and 100 μM GDP to quench postlytic GTP-loading and GAP-dependent Ras-bound GTP hydrolysis, respectively. Cell extracts were cleared by centrifugation and GST-RBD/Ras-GTP complexes were collected on glutathione-Sepharose, washed once with lysis buffer, and processed for SDS-PAGE analysis.

Mammalian two hybrid system

A modified Clontech MatchMaker (BD Biosciences) mammalian two-third-hybrid assay was used. Full-length human SAP and its point-mutated variants were cloned into the pM series vectors as GAL4-binding domain fusions.

Either full-length DGKα or the N-terminal DGKα fragment was cloned into a pVP vector to direct expression of VP16-activation domain fusion proteins. These were cotransfected into subconfluent HEK293 cells with a GAL4-luciferase reporter plasmid and a pVAX-based expression plasmid containing full-length human FynT. Luciferase activity was measured after 24 h using a commercial kit (Promega).

NF-AT assay

Jurkat cells (4×10^6/ml) were cotransfected with pNF-AT-TA-luc and pRL-TK plasmids. After 48 h, cells were stimulated as indicated for 16 h. Luciferase was assayed with a Dual-Luciferase reporter assay system (Promega) according to the manufacturer's instructions and assessed using a Victor^3 V multilabel counter (PerkinElmer). NF-AT–driven firefly luciferase activity was normalized for the reference *Renilla* luciferase activity to take in account differences in transfection and expression efficiency, and all values were expressed as fold increase upon unstimulated controls.

IL-2 assay

Jurkat cells (1×10^5) were plated in 100 μl medium supplemented with 10% FBS and stimulated as indicated for 72 h. IL-2 released in the media was measured by ELISA (GE Healthcare).

Statistical analysis

The data were expressed as means ± SE. Statistical analysis was determined by a Student *t* test.

Results

Negative regulation of DGKα during T cell activation

Because DGKα negatively regulates T cell activation (17, 19), we set out to investigate whether it is regulated in the early phase of lymphocyte activation. To this purpose, we assayed the enzymatic activity and subcellular localization of DGKα upon activation of primary lymphocytes (PBLs) and Jurkat leukemic T cells. DGKα activity was measured in vitro in the presence of exogenous substrates in anti-DGKα immunoprecipitates obtained from either control or stimulated lymphocytes. Following 15 min costimulation of PBLs with agonistic anti-CD3 and anti-CD28 Abs, the enzymatic activity of DGKα was reduced by ~60% as compared with unstimulated cells (Fig. 1*A*), without any change in DGKα protein content (Fig. 1*A*, *lower right panel*). Stimulation of PBLs with anti-CD3 Ab alone did not significantly affect DGKα activity (data not shown). Because activation of SLAM family receptors was reported to enhance TCR signaling (28, 29), we investigated whether SLAM might regulate the enzymatic activity of DGKα. Indeed, 15 min costimulation of PBLs with anti-CD3 and anti-SLAM agonist Abs resulted in an even stronger inhibition of DGKα activity without affecting DGKα protein content (Fig. 1*A*). We then measured DGKα activity in anti-DGKα immunoprecipitates from Jurkat leukemia cells following costimulation with anti-CD3 and either anti-CD28 or anti-SLAM agonist Abs. Similar to the data on PBLs, DGKα enzymatic activity was strongly reduced upon 15 min costimulation via the TCR and either SLAM or CD28 and lasted for at least 1 h, without changes in DGKα protein content (Fig. 1*B*, 1*C*). Finally, to address the reported ambiguity of how anti-SLAM Abs may affect SLAM signaling, we used an alternative approach to induce SLAM signaling. We used a chimeric receptor featuring SLAM intracellular domain and the extracellular and transmembrane regions of the human IL-2 receptor α-chain coexpressed with SAP in BI-141 lymphocytes (30). Crosslinking of the chimeric receptor with TAC triggers SLAM signaling (30) and it was sufficient to induce a strong decrease of DGKα activity without changes in DGKα protein content (Fig. 1*D*). This result indicates that signals originating from the intracellular domain of SLAM lead to DGKα inhibition. Taken together, these observations indicate that upon costimulation of the TCR with either CD28 or SLAM, the enzymatic activity of DGKα undergoes a negative regulation, which likely contributes to the accumulation of DAG required for RasGRP-mediated activation of Ras and full T cell activation.

To verify whether this regulation was specific to DGKα, we first examined whether anti-CD3 costimulation with either anti-CD28 or anti-SLAM Abs regulated DGKζ, which, along with DGKα, is highly expressed in T cells. We observed that neither CD3/CD28 nor CD3/SLAM costimulation of T cells did affect the enzymatic activity of DGKζ in anti-DGKζ immunoprecipitates from either

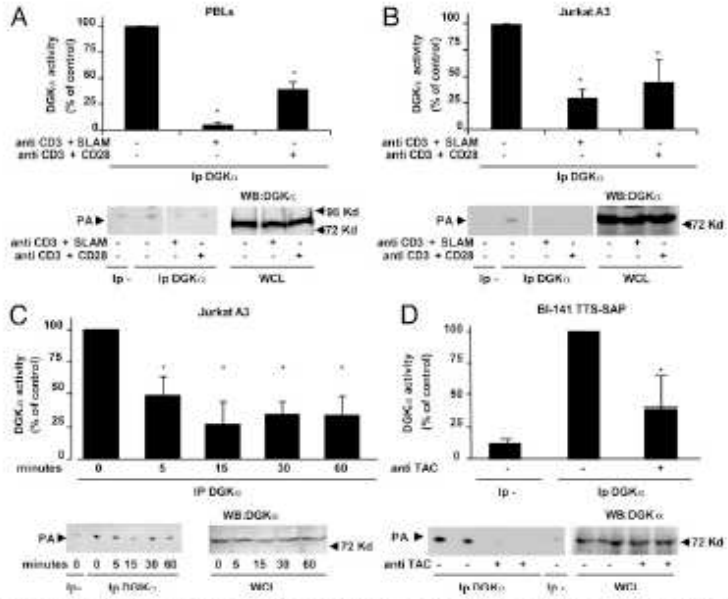

FIGURE 1. DGKα is inhibited upon T cell activation. PBLs (*A*) and Jurkat A3 cells (*B*) were stimulated for 15 min with 10 μg/ml indicated Abs and lysed. Anti-DGKα immunoprecipitates were assayed for DGK enzymatic activity while an aliquot of whole-cell lysate was analyzed by Western blot with anti-DGKα Ab to ensure equal loading. A representative experiment is shown (*lower panel*) together with a graph showing the mean ± SE of four independent experiments shown as percentage of control (*upper panel*). $^*p < 0.05$, *t* test versus control. *C*, Jurkat A3 cells were stimulated with 10 μg/ml anti-CD3 and anti-SLAM Abs and lysed at the indicated times. Anti-DGKα immunoprecipitates were assayed for DGK enzymatic activity while an aliquot of whole-cell lysate was analyzed by Western blot with anti-DGKα Ab to ensure equal loading. A representative experiment is shown (*lower panel*) together with a graph showing the mean ± SE of four independent experiments shown as percentage of control (*upper panel*). $^*p < 0.05$, *t* test versus control. *D*, BI-141 TTS-SAP cells were stimulated for 15 min with 5 mg/ml anti-TAC and 4 mg/ml anti-IgG and lysed. Anti-DGKα immunoprecipitates were assayed for DGK enzymatic activity while an aliquot of whole-cell lysate was analyzed by Western blot with anti-DGKα Ab to ensure equal loading. A representative experiment is shown (*lower panel*) together with a graph showing the mean ± SE of three independent experiments shown as percentage of control (*upper panel*). $^*p < 0.05$, *t* test versus control.

control or costimulated cells (Supplemental Fig. 1). These observations indicate that TCR activation specifically regulates DGKα enzymatic activity while not affecting DGKζ. To verify the contribution of DGKα regulation to the total cellular DGK activity, we measured DGK activity in whole-lymphocyte homogenates using exogenous substrates. Following 15 min TCR/CD28 costimulation of either PBLs or Jurkat cells, total DGK activity was not significantly affected, even when the costimulation was sufficient to activate ERK1/2 (Supplemental Fig. 2*A*, 2*B*). Conversely, upon 15 min TCR/SLAM costimulation, total DGK activity was significantly reduced (Supplemental Fig. 2*C*, 2*D*). Given the specific subcellular localization of DGK isoforms, these observations suggest that DGKα inhibition does not affect the bulk of DAG metabolism while selectively promoting DAG accumulation at specific compartments.

As DGKα recruitment from the cytoplasm to the plasma membrane is highly regulated both upon growth factor stimulation of epithelial cells and TCR/CD28-mediated costimulation of lymphocytes (20, 24), we assessed DGKα localization following costimulation of the TCR with either CD28 or SLAM. Both endogenous DGKα in $CD3^+$ PBLs and YFP-DGKα transiently expressed in Jurkat cells localize diffusely in the nucleus and in the cytoplasm of unstimulated or TCR-stimulated cells. Upon 1 h costimulation of the TCR with either CD28 or SLAM, DGKα was almost entirely excluded from the nucleus and recruited to the cell periphery in both PBLs and Jurkat cells (Fig. 2*A*, 2*B*, Supplemental Fig. 3*A*, 3*B*). Whereas inhibition of DGKα enzymatic activity was an early event, starting 5 min following costimulation, reaching maximal inhibition at 15 min, and lasting up to 1 h (Fig. 1*C*), translocation of DGKα became detectable 15 min after costimulation, reached its maximum at 30 min, and lasted for several hours (Fig. 2*B*).

To distinguish between plasma membrane and cytoplasmic localization, we labeled plasma membrane with either K-Ras-V12/A28 (31) or wheat germ agglutinin. Upon T cell costimulation, DGKα only partially colocalized with K-Ras-V12/A28 (Fig. 2*B*) or with wheat germ agglutinin (Supplemental Fig. 3*B*). Accordingly, ~10% of cytoplasmic DGKα sedimented in the 100,000 RCF fraction of CD3/CD28-costimulated Jurkat cells (Fig. 2*C*). These findings indicate that, upon lymphocyte activation, DGKα undergoes both negative regulation of its enzymatic activity and translocation from the nucleus to the cell periphery, although with different kinetics.

Regulation of DGKα inhibition and recruitment to the cell periphery

We explored whether translocation to the cell periphery and negative regulation of DGKα were regulated by common signaling pathways. DGKα activity and localization are regulated by Src-mediated tyrosine phosphorylation (21, 24, 25), calcium binding (17, 32), and D-3 phosphoinositides (33). Pharmacological inhibition of PLC by U73122 and calcium chelation by BAPTA-AM blunted DGKα translocation from the nucleus to the cell periphery induced by costimulation of TCR with either SLAM or CD28

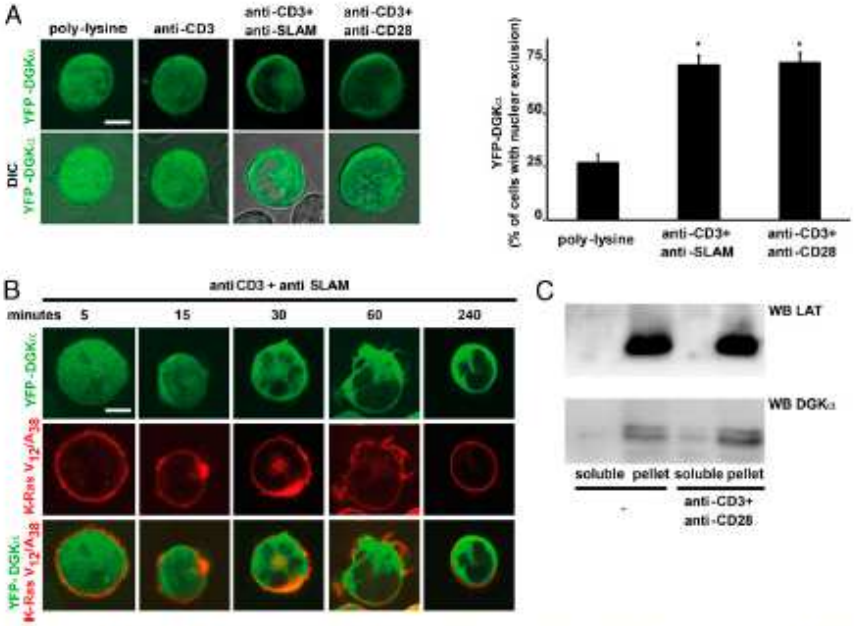

FIGURE 2. YFP-DGKα localization upon T cell stimulation. *A*, Jurkat A3 cells were transfected with YFP-DGKα (green) and after 24 h were serum starved for 2 h and seeded for 1 h on either poly-L-lysine, anti-CD3, anti-CD3 plus anti-SLAM, or anti-CD3 plus anti-CD28 (10 μg/ml each)-coated glass-bottom dishes and microscope images were acquired. Representative images are shown along with a quantification from three independent experiments. $^*p < 0.0005$, *t* test versus control. Scale bar, 5 μm. *B*, Jurkat A3 cells were transfected with YFP-DGKα (green) and DS-Red-K-Ras V12/A38 (red) and after 72 h were serum starved for 2 h and seeded on anti-CD3 plus anti-SLAM agonistic Ab (10 μg/ml each)-coated glass-bottom dishes and images were acquired at the indicated times. Representative images are shown. Scale bar, 5 μm. *C*, Jurkat A3 cells were stimulated with anti-CD3 and anti-CD28 agonistic Abs (10 μg/ml each) and homogenized 1 h later. The postnuclear and postmitochondrial fraction was separated by centrifugation (100,000 RCF) in a soluble fraction and in a membrane-associated fraction. One fiftieth of the soluble fraction and the entire membrane-associated fraction were analyzed by Western blotting for DGKα and LAT content.

(Fig. 3*A*). Interestingly, PP2-mediated inhibition of Src family tyrosine kinases (SFKs) inhibited only CD3/SLAM-induced translocation. Conversely, wortmannin did not affect DGKα localization, indicating that phosphoinositide 3-kinases are not involved (Fig. 3*A*). Similarly, pharmacological inhibition of PLC and calcium signaling prevented the negative regulation of DGKα activity induced by TCR/SLAM costimulation (Fig. 3*B*). These data indicate that PLC activity and calcium release mediate both inhibition of DGKα activity and its translocation to the cell periphery. Conversely, inhibition of SFKs impaired specifically negative regulation of DGKα activity and its translocation to the cell periphery induced by TCR/SLAM costimulation, but not by TCR/CD28 costimulation (Fig. 3*A*, 3*C*), indicating that the requirement of SFKs is restricted to SLAM-induced regulation of DGKα. Despite that SAP overexpression regulates cdc42, IPA-3–mediated inhibition of PAK, a cdc42 effector, does not affect DGKα activity (Fig. 3*B*).

Upon SLAM engagement, SAP mediates the recruitment of Fyn, thereby promoting tyrosine phosphorylation of SLAM and activation of its downstream signaling (34). Thus, we investigated the role of SAP in negative regulation and membrane recruitment of DGKα. SAP expression was downregulated in Jurkat cells by lentiviral-mediated stable expression of a SAP-specific shRNA (Fig. 4*A*, 4*B*). In SAP-deficient Jurkat cells, but not in control shRNA cells, DGKα activity was not inhibited following stimulation of TCR and SLAM (Fig. 4*A*), consistent with the essential role of SAP in SLAM-induced signaling. Surprisingly, in SAP-deficient cells, DGKα activity was not inhibited by TCR/CD28 costimulation. This observation suggests that SAP is not only required for SLAM signaling, but may also play a more direct role in promoting negative regulation of DGKα enzymatic activity (Fig. 4*B*). Indeed, overexpression of SAP and myc-DGKα in Jurkat cells resulted in the reduction of DGKα activity by 60% as measured in anti-myc immunoprecipitates, whereas myc-DGKα protein content was not affected (Fig. 4*C*). Conversely, in the same assay SAP mutants unable to bind either SH3 domains (SAP-R78A) or both tyrosine-phosphorylated proteins and SH3 domains (SAP-R55L) (3, 35) failed to inhibit DGKα (Fig. 4*C*). These findings indicate that SAP overexpression is sufficient to inhibit DGKα through a mechanism that requires SH3-binding ability of SAP.

The sequence surrounding tyrosine 335 of DGKα (SIY335PSV) features a high similarity to the SAP-SH_2 binding motif on SLAM (TIY281AQV) (36), suggesting that DGKα might bind directly to SAP. However, we could not detect a direct physical association between SAP and DGKα in a mammalian two-hybrid assay (Supplemental Fig. 4*A*) or in coimmunoprecipitation assays using transfected 293T cells (Supplemental Fig. 4*B*), even when the two proteins were coexpressed with SLAM and Fyn. Taken together, these results indicate that SAP does not inhibit DGKα by directly binding to it, but through the SAP-mediated recruitment of a yet unidentified SH3-containing protein.

The role of SAP in DGKα membrane recruitment in Jurkat cells was investigated by shRNA-mediated stable knockdown of SAP. SAP silencing selectively impaired the recruitment of DGKα to the cell periphery induced by TCR/SLAM costimulation, but not by TCR/CD28 costimulation (Fig. 4*D*). Similar results were obtained upon transient siRNA-mediated downregulation of SAP in Jurkat

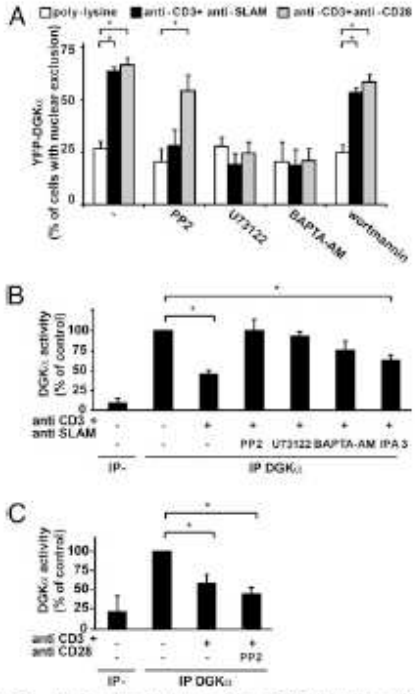

FIGURE 3. PLC and calcium mediate TCR-induced regulation of DGKα. *A*, Jurkat A3 cells were transfected with YFP-DGKα and after 24 h were serum starved for 2 h, seeded for 1 h on poly-L-lysine, CD3 plus SLAM, or CD3 plus CD28 agonistic Ab (10 μg/ml each)-coated glass-bottom dishes in the presence or absence of the indicated inhibitors (50 μM PP2, 5 μM U73122, 10 μM BAPTA-AM, or 100 nM wortmannin) and images were acquired. The quantification of three independent experiments is shown. $*p < 0.0005$, *t* test versus control. *B*, Jurkat A3 cells were treated with the indicated inhibitors (10 μM PP2, 5 μM U73122, 10 μM BAPTA-AM, 10 μM IPA-3) or vehicle for 30 min before stimulation with 10 μg/ml anti-CD3 and anti-SLAM Abs. After 15 min, cells were lysed and anti-DGKα immunoprecipitates were assayed for DGK enzymatic activity. The graph shows the mean ± SE of at least three independent experiments for each inhibitor. $*p < 0.05$, *t* test versus control. *C*, Jurkat A3 cells were treated with 10 μM PP2 or vehicle for 30 min before stimulation with 10 μg/ml anti-CD3 and anti-CD28 Abs. After 15 min, cells were lysed and anti-DGKα immunoprecipitates were assayed for DGK enzymatic activity. The graph shows the mean ± SE of at least three independent experiments. $*p < 0.05$, *t* test versus control.

cells (data not shown). Thus, following engagement of the TCR and SLAM, SAP is required for DGKα enzymatic inhibition and recruitment to the cell periphery. In contrast, whereas SAP is required for TCR/CD28-induced enzymatic inhibition of DGKα, it is not essential for translocation of DGKα to the cell periphery. These findings indicate that the localization and enzymatic activity of DGKα are regulated through distinct processes and kinetics, although the mechanisms involved are still partially unknown.

Inhibition of DGKα rescues the functional defects caused by SAP deficiency in XLP

Collectively, these data demonstrate that SAP is essential for regulation of DGKα activity upon T cell activation via the TCR/SLAM or TCR/CD28. We therefore reasoned that, similarly to SAP-deficient Jurkat cells, T cells of XLP patients lacking functional SAP might be defective in the negative regulation of DGKα, thereby contributing to the defective lymphocyte responses observed in both XLP patients and in SAP-null mice. To address this hypothesis, we first characterized the signaling capacity of SAP-deficient Jurkat cells following stimulation via the TCR and CD28. We then assessed whether pharmacological inhibition of DGKα by R59949, or its siRNA-mediated downregulation, might rescue those aberrant T cell responses.

DAG-dependent recruitment of PKCθ to the plasma membrane is defective in T cells from SAP-null mice, it is potentiated upon SAP overexpression (7, 37) and it is negatively regulated by constitutive activation of DGKα (38). Consistently, in SAP-deficient Jurkat cells, PKCθ recruitment to the immune synapse with super Ag-loaded APCs was impaired (Fig. 5*A*). Both pharmacological inhibition (Fig. 5*A*) and siRNA-mediated silencing of DGKα (Fig. 5*B*) nearly completely rescued the defective translocation of PKCθ to the immune synapse observed in SAP-deficient Jurkat cells, pointing to a rescue of DAG-mediated signaling.

Upon TCR/CD28 costimulation, both T cells from XLP patients and Jurkat cells made SAP-deficient by siRNA-mediated downregulation exhibit defective ERK1/2 activation (5, 39), suggesting that DAG-mediated Ras-GTP signaling is impaired. Indeed, upon TCR/CD28 costimulation, Jurkat SAP-shRNA cells showed both a decrease in ERK1/2 phosphorylation and a marked reduction of Ras-GTP loading, as measured by Ras-GTP pull-down with GST-RBD (Fig. 5*C*). Pharmacological inhibition of DGKα with R59949 fully restored both ERK1/2 phosphorylation and Ras-GTP loading (Fig. 5*C*). These findings confirm that SAP is required for Ras activation in human T cells and provide further support to the hypothesis that negative regulation of DGKα is a critical step in the activation of the Ras pathway downstream of TCR/CD28. Interestingly, R59949 raised basal levels of ERK1/2 phosphorylation without significantly affecting Ras-GTP loading, suggesting that under these conditions ERK1/2 phosphorylation may be enhanced through a Ras-independent mechanism, likely through DAG-dependent PKCθ activation (40).

Activation of PKCθ and Ras pathways upon TCR/CD28 costimulation triggers NF-AT transcriptional activity, which plays a central role in cytokine production (8, 41). Moreover, NF-AT is activated upon SAP overexpression in Jurkat cells (42). Consistently, SAP downregulation in Jurkat cells impaired TCR/CD28-induced stimulation of NF-AT activity, as measured by luciferase reporter system (Fig. 5*D*, 5*E*). In SAP-deficient cells, pharmacological inhibition of DGK with 1 μM R59949 fully restored TCR/CD28-induced activation of NF-AT without affecting basal NF-AT activity (Fig. 5*D*), whereas siRNA-mediated DGKα silencing resulted only in partial rescue (Fig. 5*E*). These data suggest either that DGKα along with other R59949-sensitive DGKs mediate NF-AT activation downstream from SAP or that the low quantity of DGKα remaining after RNA interference may still transduce the signaling.

Upon T cell stimulation, activation of Ras, PKCθ, and NF-AT signaling pathways leads to IL-2 production (41, 43, 44), which has been reported to be reduced in lymphocytes from XLP patients (5). Indeed, in Jurkat cells, shRNA-mediated SAP silencing reduced TCR/CD28-induced IL-2 secretion (Fig. 5*F*). Pharmacological inhibition of DGKα by R59949 enhanced TCR/CD28-induced IL-2 production in control cells and fully rescued the defective IL-2 secretion of SAP-deficient Jurkat cells. These findings suggest that SAP-mediated negative regulation of DGKα is a key event in the modulation of T cell activation.

Discussion

In this study, we demonstrate that within minutes following costimulation of the TCR with either CD28 or SLAM, the enzymatic activity of DGKα, as assayed in immunoprecipitates in the pres-

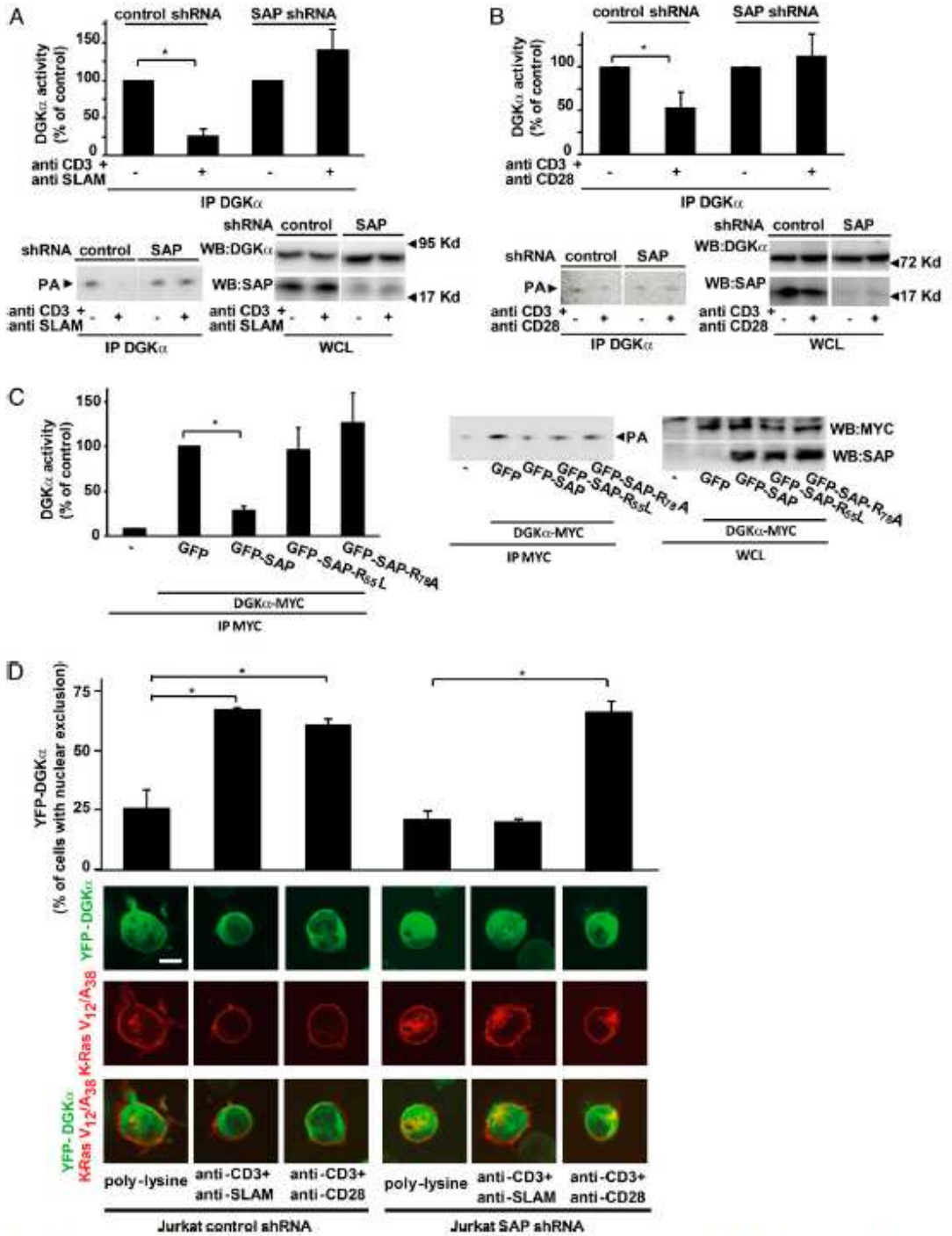

FIGURE 4. SAP negatively regulates DGKα activity. *A*, Jurkat control-shRNA or Jurkat SAP-shRNA cells were stimulated for 15 min with 10 μg/ml anti-CD3 and anti-SLAM Abs and lysed. Anti-DGKα immunoprecipitates were assayed for DGK enzymatic activity while an aliquot of whole-cell lysate was analyzed by Western blot with anti-DGKα Ab to ensure equal loading and with anti-SAP Ab to verify the downregulation of SAP expression. A representative experiment is shown together with a graph of the mean ± SE of three independent experiments shown as percentage of control. $^*p < 0.05$, *t* test versus control. *B*, Jurkat control-shRNA or Jurkat SAP-shRNA cells were stimulated for 15 min with 10 μg/ml anti-CD3 and *(Figure legend continues)*

ence of saturating DAG substrate concentration, undergoes a strong negative regulation without protein downregulation. This finding is surprising, given accumulating evidence that synthesis of PA is increased upon T cell stimulation (15, 16, 45) and that DGK activity is increased in whole-cell lysates from in vivo-activated T cells (19). However, increased PA synthesis through DAG phosphorylation may depend on both positive regulation of one or more DGK isoforms and on increased availability of DAG, whose production by PLCγ is increased upon TCR/CD28 co-stimulation (46). A parallel increase of DAG and PA levels upon TCR stimulation has been indeed observed (45, 47). Several pieces of evidence suggest that most of the PA generated upon T cell activation derives from phospholipase D2-mediated phospholipid hydrolysis and from DGKζ-mediated phosphorylation of DAG, whereas deletion of DGKα does not significantly affect PA production upon T cell stimulation (15, 16, 45). Nevertheless, recent genetic and biochemical data indicating that DGKα is a negative regulator of DAG-mediated TCR signaling (15, 17) are highly consistent with our finding that enzymatic activity of DGKα is reduced upon TCR costimulation with either CD28 or SLAM. This regulation appears to be isoform-specific, as DGKζ activity is unaffected by TCR triggering (Supplemental Fig. 1). Interestingly, the previous finding that stimulation of the sole TCR is not sufficient to promote sustained DAG signaling (48) is consistent with our observation that TCR activation in PBLs is not sufficient to inhibit DGKα activity in the absence of costimulation. Moreover, costimulation of TCR/CD28, compared with TCR alone, strongly enhances production of DAG but not of PA (15), suggesting a slowdown in the rate of DAG conversion to PA that is consistent with a negative regulation of DGK activity.

The molecular mechanisms underlying the negative regulation of DGKα have not yet been elucidated. In this study, we report that the adaptor function of SAP is required for DGKα inhibition induced by TCR costimulation with either SLAM or CD28. SAP is essential for SLAM tyrosine phosphorylation by recruiting the Src-related kinase FynT (3, 34); however, a growing body of evidence indicates that SAP is also involved in T cell responses to antigenic stimulation (2). Indeed, SAP binds directly to ITAM sequences of CD3ζ subunit (29), whereas TCR activation promotes the recruitment of SAP and SLAM family receptors to the signalosome (28, 29, 49). Furthermore, genetic deletion of SAP in mice results in the impairment of TCR/CD28-induced DAG-mediated activation of PKCθ and of downstream signaling events (7). Moreover, TCR/CD28-induced ERK1/2 activation and IL-2 production, which are both dependent on DAG-mediated activation of RasGRP, are impaired in T cells from SAP-deficient XLP patients (5). Intriguingly, SAP is physically associated to PKCθ, and it has been demonstrated that SAP overexpression, which is sufficient to inhibit DGKα, promotes PKCθ recruitment to the immune synapse (37). Finally, we and others have shown that, in Jurkat cells, SAP silencing impairs TCR-induced Ras-GTP loading, ERK1/2 activation, PKCθ recruitment, NF-AT activation, and IL-2 production (5–7). Taken together, these observations suggest that, upon TCR/CD28 costimulation, SAP is required for optimal DAG signaling. The finding that SAP is required for inhibition of DGKα might provide a mechanistic link between SAP and the regulation of DAG signaling. Thus, we propose that, upon stimulation of T cells from either SAP-deficient XLP patients or SAP-null mice, DGKα may inappropriately retain a high enzymatic activity, thereby converting DAG to PA and decreasing DAG signaling.

If this hypothesis holds true, we would expect that inhibition or downregulation of DGKα would rescue, at least partially, the defective signaling of SAP-deficient T cells. Accordingly, we observed that the inhibition of DGKα enzymatic activity in SAP-deficient Jurkat cells rescued defective DAG-dependent PKCθ membrane recruitment, Ras-GTP loading, ERK1/2 and NF-AT activation, and IL-2 production. These findings indicate that the excess of DGKα activity contributes to the defective signaling of SAP-deficient cells and, along with the demonstration that SAP overexpression inhibits DGKα, provide further support to the hypothesis that SAP negatively regulates DGKα. According to these findings, the negative regulation of DGKα activity represents a key event controlling the early phase of T cell activation by contributing to fine tuning of DAG levels required for appropriate signaling.

In this study, we observed that costimulation of the TCR with either SLAM or CD28 induces DGKα exit from the nucleus and accumulation in the cytoplasm with only partial localization at the plasma membrane. This finding appears to contrast previous studies reporting GFP-DGKα localization at the plasma membrane of CD3/CD28 costimulated Jurkat cells; however, according to the same authors, DGKα membrane translocation is rapid and transient and can be visualized in conditions that inhibit its relocalization to the cytoplasm (17, 21). Moreover, DGKα plasma membrane localization was clearly induced by stronger stimuli, such as the activation of ectopically overexpressed muscarinic receptor (20, 21, 50, 51) or Ag challenge in vivo (19). Further support to the hypothesis that enzymatic activity of DGKα regulates DAG level at the plasma membrane of T cells derives both from our finding that uncoupling of DGKα inhibition from TCR stimulation impairs PKCθ recruitment to the immune synapses (Fig. 5A) and from the observation that pharmacological inhibition of DGKα allows accumulation of DAG at the plasma membrane of T cells, thereby triggering activation of Ras signaling (52).

Interestingly, stimulation with either SLAM or TCR alone did not induce DGKα translocation from the nucleus, indicating that the concerted signaling via both receptors is required. Moreover, the finding that SAP, which is essential for SLAM tyrosine phosphorylation and signaling, is required for translocation induced exclusively by TCR/SLAM, but not by TCR/CD28, suggests that SAP may not directly regulate DGKα subcellular localization. Additionally, the fact that upon TCR/CD28 costimulation, SAP is required for inhibition of DGKα activity, but not

anti-CD28 Abs and lysed. Anti-DGKα immunoprecipitates were assayed for DGK enzymatic activity while an aliquot of whole-cell lysate was analyzed by Western blot with anti-DGKα Ab to ensure equal loading and with anti-SAP Ab to verify the downregulation of SAP expression. A representative experiment is shown together with a graph of the mean ± SE of three independent experiments shown as percentage of control. $*p < 0.05$, *t* test versus control. *C*, Jurkat A3 cells were transiently cotransfected with myc-DGKα and the indicated GFP-SAP mutants. After 48 h, cells were lysed and anti-myc immunoprecipitates were assayed for DGK enzymatic activity while an aliquot of whole-cell lysate was assayed by Western blot with anti-myc and anti-SAP Abs to verify transfection efficiency. A representative experiment is shown along with a graph showing the mean ± SE of three independent experiments shown as percentage of control. $*p < 0.05$, *t* test versus control. *D*, Jurkat control-shRNA and Jurkat SAP-shRNA cells were transfected with YFP-DGKα (green) and DS-Red-K-Ras V12/A38 (red). After 24 h, cells were serum starved for 2 h, seeded for 1 h on poly-L-lysine, anti-CD3 plus anti-SLAM, or anti-CD3 plus antiCD28 agonistic Ab (10 μg/ml each)-coated glass-bottom dishes, and images were acquired. Representative images are shown together with a quantification from three independent experiments. $*p < 0.05$, *t* test versus control. Scale bar, 5 μm.

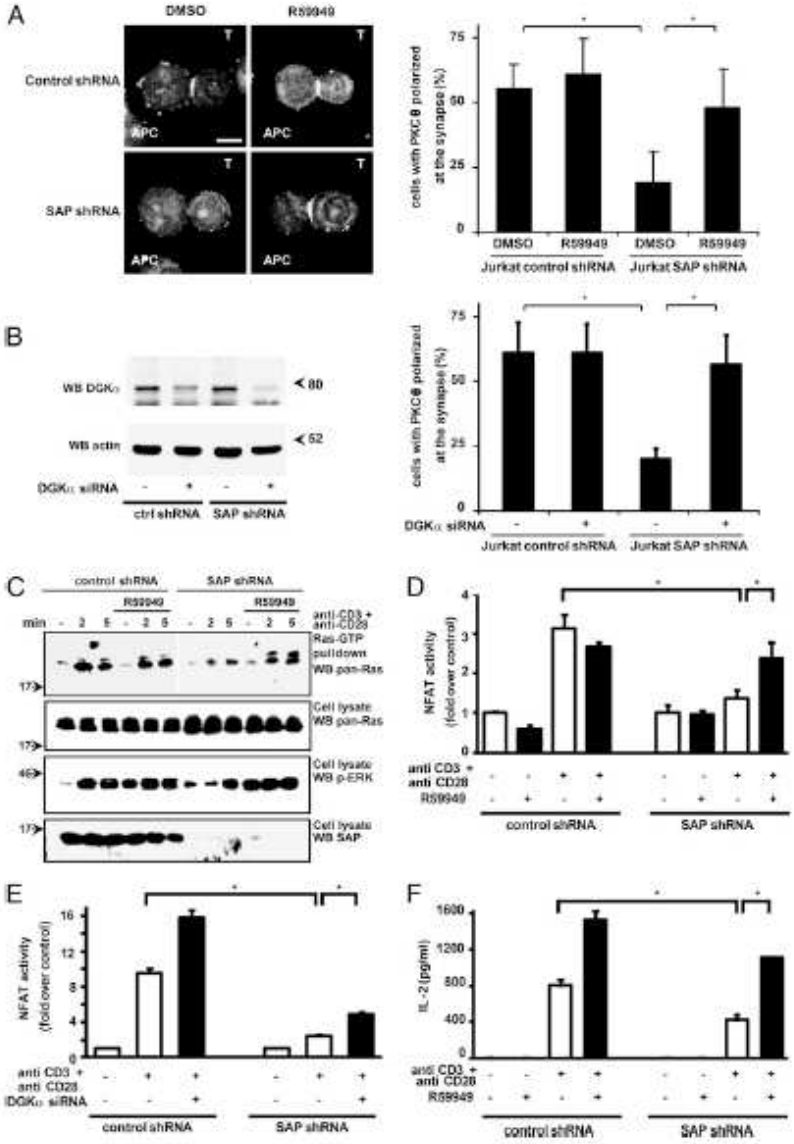

FIGURE 5. DGKα inhibition rescues defective TCR-induced DAG-dependent signaling and IL-2 production of SAP-deficient T lymphocytes. *A*, Jurkat control-shRNA and Jurkat SAP-shRNA cells (T) were pretreated with R59949 (10 μM 30) min) incubated with super Ag-loaded Raji cells (APCs) for 15 min, fixed, and stained for PKCθ. Representative images are shown. Scale bar, 5 μm. Cells displaying PKCθ at the immune synapse were counted. The histogram shows data from three independent experiments as mean ± SE (*$p < 0.05$, *t* test). *B*, Jurkat control-shRNA and Jurkat SAP-shRNA cells (T) were transfected with DGKα-specific siRNA or control siRNA. After 72 h, cells were lysed and analyzed by Western blot with anti-DGKα and anti-actin Abs (*left panel*). At the same time cells were incubated with super Ag-loaded Raji cells (APCs) for 15 min, fixed, and stained for PKCθ. Cells displaying PKCθ at the synapse were counted (*right panel*). The histogram shows data from three independent experiments as mean ± SE (*$p < 0.05$, *t* test). *C*, Control shRNA Jurkat or SAP shRNA Jurkat cells were stimulated with 1 μg/ml anti-CD3 and 0.1 μg/ml anti-CD28 Abs in the presence or in absence of 1 μM R59949. After 15 min, cells were lysed and Ras-GTP was separated by pull-down with Raf-RBD and quantified by Western blotting with anti pan-Ras Ab. Total Ras, phospho-ERK1/2, and SAP contents were revealed in whole-cell lysates by Western blotting. *D*, Jurkat control-shRNA and Jurkat SAP-shRNA cells were transfected with a Dual-Luciferase NF-AT reporter system. After 48 h, cells were stimulated with 1 μg/ml anti-CD3 and anti-CD28 Abs in the presence or absence of 1 mM R599-49. After 16 h stimulation, cells were lysed and analyzed for NF-AT–driven luciferase activity. Graph shows the mean ± SE of quadruplicates of a representative experiment. *$p < 0.05$, *t* test versus control. *E*, Jurkat control-shRNA or Jurkat SAP-shRNA cells were transfected with a siRNA targeting DGKα or a control siRNA and a Dual-Luciferase NF-AT reporter system. After 48 h, cells were stimulated with 1 μg/ml anti-CD3 and anti-CD28 Abs. After 16 h stimulation, cells were lysed and analyzed for NF-AT–driven luciferase activity. Graph shows the mean ± SE of quadruplicates of a representative experiment. *$p < 0.05$, *t* test versus control. *F*, Jurkat control-shRNA or Jurkat SAP-shRNA cells were stimulated with 1 μg/ml anti-CD3 and 0.1 μg/ml anti-CD28 Abs. After 72 h, cells were lysed and the amount of IL-2 released in the medium was measured by ELISA. Graph shows the mean ± SE of four replicates of a representative experiment. *$p < 0.05$, *t* test versus control.

for its exit from the nucleus, indicates that enzymatic activity and localization of DGKα are regulated independently of each other, as suggested also by the different kinetics of the two processes. Importantly, these findings also indicate that DGKα exit from the nucleus is not required for the inhibition of its enzymatic activity. The massive exit from the nucleus may reflect a potential increase in the availability of DGKα outside the nucleus for control of DAG signaling both at the plasma membrane and at intracellular vesicles. Indeed, several reports indicate a role of DGKs in T cells intracellular trafficking (50, 53, 54). Conversely, DGKα exit from the nucleus may contribute to regulate nuclear pools of DAG and PA. Indeed, several DGK isoforms have been reported to localize in the nucleus where they contribute to regulate transcription and cell cycle progression (55).

Previous evidence indicates that SFK-induced phosphorylation of DGKα on tyrosine 335 mediates its activation and membrane localization upon growth factor stimulation of epithelial and large cell lymphoma cells (24, 56). Moreover, in T cells DGKα phosphorylation by LCK on tyrosine 335 mediates CD3/CD28-induced recruitment of DGKα to the plasma membrane (21). Surprisingly, in our study pharmacological inhibition of SFKs did not affect either TCR/CD28-induced inhibition of DGKα or its exit from the nucleus, suggesting that both events are independent from SFK-mediated tyrosine phosphorylation of DGKα. Conversely, PP2 completely blocks DGKα inhibition and exit from the nucleus induced by CD3/SLAM, as SLAM signaling is dependent on Fyn tyrosine kinase.

The mechanism by which SAP regulates DGKα still remains to be elucidated. Based on the high similarity between the sequences surrounding tyrosine 335 of DGKα and tyrosine 281 of SLAM, we investigated the hypothesis that SAP may regulate DGKα by associating with it in a complex. However, we could not detect any direct or indirect physical interaction between the two proteins, even in a reconstituted association assay in a mammalian two-hybrid system. Our data demonstrate that SAP ability to inhibit DGKα requires the interaction with a yet unidentified SH3 domain-containing protein. The finding that inhibition of DGKα is independent of activity by SFKs suggests that the SAP interactor required for DGKα inhibition is not Fyn. The previous observation that SAP overexpression activates Cdc42 signaling by interacting with SH3-containing βPIX and independently of Fyn suggests that DGKα may be regulated by Cdc42-dependent PAK activation. However, the PAK-specific inhibitor IPA-3 did not affect the inhibition of DGKα following TCR/SLAM costimulation (Fig. 3*B*). Finally, upon TCR stimulation of Jurkat cells, SAP silencing results in defective tyrosine phosphorylation of several proteins, including LAT and SLP76 (39). As both LAT and SLP76 regulate PLCγ activation (57), it is possible to speculate that SAP regulates DGKα by controlling PLCγ activity. Consistent with this possibility, PLC activity and cytosolic-free calcium are both required for DGKα inhibition and membrane recruitment. However, lack of SAP in T cells of both SAP-null mice and XLP patients does not affect PLCγ-mediated intracellular calcium increase (5, 58). Moreover, cell stimulation with a calcium ionophore and phorbol ester failed to inhibit DGKα activity and to recruit it to the plasma membrane, indicating that activation of PLC is necessary but not sufficient to regulate both enzymatic activity and membrane localization (data not shown). Furthermore, the requirement for PLC activity in regulating DGKα suggests that the two enzymes may act as a bicomponent unit able to finely modulate the extent and the duration of DAG signaling.

In conclusion, our findings suggest that the coordinated, but independent, control of DGKα enzymatic activity and of its localization regulates both its access to DAG and its rate of conversion to PA. Upon T cell stimulation, such a coordinated and complementary mechanism of regulation might finely tune the intensity and the duration of DAG-mediated signaling. Indeed, SAP silencing, by uncoupling TCR/CD28 costimulation from DGKα inhibition, results in the impairment of TCR/CD28-induced DAG-mediated signaling, providing further evidence that the SAP-mediated negative regulation of DGKα is crucial for the ability of T cells to trigger DAG-mediated responses.

Similar to cAMP signaling, which is triggered by G protein-coupled receptors by reciprocal regulation of both adenylate cyclase and phosphodiesterase activities (59), the findings presented in this study suggest that TCR/CD28 controls DAG signaling both by means of PLCγ activation and DGKα inhibition. Similarly, genetic and biochemical studies in *Caenorhabditis elegans* motoneurons and murine hepatocytes showed that DAG-mediated signaling is controlled by G protein-coupled receptor-dependent reciprocal regulation of both PLC and DGKθ (60–62).

In summary, our findings demonstrate that SAP-mediated DGKα inhibition is an early event in TCR signaling, which might be required for efficient T cell activation. The impaired regulation of DGKα activity in SAP-deficient lymphocytes may contribute to their defective TCR-induced responses, suggesting that pharmacological inhibition of DGKα could be useful in the treatment of certain manifestations of XLP.

Acknowledgments

M.C. Zhong and A. Veillette (Montréal, QC, Canada) provided BI-141 cells expressing IL-2R/SLAM chimera and SAP. M. Topham provided anti-DGKζ Abs. P. Schwartzberg (National Institutes of Health, Bethesda, MD) provided GFP-SAP constructs.

Disclosures

The authors have no financial conflicts of interest.

References

1. Kinoczek, R. A., H. W. Mages, and A. Hutloff. 2004. Emerging paradigms of T-cell co-stimulation. *Curr. Opin. Immunol.* 16: 321–327.
2. Veillette, A. 2010. SLAM-family receptors: immune regulators with or without SAP-family adaptors. *Cold Spring Harb. Perspect. Biol.* 2: a002469.
3. Chen, R., S. Latour, X. Shi, and A. Veillette. 2006. Association between SAP and FynT: inducible SH3 domain-mediated interaction controlled by engagement of the SLAM receptor. *Mol. Cell. Biol.* 26: 5559–5568.
4. Rezaei, N., E. Mahmoudi, A. Aghamohammadi, R. Das, and K. E. Nichols. 2011. X-linked lymphoproliferative syndrome: a genetic condition typified by the triad of infection, immunodeficiency and lymphoma. *Br. J. Haematol.* 152: 13–30.
5. Sansone, S., M. Zeyda, M. D. Saemann, M. Soncini, W. Holter, G. Pritsch, W. Knapp, F. Candotti, T. M. Stulnig, and O. Parolini. 2008. SLAM-associated protein deficiency causes imbalanced early signal transduction and blocks downstream activation in T cells from X-linked lymphoproliferative disease patients. *J. Biol. Chem.* 278: 29593–29599.
6. Ma, C. S., N. J. Hare, K. E. Nichols, L. Dupré, G. Andolfi, M. G. Roncarolo, S. Adelstein, P. D. Hodgkin, and S. G. Tangye. 2005. Impaired humoral immunity in X-linked lymphoproliferative disease is associated with defective IL-10 production by CD4$^+$ T cells. *J. Clin. Invest.* 115: 1049–1059.
7. Cannons, J. L., L. J. Yu, B. Hill, L. A. Mijares, D. Dombroski, K. E. Nichols, A. Antonellis, G. A. Koretzky, K. Gardner, and P. L. Schwartzberg. 2004. SAP regulates T_H2 differentiation and PKC-θ-mediated activation of NF-κB1. *Immunity* 21: 693–706.
8. Baldari, C. T., A. Heguy, and J. L. Telford. 1993. ras protein activity is essential for T-cell antigen receptor signal transduction. *J. Biol. Chem.* 268: 2693–2698.
9. Woodrow, M. A., S. Rayter, J. Downward, and D. A. Cantrell. 1993. p21ras function is important for T cell antigen receptor and protein kinase C regulation of nuclear factor of activated T cells. *J. Immunol.* 150: 3853–3861.
10. Altman, A., and M. Villalba. 2003. Protein kinase C-θ (PKCθ): it's all about location, location, location. *Immunol. Rev.* 192: 53–63.
11. Ebinu, J. O., S. L. Stang, C. Teixeira, D. A. Bottorff, J. Hooton, P. M. Blumberg, M. Barry, R. C. Bleakley, H. L. Ostergaard, and J. C. Stone. 2000. RasGRP links T-cell receptor signaling to Ras. *Blood* 95: 3199–3203.
12. Asada, A., Y. Zhao, H. Komano, T. Kawata, M. Mukai, K. Fujita, Y. Tozawa, R. Iseki, H. Tian, K. Sato, et al. 2000. The calcium-independent protein kinase C participates in an early process of CD3/CD28-mediated induction of thymocyte apoptosis. *Immunology* 101: 309–315.

13. Zha, Y., R. Marks, A. W. Ho, A. C. Peterson, S. Janardhan, I. Brown, K. Praveen, S. Stang, J. C. Stone, and T. F. Gajewski. 2006. T cell anergy is reversed by active Ras and is regulated by diacylglycerol kinase-α. *Nat. Immunol.* 7: 1166–1173.
14. Wattenberg, B. W., and D. M. Raben. 2007. Diacylglycerol kinases: put the brakes on immune function. *Sci. STKE* 2007: pe43.
15. Olienchock, B. A., R. Guo, J. H. Carpenter, M. Jordan, M. K. Topham, G. A. Koretzky, and X. P. Zhong. 2006. Disruption of diacylglycerol metabolism impairs the induction of T cell anergy. *Nat. Immunol.* 7: 1174–1181.
16. Zhong, X. P., E. A. Hainey, B. A. Olienchock, M. S. Jordan, J. S. Maltzman, K. E. Nichols, H. Shen, and G. A. Koretzky. 2003. Enhanced T cell responses due to diacylglycerol kinase ζ deficiency. *Nat. Immunol.* 4: 882–890.
17. Sanjuán, M. A., D. R. Jones, M. Izquierdo, and I. Mérida. 2001. Role of diacylglycerol kinase α in the attenuation of receptor signaling. *J. Cell Biol.* 153: 207–220.
18. Zhong, X. P., E. A. Hainey, B. A. Olienchock, H. Zhao, M. K. Topham, and G. A. Koretzky. 2002. Regulation of T cell receptor-induced activation of the Ras-ERK pathway by diacylglycerol kinase ζ. *J. Biol. Chem.* 277: 31089–31098.
19. Sanjuán, M. A., B. Pradet-Balade, D. R. Jones, C. Martínez-A, J. C. Stone, J. A. García-Sanz, and I. Mérida. 2003. T cell activation in vivo targets diacylglycerol kinase α to the membrane: a novel mechanism for Ras attenuation. *J. Immunol.* 170: 2877–2883.
20. Merino, E., M. A. Sanjuán, I. Moraga, A. Cipres, and I. Mérida. 2007. Role of the diacylglycerol kinase α-conserved domains in membrane targeting in intact T cells. *J. Biol. Chem.* 282: 35396–35404.
21. Merino, E., A. Avila-Flores, Y. Shirai, I. Moraga, N. Saito, and I. Mérida. 2008. Lck-dependent tyrosine phosphorylation of diacylglycerol kinase α regulates its membrane association in T cells. *J. Immunol.* 180: 5805–5815.
22. Schaap, D., J. van der Wal, W. J. van Blitterswijk, R. L. van der Bend, and H. L. Ploegh. 1993. Diacylglycerol kinase is phosphorylated in vivo upon stimulation of the epidermal growth factor receptor and serine/threonine kinases, including protein kinase C-α. *Biochem. J.* 289: 875–881.
23. Baldanzi, G., S. Mitola, S. Cutrupi, N. Filigheddu, W. J. van Blitterswijk, F. Sinigaglia, F. Bussolino, and A. Graziani. 2004. Activation of diacylglycerol kinase α is required for VEGF-induced angiogenic signaling in vitro. *Oncogene* 23: 4828–4838.
24. Baldanzi, G., S. Cutrupi, F. Chiarle, V. Gnocchi, E. Rainero, P. Porporato, N. Filigheddu, W. J. van Blitterswijk, O. Parolini, F. Bussolino, et al. 2008. Diacylglycerol kinase-α phosphorylation by Src on Y335 is required for activation, membrane recruitment and Hgf-induced cell motility. *Oncogene* 27: 942–956.
25. Cutrupi, S., G. Baldanzi, D. Gnirnaglia, A. Maffè, D. Schaap, E. Giraudo, W. van Blitterswijk, F. Bussolino, P. M. Comoglio, and A. Graziani. 2000. Src-mediated activation of α-diacylglycerol kinase is required for hepatocyte growth factor-induced cell motility. *EMBO J.* 19: 4614–4622.
26. Chiarle, F., E. Rainero, C. Cianflone, V. Bertio, A. Pighini, P. E. Porporato, N. Filigheddu, G. Serini, F. Sinigaglia, G. Baldanzi, and A. Graziani. 2010. Diacylglycerol kinase α mediates HGF-induced Rac activation and membrane ruffling by regulating atypical PKC and RhoGDI. *Proc. Natl. Acad. Sci. USA* 107: 4182–4187.
27. Rubio, I., and R. Wetzker. 2000. A permissive function of phosphoinositide 3-kinase in ras activation mediated by inhibition of GTPase-activating proteins. *Curr. Biol.* 10: 1225–1228.
28. Howie, D., M. Simarro, J. Sayos, M. Guirado, J. Sancho, and C. Terhorst. 2002. Molecular dissection of the signaling and costimulatory functions of CD150 (SLAM): CD150/SAP binding and CD150-mediated costimulation. *Blood* 99: 957–965.
29. Bida, A. T., J. L. Upshaw Neff, C. J. Dick, R. A. Schoon, A. Brickshawana, C. C. Chini, and D. D. Billadeau. 2011. 2B4 utilizes ITAM-containing receptor complexes to initiate intracellular signaling and cytolysis. *Mol. Immunol.* 48: 1149–1159.
30. Latour, S., G. Gish, C. D. Helgason, R. K. Humphries, T. Pawson, and A. Veillette. 2001. Regulation of SLAM-mediated signal transduction by SAP, the X-linked lymphoproliferative gene product. *Nat. Immunol.* 2: 681–690.
31. Augsten, M., R. Pusch, C. Biskup, K. Rennert, U. Wittig, K. Beyer, A. Blume, R. Wetzker, K. Friedrich, and I. Rubio. 2006. Live-cell imaging of endogenous Ras-GTP illustrates predominant Ras activation at the plasma membrane. *EMBO Rep.* 7: 46–51.
32. Jiang, Y., W. Qian, J. W. Hawes, and J. P. Walsh. 2000. A domain with homology to neuronal calcium sensors is required for calcium-dependent activation of diacylglycerol kinase alpha. *J. Biol. Chem.* 275: 34092–34099.
33. Cipres, A., S. Carrasco, E. Merino, E. Díaz, U. M. Krishna, J. R. Falck, C. Martínez-A, and I. Mérida. 2003. Regulation of diacylglycerol kinase α by phosphoinositide 3-kinase lipid products. *J. Biol. Chem.* 278: 35629–35635.
34. Chan, B., A. Lanyi, H. K. Song, J. Griesbach, M. Simarro-Grande, F. Poy, D. Howie, J. Sumegi, C. Terhorst, and M. J. Eck. 2003. SAP couples Fyn to SLAM immune receptors. *Nat. Cell Biol.* 5: 155–160.
35. Li, C., C. Iosef, C. Y. Jia, T. Gkourmas, V. K. Han, and S. Shun-Cheng Li. 2003. Disease-causing SAP mutants are defective in ligand binding and protein folding. *Biochemistry* 42: 14885–14892.
36. Hwang, P. M., C. Li, M. Morra, J. Lillywhite, D. R. Muhandiram, F. Gertler, C. Terhorst, L. E. Kay, T. Pawson, J. D. Forman-Kay, and S. C. Li. 2002. A "three-pronged" binding mechanism for the SAP/SH2D1A SH2 domain: structural basis and relevance to the XLP syndrome. *EMBO J.* 21: 314–323.
37. Cannons, J. L., J. Z. Wu, J. Gomez-Rodriguez, J. Zhang, B. Dong, Y. Liu, S. Shaw, K. A. Siminovitch, and P. L. Schwartzberg. 2010. Biochemical and genetic evidence for a SAP-PKC-theta interaction contributing to IL-4 regulation. *J. Immunol.* 185: 2819–2827.
38. Carrasco, S., and I. Merida. 2004. Diacylglycerol-dependent binding recruits PKCθ and RasGRP1 C1 domains to specific subcellular localizations in living T lymphocytes. *Mol. Biol. Cell* 15: 2932–2942.
39. Li, C., D. Schibli, and S. S. Li. 2009. The XLP syndrome protein SAP interacts with SH3 proteins to regulate T cell signaling and proliferation. *Cell. Signal.* 21: 111–119.
40. Witte, V., B. Laffert, P. Gimtschel, E. Knuttkrämer, K. Blume, O. T. Fackler, and A. S. Baur. 2008. Induction of HIV transcription by Nef involves Lck activation and protein kinase Cθ raft recruitment leading to activation of ERK1/2 but not NFκB. *J. Immunol.* 181: 8425–8432.
41. Pfeifhofer, C., K. Kofler, T. Gruber, N. G. Tabrizi, C. Lutz, K. Maly, M. Leitges, and G. Baier. 2003. Protein kinase Cθ affects Ca^{2+} mobilization and NFAT cell activation in primary mouse T cells. *J. Exp. Med.* 197: 1525–1535.
42. Gu, C., S. G. Tangye, X. Sun, Y. Luo, Z. Lin, and J. Wu. 2006. The X-linked lymphoproliferative disease gene product SAP associates with PAK-interacting exchange factor and participates in T cell activation. *Proc. Natl. Acad. Sci. USA* 103: 14447–14452.
43. Baldari, C. T., G. Macchia, and J. L. Telford. 1992. Interleukin-2 promoter activation in T-cells expressing activated Ha-ras. *J. Biol. Chem.* 267: 4289–4291.
44. Altman, A., and M. Villalba. 2002. Protein kinase C-θ (PKCθ): a key enzyme in T cell life and death. *J. Biochem.* 132: 841–846.
45. Stewart, S. J., G. R. Cunningham, J. A. Strupp, F. S. House, L. L. Kelley, G. S. Henderson, I. H. Exton, and S. B. Bocclino. 1991. Activation of phospholipase D: a signaling system set in motion by perturbation of the T lymphocyte antigen receptor/CD3 complex. *Cell Regul.* 2: 841–850.
46. Bonvini, E., K. E. DeBell, M. C. Veri, L. Graham, B. Stoica, J. Laborda, M. J. Aman, A. DiBaldassarre, S. Miscia, and B. L. Rellahan. 2003. On the mechanism coupling phospholipase Cγ1 to the B- and T-cell antigen receptors. *Adv. Enzyme Regul.* 43: 245–269.
47. Tocchioni, M., C. Aussel, J. P. Breittmayer, S. Manié, C. Pelassy, and A. Bernard. 1993. Suppressive effect of T cell proliferation via the CD29 molecule: the CD29 mAb 1 "K20" decreases diacylglycerol and phosphatidic acid levels in activated T cells. *J. Immunol.* 151: 119–127.
48. Mor, A., G. Campi, G. Du, Y. Zheng, D. A. Foster, M. L. Dustin, and M. R. Philips. 2007. The lymphocyte function-associated antigen-1 receptor costimulates plasma membrane Ras via phospholipase D2. *Nat. Cell Biol.* 9: 713–719.
49. Snow, A. L., R. A. Marsh, S. M. Krummey, P. Roehrs, L. R. Young, K. Zhang, J. van Hoff, D. Dhar, K. E. Nichols, A. H. Filipovich, et al. 2009. Restimulation-induced apoptosis of T cells is impaired in patients with X-linked lymphoproliferative disease caused by SAP deficiency. *J. Clin. Invest.* 119: 2976–2989.
50. Alonso, R., C. Mazzeo, M. C. Rodriguez, M. Marsh, A. Fraile-Ramos, V. Calvo, A. Avila-Flores, I. Merida, and M. Izquierdo. 2011. Diacylglycerol kinase α regulates the formation and polarization of mature multivesicular bodies involved in the secretion of Fas ligand-containing exosomes in T lymphocytes. *Cell Death Differ.* 18: 1161–1173.
51. Alonso, R., M. C. Rodriguez, J. Pindado, E. Merino, I. Mérida, and M. Izquierdo. 2005. Diacylglycerol kinase α regulates the secretion of lethal exosomes bearing Fas ligand during activation-induced cell death of T lymphocytes. *J. Biol. Chem.* 280: 28439–28450.
52. Rubio, I., S. Gründ, S. P. Song, C. Biskup, S. Bandemer, M. Fricke, M. Förster, A. Graziani, U. Wittig, and S. Kliche. 2010. TCR-induced activation of Ras proceeds at the plasma membrane and requires palmitoylation of N-Ras. *J. Immunol.* 185: 3536–3543.
53. Alonso, R., C. Mazzeo, I. Mérida, and M. Izquierdo. 2007. A new role of diacylglycerol kinase α on the secretion of lethal exosomes bearing Fas ligand during activation-induced cell death of T lymphocytes. *Biochimie* 89: 213–221.
54. Rincón, E., T. Santos, A. Avila-Flores, J. P. Albar, V. Lalioti, C. Lei, W. Hong, and I. Mérida. 2007. Proteomics identification of sorting nexin 27 as a diacylglycerol kinase ζ-associated protein: new diacylglycerol kinase roles in endocytic recycling. *Mol. Cell. Proteomics* 6: 1073–1087.
55. Raben, D. M., and B. Tu-Sekine. 2008. Nuclear diacylglycerol kinases: regulation and roles. *Front. Biosci.* 13: 590–597.
56. Bacchiocchi, R., G. Baldanzi, D. Carbonari, C. Capomagi, E. Colombo, W. J. van Blitterswijk, A. Graziani, and F. Facchetti. 2005. Activation of α-diacylglycerol kinase is critical for the mitogenic properties of anaplastic lymphoma kinase. *Blood* 106: 2175–2182.
57. Wange, R. L. 2000. LAT, the linker for activation of T cells: a bridge between T cell-specific and general signaling pathways. *Sci. STKE* 2000: re1.
58. Cannons, J. L., L. J. Yu, D. Jankovic, S. Crotty, R. Horai, M. Kirby, S. Anderson, A. W. Cheever, A. Sher, and P. L. Schwartzberg. 2006. SAP regulates T cell-mediated help for humoral immunity by a mechanism distinct from cytokine regulation. *J. Exp. Med.* 203: 1551–1565.
59. Grady, E. F. 2007. Cell signaling: β-arrestin, a two-fisted terminator. *Science* 315: 605–606.
60. Baldanzi, G., E. Akbem, C. Imarisio, M. Gaggianesi, C. Dal Ponte, M. Nitti, C. Domenicotti, W. J. van Blitterswijk, E. Albano, A. Graziani, and R. Carini. 2010. Negative regulation of diacylglycerol kinase θ mediates adenosine-dependent hepatocyte preconditioning. *Cell Death Differ.* 17: 1059–1068.
61. McMullan, R., E. Hiley, P. Morrison, and S. J. Nurrish. 2006. Rho is a presynaptic activator of neurotransmitter release at pre-existing synapses in *C. elegans*. *Genes Dev.* 20: 65–76.
62. Nurrish, S., L. Ségalat, and J. M. Kaplan. 1999. Serotonin inhibition of synaptic transmission: $Go\alpha_0$ decreases the abundance of UNC-13 at release sites. *Neuron* 24: 231–242.

OPEN ACCESS Freely available online

PLOS ONE

The Diacylglycerol Kinase α/Atypical PKC/β1 Integrin Pathway in SDF-1α Mammary Carcinoma Invasiveness

Elena Rainero[1], Cristina Cianflone[2], Paolo Ettore Porporato[2¤b], Federica Chianale[2¤a], Valeria Malacarne[2], Valentina Bettio[2], Elisa Ruffo[2], Michele Ferrara[2], Fabio Benecchia[2], Daniela Capello[2], Wolfgang Paster[3], Irene Locatelli[2¤c], Alessandra Bertoni[2], Nicoletta Filigheddu[2], Fabiola Sinigaglia[2], Jim C. Norman[1], Gianluca Baldanzi[1]*, Andrea Graziani[1]

1 Integrin Biology Laboratory, Beatson Institute for Cancer Research, Glasgow, Scotland, United Kingdom, 2 Department of Translational Medicine, Università del Piemonte Orientale, Novara, Italy, 3 Sir William Dunn School of Pathology, University of Oxford, Oxford, United Kingdom

Abstract

Diacylglycerol kinase α (DGKα), by phosphorylating diacylglycerol into phosphatidic acid, provides a key signal driving cell migration and matrix invasion. We previously demonstrated that in epithelial cells activation of DGKα activity promotes cytoskeletal remodeling and matrix invasion by recruiting atypical PKC at ruffling sites and by promoting RCP-mediated recycling of α5β1 integrin to the tip of pseudopods. In here we investigate the signaling pathway by which DGKα mediates SDF-1α-induced matrix invasion of MDA-MB-231 invasive breast carcinoma cells. Indeed we showed that, following SDF-1α stimulation, DGKα is activated and localized at cell protrusion, thus promoting their elongation and mediating SDF-1α induced MMP-9 metalloproteinase secretion and matrix invasion. Phosphatidic acid generated by DGKα promotes localization at cell protrusions of atypical PKCs which play an essential role downstream of DGKα by promoting Rac-mediated protrusion elongation and localized recruitment of β1 integrin and MMP-9. We finally demonstrate that activation of DGKα, atypical PKCs signaling and β1 integrin are all essential for MDA-MB-231 invasiveness. These data indicates the existence of a SDF-1α induced DGKα - atypical PKC - β1 integrin signaling pathway, which is essential for matrix invasion of carcinoma cells.

Citation: Rainero E, Cianflone C, Porporato PE, Chianale F, Malacarne V, et al. (2014) The Diacylglycerol Kinase α/Atypical PKC/β1 Integrin Pathway in SDF-1α Mammary Carcinoma Invasiveness. PLoS ONE 9(6): e97144. doi:10.1371/journal.pone.0097144

Editor: Donald Gullberg, University of Bergen, Norway

Received November 27, 2013; **Accepted** April 15, 2014; **Published** June 2, 2014

Funding: This work was supported by: AIRC, Italian Association for Cancer Research, (IG 13524 and IG 5392 grants) www.airc.it, and CARIPLO Foundation (2010-0737 grant) www.fondazionecariplo.it. CC was supported by a mobility grant of CIB, Consorzio Interuniversitario Biotecnologie www.cibiotech.it. GB was supported by EMBO (short term fellowships) www.embo.org and University Piemonte Orientale (Young Investigators) www.unipmn.it. VM was supported by Compagnia di San Paolo www.compagniadisanpaolo.it/. DC was supported by Fondo Di Solidarieta' Edo Tempia Valenta Per Lotta Contro I Tumori www.fondoedotempia.it. The funders had no role in study design, data collection and analysis, decision to publish, or preparation of the manuscript.

Competing Interests: The authors have declared that no competing interests exist.

* E-mail: gianluca.baldanzi@med.unipmn.it

¤a Current address: Physical Biology of the Cancer Cell, IRCC Institute for Cancer Research and Treatment, Candiolo, Turin, Italy
¤b Current address: Unit of Pharmacology & Therapeutics, Angiogenesis and Cancer Research Group, University of Louvain Medical School, Brussels, Belgium
¤c Current address: Department of Health Sciences, Università del Piemonte Orientale, Novara, Italy

Introduction

Most cancer-associated mortality is caused by metastatic dissemination of primary tumors and the outgrowth of secondary tumors at distant sites. Among the microenvironment signals sustaining the invasive phenotype of cancer cells, stromal cell-derived factor-1α (SDF-1α, also named CXCL12), plays a major role in promoting cancer metastasis in several cancers, including breast cancer [1]. SDF-1α is a chemokine secreted by tumor-associated fibroblasts and bone marrow stromal cells, which through activation of its CXCR4 receptor, promotes migration and invasion of malignant cells and their homing to target organs [2,3]. Indeed CXCR4 is a poor prognosis predictor in several cancer types [4].

In breast cancer, the chemotactic and invasive activity of SDF-1α/CXCR4 is mediated by both $G\alpha_{i2}$-mediated activation of RhoA and Gαi-mediated activation of Rac1 via DOCK180/ELMO, which regulate cytoskeletal remodeling [5,6]. In myeloid cells, Rac1 mediates SDF-1α-induced increase of integrin affinity, while RhoA mediates formation of membrane protrusions and CXCR4 trafficking to the cell surface in Rab11+ endosomes [7,8]. Moreover, in gastric cancer cells SDF-1α invasive and proliferative activity is also stimulated by Gαi- and PI3Kβ-mediated activation of mTOR complex 1, which contributes to Rac1 activation as well [9]. Finally, atypical protein kinases C (PKCζ and ι, hereafter aPKCs), which do not bind diacylglycerol (DG), play a key role in mediating chemotaxis of bone marrow and muscle stem cells, and of lymphocytes [10,11]. However neither the mechanisms by which SDF-1α stimulates aPKCs nor their role in SDF-1α invasive signaling in breast cancer cells have been elucidated.

DGKs are a multigenic family of ten enzymes phosphorylating DG to generate phosphatidic acid (PA), thus reciprocally regulating in a highly compartmentalized manner the concentration of both lipid second messengers and their signaling activities [12]. Indeed, activation of DGKs results in the termination of DG-mediated signals, while triggering PA-mediated ones. Increasing evidence points to DGKα as a critical node in oncogenic signaling

and as a putative novel therapeutic target in cancer: inhibition or silencing of DGKα has been shown to reduce tumor growth and mortality in glioblastoma and hepatic carcinoma xenograft models [13,14]. Moreover, we recently showed that DGKα activity sustains the pro-invasive activity of metastatic p53 mutations, by promoting the recycling of α5β1 integrin to the tip of invasive protrusions in tridimensional matrix [15]. DGKα is activated and recruited to the membrane by growth factors, estrogen and tyrosine kinase oncogenes through Src-mediated phosphorylation. Upon growth factor stimulation, activation of DGKα mediates cell migration, invasion and anchorage-independent growth [16–21]. Indeed, activation of DGKα is a central element of a novel lipid signaling pathway involving PA-mediated recruitment at the plasma membrane and activation of aPKCs in a complex with RhoGDI and Rac1, thus providing a positional signal regulating Rac1 activation and association to the membrane [22,23].

Altogether these data suggest that DGKα and aPKCs may act as signaling nodes in the molecular crosstalk between soluble chemotactic factors and the extracellular matrix, thus prompting us to investigate the involvement of DGKα in cell migration and invasion induced by SDF-1α in breast cancer cells. In here we show that upon SDF-1α stimulation of breast cancer cells, DGKα activity mediates aPKCs localization at protrusion sites and the subsequent recruitment of β1 integrin and MMP-9 secretion. Conversely over-expression of DGKα is sufficient to induce aPKCs-dependent cell elongation. Finally, we observed that the DGKα – aPKCs – β1 integrin pathway is an essential mediator of chemokine-promoted cell migration and matrix invasion.

Materials and Methods

Cells Culture and Reagents

MDA-MB-231 cells were from ATCC, 293FT were from Life Technologies. Cells were cultured in DMEM (Life Technologies) with 10% FCS (LONZA) and antibiotics/antimycotics (Sigma-Aldrich) in humidified atmosphere 5% CO_2 at 37°C.

R59949 (Sigma-Aldrich) was dissolved in DMSO; equal amounts of DMSO were used in the control samples. All reagents are from Sigma-Aldrich apart: matrigel growth factor reduced (BD Biosciences), human recombinant SDF-1α and HGF (Peprotech), Myr-PKCζ/ι peptide inhibitor (BIOMOL) and NSC23766 (Tokris bioscience).

Antibodies: myc (clone 9E10 Santa Cruz), MMP-9 (2C3 Santa Cruz for western blotting and immunofluorescence or IC9111F RDsystems); PKCζ/ι (P0713 Sigma); β1 integrin (cat. 610467 BD Transduction Laboratories for western blotting and immunofluorescence or BV7 Abcam for cytofluorimetry); StrepMab-tag II (2-1507-001 IBA); actin (C-2 Santa Cruz); tubulin (DM1A Sigma-Aldrich); DGKα (Shaap et al., 1993), human RCP (rabbit in-house Ab raised against RCP residues 379–649); Cdc42 (2462 Cell signaling). Secondary antibodies HRP-mouse and HRP-rabbit were from Perkin Elmer. Secondary antibodies anti-rabbit Ig Alexa Flour-488 and anti-mouse Ig Alexa Flour-488 were from Life Technologies as well as Alexa Flour 546-phalloidin, TO-PRO-3 is from Life Technologies.

Invasion Assay

Invasion assay were performed in BD BioCoat Matrigel Chambers. 50,000 cells/well were plated in the upper chamber whereas SDF-1α (100 ng/ml) or 10% FCS were added to the lower chamber in serum free medium. After 22 hours of incubation in a humidified atmosphere 5% CO_2 at 37°C, non invading cells were removed from the upper surface of the membrane and invading cells were fixed and stained with Diff-Quik (Medion Diagnostic) before counting.

Wound Healing Assay

Cells were grown to confluence in 12 wells plates and the monolayer wounded with a pipet tip. Cell debris were removed and monolayer maintained in serum free medium for 24 hours with or without HGF (50 ng/ml). The cells were stained with Diff-Quik (Medion Diagnostic) and for each experimental point 8 fields photographed (Axiovert inverted microscope with a 4x objective and a digital camera). Cells migrating inside 2.3 mm of wound were counted.

DGKα Activation Assay

Cells homogenates were prepared by collecting the cells with a rubber scraper in buffer B (25 mM Hepes (pH 8), 10% glycerol, 150 mM NaCl, 5 mM EDTA, 2 mM EGTA, 1 mM $ZnCl_2$, 50 mM ammonium molibdate, 10 mM NaF, 1 mM sodium orthovanadate and Protease Inhibitor Cocktail), homogenizing them with a 23 G syringe and by spinning at 500 g for 15 min. Protein concentration was determined by the bicinchoninic acid method (Pierce) and equalized for each point with buffer.

DGKα activity in cell homogenates (25 µl) was assayed by measuring initial velocities (5 min at 30°C) in presence of saturating substrates concentration (1 mg/ml diolein, 5 mM ATP, 3 µCi/ml γ^{32}P-ATP (Perkin Elmer), 10 mM $MgCl_2$, 1 mM $ZnCl_2$, 1 mM EGTA in 25 mM Hepes pH 8, final reaction volume 50 ml). Reaction was terminated with 0.1 M HCl and lipids were extracted with cloroform methanol (1:1). PA was separated by TLC in chloroform:methanol:water:25% ammonium hydroxide (60:47:11:4). ^{32}P-PA was identified by co-migration with PA standards stained by incubation in iodine chamber. Radioactive signals were detected and quantified by Molecular Imager (Bio-Rad).

Immunofluorescence

Cells (30,000/well) were plated on matrigel coated coverlips in 24 wells cell culture plate and serum deprived for 16–24 hours before stimulation. After stimulation cells were washed with PBS, fixed in PBS containing 3% paraformaldehyde and 4% sucrose and permeabilized in cold Hepes-Triton buffer (20 mM Hepes, 300 mM sucrose, 50 mM NaCl, 3 mM $MgCl_2$, 0.5% Triton X-100, pH 7.4). PBS containing 2% BSA was used as blocking reagent for 15 minutes and as diluting agent for primary and secondary antibodies (incubated for at least 1 hour). Intermediate washing was performed with PBS containing 0.2% BSA.

Antibodies were added directly onto each glass coverslip in a humidified chamber. Finally, each glass coverslip was washed briefly in water and mounted onto a glass microscope slide using Mowiol (20% Mowiol 4–88, 2.5% 1, 4-diazabicyclo [2.2.2] octane in PBS, pH 7.4).

Confocal images were acquired with Leica confocal microscope TCS SP2 using a 63x objective, NA = 1.32, equipped with LCS Leica confocal software. Basal planes are shown. Each experimental point was performed in duplicate. Depending on preparation quality in each replicate roughly 30 images were taken, containing between 70 and 100 cells.

Morphometry

For cell length analysis cells were plated in 24 wells plates and phase contrast images of live cell were acquired with an Axiovert inverted microscope equipped with a 40x objective and a digital camera (Carl-Zeiss) and total cell length was measured with

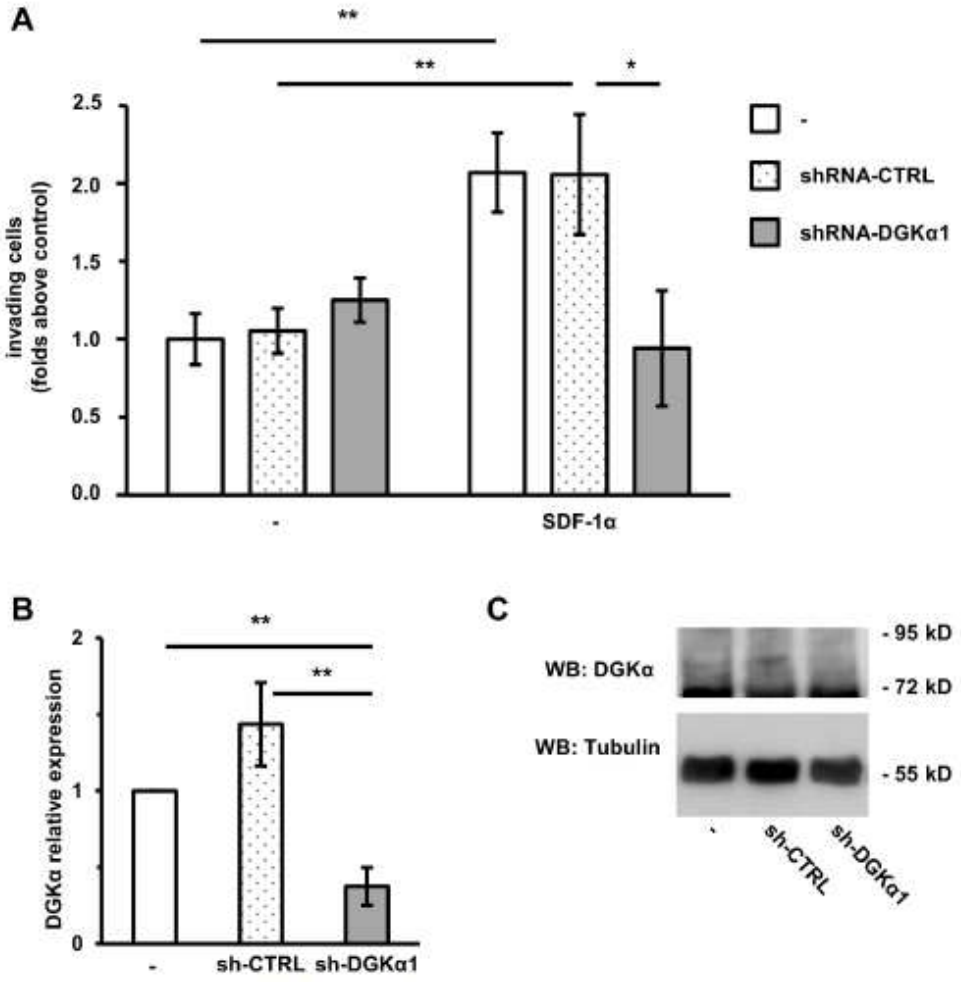

Figure 1. DGKα is necessary for SDF-1α-induced cell invasion. MDA-MB-231 cells were infected with lentiviral vectors expressing an inducible shRNA against DGKα (shRNA-DGKα1) or an inducible control shRNA (shRNA-CTRL). Parental and infected cells were treated with 1 μg/ml doxycycline for 72 hours to promote shRNA transcription. A) 50,000 cells were plated on matrigel invasion chamber and incubated for 24 hours in presence or in absence of SDF-1α (100 ng/ml). Histogram reports mean ± SE of fold over control values from 3 independent experiments with *t-test $p<0.05$, **t-test $p<0.01$. B) The efficiency of DGKα down-regulation by shRNA was verified by quantitative RT-PCR. **t-test $p<0.01$. A) Cells were lysed and the efficiency of DGKα down-regulation by shRNA was verified by western blot, tubulin was used as a loading control.
doi:10.1371/journal.pone.0097144.g001

Image-Pro Plus software (MediaCybernetics). Alternatively in Fig. 6D and Fig. S5B we used a 10x Plan Fluor objective, NA 0.3, and an inverted microscope (TE200; Nikon) with a digital camera (CoolSNAP HQ; Photometrics) and Metamorph software (Molecular Devices). For each experimental condition 5 random fields were photographed containing more than 100 cells.

Cytofluorimetry

Cells were detached with ice could PBS 4 mM EDTA, fixed with PBS containing 3% paraformaldehyde and stained as indicated for 30 min. After washing with PBS containing 0.2% BSA cells were analyzed with a FACScalibur instrument an CellQuest software (BD) or Flowing software (Turku Bioimaging).

siRNA for Transient Silencing

Transient silencing was obtained by transfection of siRNA (Sigma Genosys or Life Technologies). Briefly were plated on matrigel coated coverlips to 30–50% confluence the day before transfection and transfected using lipofectamine 2000 (Life Technologies) according to manufacturer's instructions. The day after transfection cells were serum deprived for further 18 hours before immunofluorescences or western blotting.

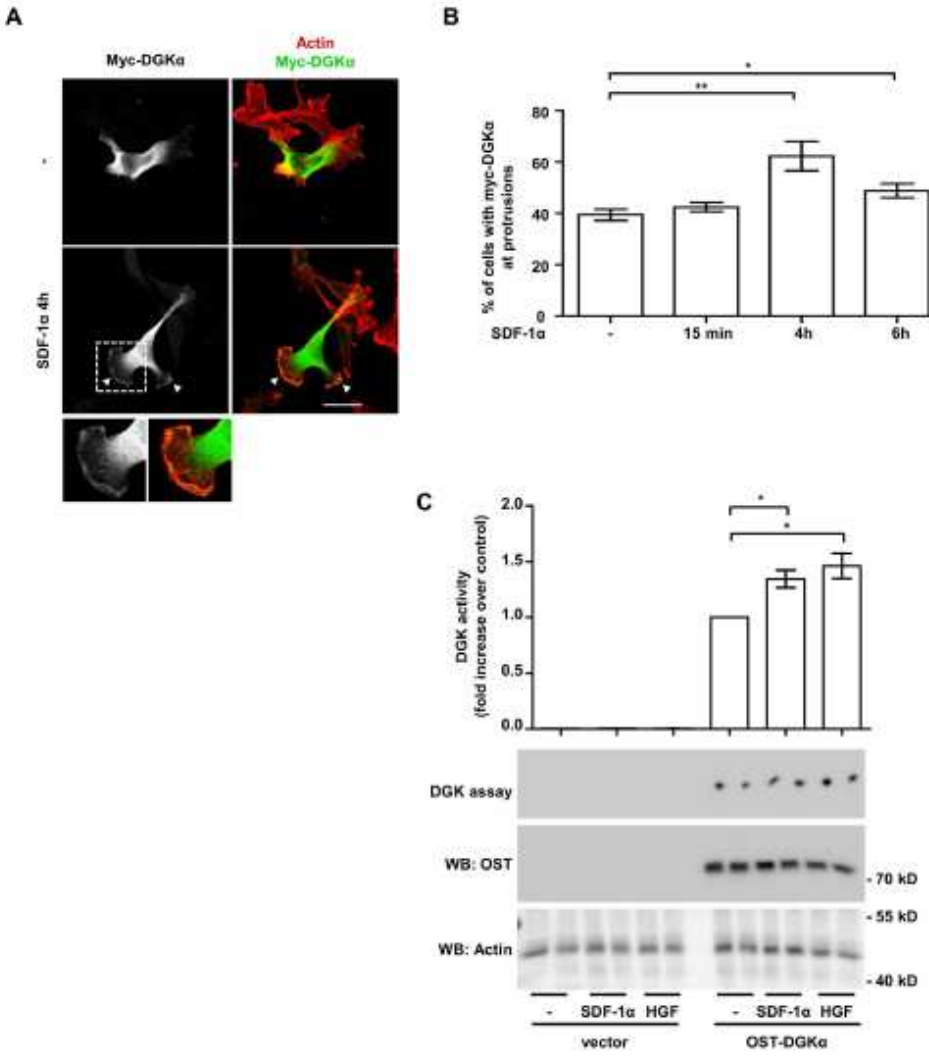

Figure 2. SDF-1α stimulates DGKα activity and localization at protrusions site. A) MDA-MB-231 cells, stably expressing myc-DGKα, were plated on matrigel-coated coverslips for 20 hours in FCS containing medium and cultured for further 20 hours in serum free medium. Cells were then stimulated with 50 ng/ml of SDF-1α for the indicated times, fixed and stained for actin (red) and myc-DGKα (green). Representative images at 4 hours after stimulation. Arrowheads indicate DGKα at protrusions. Histogram (B) reports the percentage of cells displaying myc-DGKα at protrusion as mean ± SE of 5 independent experiments, *t-test $p<0.05$, **t-test $p<0.005$. Scale bar 24 μm. C) MDA-MB-231 cells were infected with a lentiviral vector expressing inducible OST-tagged DGKα or an empty vector. To induce DGKα expression, cells were treated overnight with doxycycline (1 μg/ml) in serum free medium. Cell were homogenized with buffer B in absence of detergent and analysed for DGK activity (upper panel). Values are mean ± SE of 4 independent experiments with *t-test $p<0.05$. OST-DGKα and actin protein expression was verified by anti-OST and anti-actin western blot (lower panel).
doi:10.1371/journal.pone.0097144.g002

Validated siRNA DGKα [17] sense 5' GGAUGGCGAGAUGGCUAAAtt 3' antisense 5'UUUAGCCAUCUCGCCAUCCgg 3'.

siRNA PKCζ sense 5'CGUUCGACAUCAUCACCGAtt3'antisense 5'UCGGUGAUGAUGUCGAACGgg3'.

siRNA PKCι sense 5'CGUUCGACAUCAUCACCGAtt3' antisense 5'UCGGUGAUGAUGUCGAACGgg3'.

siRNA β1 integrin sense 5'GGAGGAAUGUUACACGGCU3' antisense 5' AGCCGUGUAACAUUCCUCCag 3'.

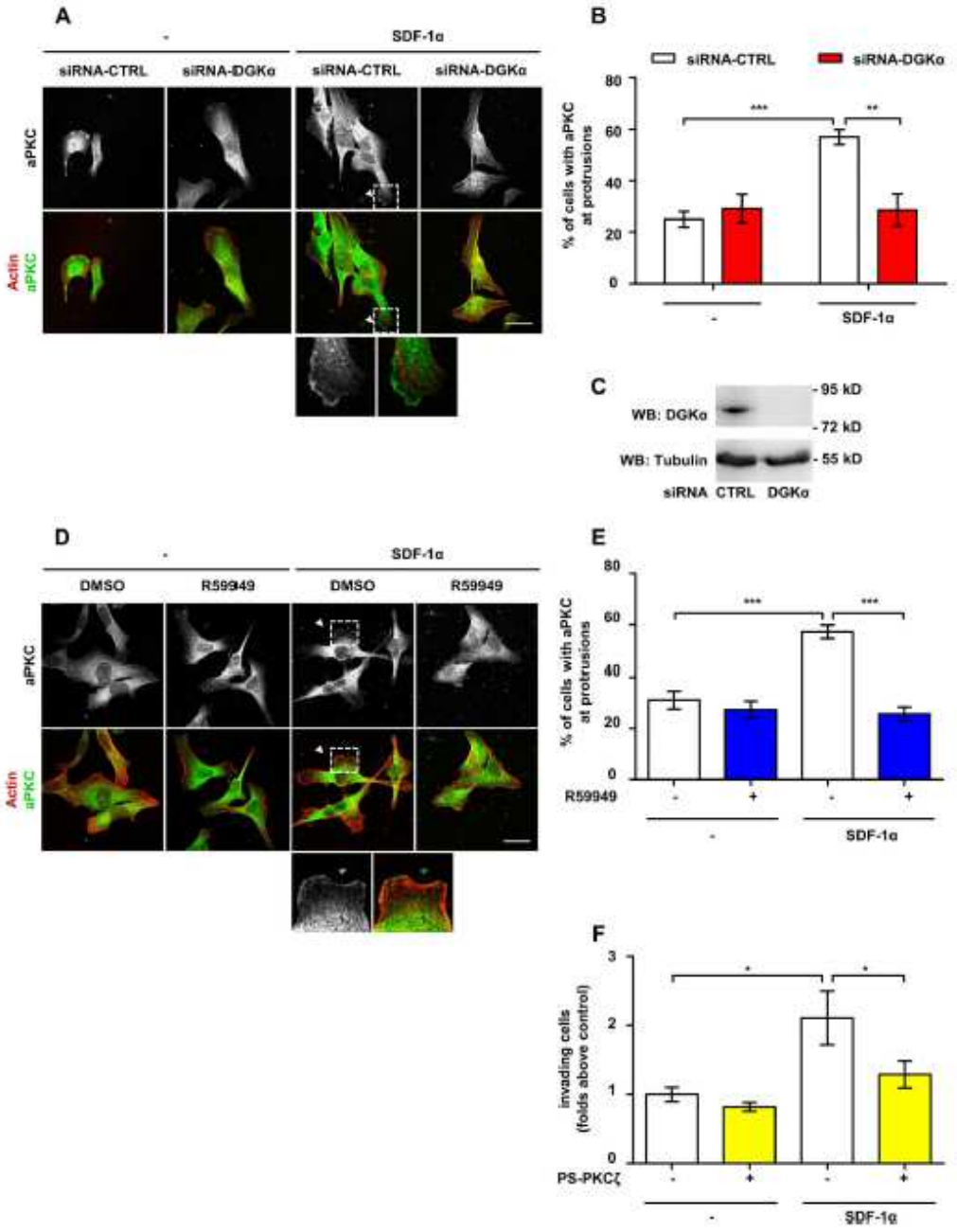

Figure 3. DGKα mediates SDF-1α-induced cell invasion by regulating aPKCs recruitment to cell pseudopods. A) MDA-MB-231 cells were plated on matrigel-coated coverslips for 20 hours in FCS containing medium, transfected with CTRL or DGKα -specific siRNA and cultured for further 20 hours in serum free medium. Cells were then stimulated for 6 hours with 50 ng/ml SDF-1α, fixed, and stained for actin (red) and aPKCs (green). Arrowhead indicates aPKCs at protrusions. Scale bar 24 μm. B) Histogram reports the percentage of cells displaying aPKCs at protrusions as mean ± SE of 3 independent experiments with **t-test $p<0.005$, ***t-test $p<0.0005$. C) MDA-MB-231 cells were transfected with CTRL or DGKα -

specific siRNA and lysed. The efficiency of DGKα down-regulation by siRNA was verified at 48 hours after transfection by western blot, tubulin was used as loading control. D) MDA-MB-231 cells were plated on matrigel-coated coverslips for 20 hours in FCS containing medium and cultured for further 20 hours in serum free medium. Cells were then stimulated for 6 hours with 50 ng/ml SDF-1α in presence or in absence of 1 μM R59949, fixed and stained for actin (red) and aPKCs (green). Arrowheads indicate aPKCs at protrusions. Scale bar 24 μm. E) Histogram reports the percentage of cells displaying aPKCs at protrusions as mean ± SE of 3 independent experiments with ***t-test p<0.0005. F) MDA-MB-231 cells (10^6/well) were plated on matrigel invasion chamber and stimulates for 24 hours with SDF-1α (50 ng/ml) in presence or absence of PKCζ pseudosubstrate (PS-PKCζ, 10 μM). Histogram reports mean ± SE of folds over control values from 3 independent experiments with *t-test p<0.05.
doi:10.1371/journal.pone.0097144.g003

siRNA RCP: ON-TARGETplus RAB11FIP1 siRNA L-015968-00-0005 (Dharmacon). Silencer negative control siRNA AM4611 (Life Technologies) was used as negative control.

Generation of Tet-inducible Strep-tagged DGKα Construct and Cell Infection

Human DGKα was amplified from pMT2- DGKα [24] by PCR using the primers DGKα_ScII_fw (5'-CCGCGGGCAG-CATGGCCAAGGAGAGGGGC-3') and DGKα_H3_rv (5'-AAGCTTTTAGCTCAAGAAGCCAAA-3') and cloned into pEXPR-IBA-105 (IBA GmbH) via SacII and HindIII to generate pEXPR-Strep-DGKα. In a further step Strep-DGKα was amplified by PCR using primers IBA_fw_N1 (5'-GCGGCCGCA-GACCCACCATGGCTAGC-3') and 105DGKa_MluI_rv (5'-ACGCGTTTAGCTCAAGAAGCCAAA-3') and cloned via NotI and MluI in pLVX-Tight-Puro (Clontech). All constructs were verified by DNA sequencing.

The resulting pLVX-Tight-PURO-OST-DGKα presents OST-DGKα after a tetracycline controlled promoter and was used with the Lenti-X Tet-On Advanced Inducible Expression System (Clontec) according to manufacturer's instruction. Lentiviral particles were obtained in 293FT packaging cells co-transfected with helper vectors. After double infection and selection we obtained a polyclonal population of MDA-MB-231 cells expressing OST-DGKα in a tetracycline inducible manner. A control cell line was also generated with an empty vector.

Generation of MDA-MB-231 Stably Expressing Myc-DGKa

Myc-DGKα was amplified from PMT2-myc-DGKα [16] by PCR using the primers sense.

5'CTCGAGACCAATGGAACAAAAGTTGATTTCAGAA-GAAGATTTATTAATGGCCAAGGAGG3', antisense 5'GCCCCTCTCCTTGGCCATTAATAAATCTTCTTCT-GAAACAACTTTTGTTCCATGGCTCGAGTGCA3' and cloned in the pDONOR211 vector using the Gateway system (Life Technologies) according to manufacturer's instructions. The Gateway Technology (Life Technologies) was also used to subclone myc-DGKα into pLenti4/V5-DEST lentiviral vector. Lentiviral particles were obtained in 293FT packaging cells co-transfected with helper vectors. After infection and selection we obtained a polyclonal population of MDA-MB-231 cells constitutively expressing myc-DGKα.

Inducible Silencing of DGKα in MDA-MB-231

We used the commercial pTRIPZ Inducible Lentiviral Human DGKA shRNA Clone ID: V3THS_340705 (shRNA-DGKα1) or pTRIPZ Inducible Lentiviral Non-silencing shRNA Control RHS4743 (shRNA-CTRL). Those vectors express shRNA and turboRFP under a doxycycline regulated promoter (Thermo Scientific Open Biosystems). Lentiviral particles were obtained in 293FT packaging cells co-transfected with helper vectors. After infection and selection we obtained a polyclonal population of MDA-MB-231 cells which upon induction with doxycycline (1 μg/ml, 72 hours) are 100% RFP positive.

Stable Silencing DGKα in MDA-MB-231

The shRNA for DGKα (forward: 5' GATCCCCGGTCAGT-GATGTCCTAAAGTTCAAGAGACTTTAGGACATCACT-GACCTTTTTGGAAA reverse: 5' AGCTTTTC-CAAAAAGGTCAGTGATGTCCTAAAGTCTCTTGAACTT-TAGGACATCACTGACCGGG) was cloned with H1-Promoter within the lentiviral vector pCCL.sin.PPT.hPGK.GFPWpre [25]. The resulting vector co-express shRNA-DGKα and GFP (shRNA-DGKα2). Empty vector was used as a control. Lentiviral particles were obtained in 293FT packaging cells co-transfected with helper vectors (Life Technologies). At 1 week after infection nearly 100% of cells were GFP^+.

Generation of ShRNA- β1 Integrin MDA-MB-231

ShRNA-β1integrin in pLKO were a kind gift of P. Defilippi [26]. Lentiviral particles were generated with Sigma Mission Lentivaral packaging mix according to manufacturer's instruction in 293FT cells and selected with puromycin. Empty pLKO was used as a control.

Western Blotting

To verified protein down-regulation cells were lysed 48 hours after transfection. Cell were washed with ice cold PBS, scraped on ice in lysis buffer (25 mM Hepes, pH 8, 150 mMNaCl, 0.5/1% Nonidet P-40, 5 mM EDTA, 2 mM EGTA, 1 mM ZnCl2, 50 mM NaF, 10% glycerol supplemented with fresh 1 mM Na_3VO_4, and protease inhibitors) and clarified after centrifugation of 15 minutes at 12000 rpm at 4°C. Samples were then resuspended in Laemmli buffer, heat denatured, and separated by SDS/PAGE. Proteins were then transferred on PVDF membrane by using semi-dry system. Membrane was then blocked with 5% BSA in PBS and incubated at 4°C overnight with primary antibodies diluted in TBS tween 0.1%, BSA 2%, 0.01% azide. After 4 washes with TBS-Tween 0.1%, membranes were incubated with secondary antibodies and washed again. Western blot were visualized using Western Lightning Chemiluminescence Reagent Plus (Perkin Elmer).

Quantitative RT-PCR

RNA was extracted by TRI-Reagent Solution (Life Technologies) retrotrascribed with High-Capacity cDNA Reverse Transcription Kits (Life Technologies) and cDNA quantified by real time PCR using GUSB as normalizer. TaqMan gene expression assays we from Life Technologies: β1 integrin (Hs 00559595), GUSB (Hs 00939627), DGKα (Hs 00176278) and MMP-9 (Hs 00234579).

MMP-9 Secretion

MDA-MB-231 cells (250,000 cells/well) were plated in 6-well cell culture plate and transfected with the indicated siRNA. After 24 hours in serum free media cells were treated with SDF-1α (100 ng/ml in 500 μl serum-free medium). After 24 hours the MMP-9 concentration in the supernatants was determined by ELISA assay (Life Technologies).

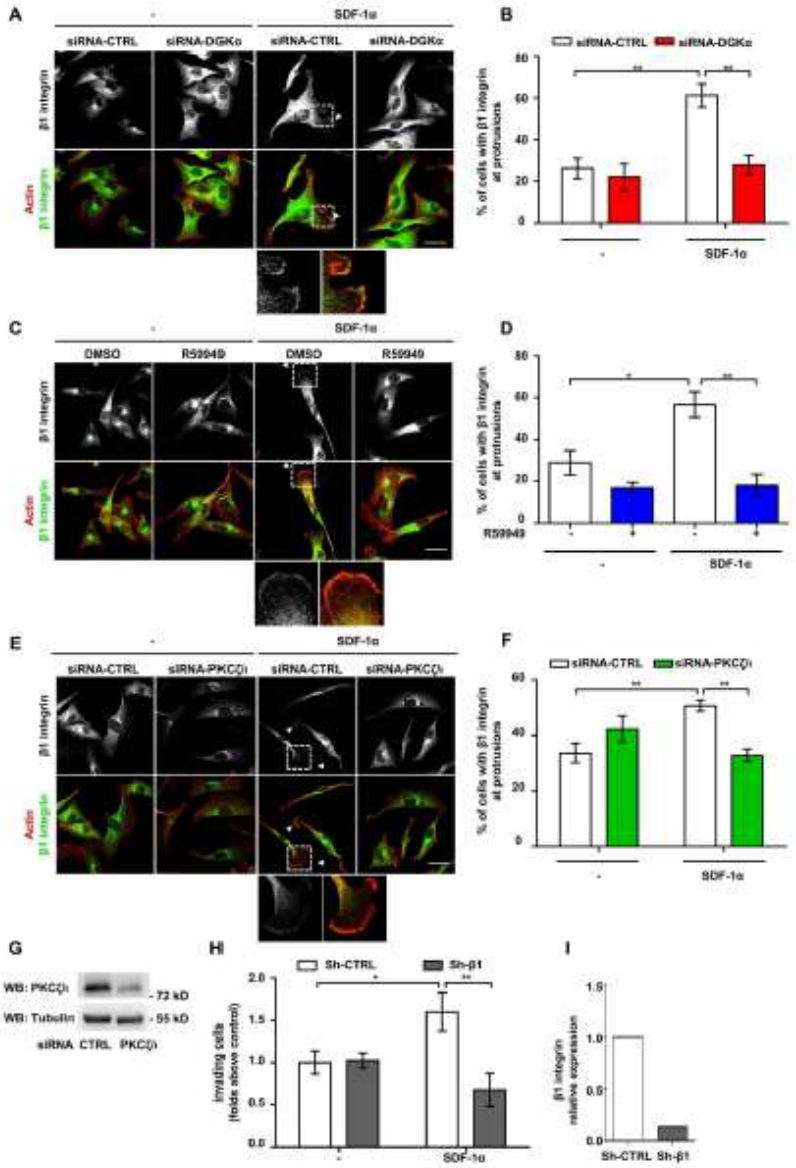

Figure 4. DGKα and aPKCs mediate SDF-1α-induced recruitment of β1 integrin to pseudopods. A) MDA-MB-231 cells were plated on matrigel-coated coverslips for 20 hours in FCS containing medium, transfected with CTRL or DGKα-specific siRNA and cultured for further 20 hours in serum free medium. Cells were then stimulated for 6 hours with 50 ng/ml SDF-1α, fixed and stained for actin (red) and β1 integrin (green). Arrows indicate β1 integrin at protrusions. Scale bar 24 μm. B) Histogram reports the percentage of cells displaying β1 integrin at protrusions as mean ± SE values of 3 independent experiments with **t-test $p<0.005$. C) MDA-MB-231 cells were plated on matrigel-coated coverslips for 20 hours in FCS containing medium and cultured for further 20 hours in serum free medium. Cells were then stimulated for 6 hours with 50 ng/ml SDF-1α, in presence or in absence of 1 μM R59949, fixed and stained for actin (red) and β1 integrin (green). Arrow indicates β1 integrin at protrusions. Scale bar 24 μm. D) Histogram reports the percentage of cells displaying β1 integrin at protrusions as mean ± SE of 3 independent experiments with *t-test $p<0.05$, **t-test $p<0.005$. E) MDA-MB-231 cells were plated on matrigel-coated coverslips for 20 hours in FCS containing medium, transfected with CTRL or PKCζ/ι –specific siRNA and cultured for further 20 hours in serum free medium. Cells were then stimulated for 6 hours with 50 ng/ml SDF-1α, fixed and stained for actin (red) and β1 integrin (green). Arrowheads indicate β1 integrin at protrusions. Scale bar 24 μm. F) Histogram reports the percentage of cells displaying β1 integrin at protrusions as mean ± SE of 3 independent experiments with **t-test $p<0.005$. G) MDA-MB-231 cells

were transfected with CTRL and PKCζ/ι –specific siRNA and lysed. The efficiency of PKCζ/ι down–regulation by siRNA was verified by western bloting, tubulin was used as a loading control. H) MDA-MB-231 cells were infected with lentiviral vectors expressing a shRNA against β1-integrin (shRNA-β1) or a control sequence (shRNA-CTRL). 50,000 cells were plated on matrigel invasion chamber and incubated for 24 hours in presence or in absence of SDF-1α (100 ng/ml). Histogram reports mean ± SE of fold over control values from 3 independent experiments with *t-test $p<0.05$, **t-test $p<0.01$. I) The efficiency of β1-integrin down–regulation by shRNA was verified by quantitative RT-PCR.
doi:10.1371/journal.pone.0097144.g004

Statistical Analysis

Data are shown as the mean ± SEM. For statistical analysis, Student's t-test or *ANOVA* were used. Experiments shown are representative at least 3 independent experiments.

Results

DGKα Is Necessary for SDF-1α-induced Cell Invasion

We previously showed that DGKα is necessary for matrix invasion promoted by Epidermal Growth Factor (EGF) [15] or Hepatocyte Growth Factor (HGF) in MDA-MB-231 breast carcinoma cells [27]. In order to investigate the role of DGKα in chemokine invasive signaling in breast cancer, we knocked down DGKα in MDA-MB-231 using a lentiviral construct expressing a DGKα-specific shRNA under an inducible promoter (shRNA-DGKα1). This construct strongly downregulated DGKα expression when compared with parental cells or a non-targeting control sequence (shRNA-CTRL, Fig. 1 B and C). The invasive ability of parental, DGKα-knocked down and control cells were evaluated in a Matrigel invasion assay. SDF-1α (100 ng/ml) doubles the number of parental as well as shRNA-CTRL MDA-MB-231 invading across the matrigel insert (Fig. 1 A). Conversely, shRNA-DGKα1 cells were unresponsive to SDF-1α stimulation. We confirmed this finding with an independent shRNA (shRNA-DGKα2) giving a comparable inhibition of SDF-1α stimulated matrix invasion (Fig. S1), making off-target effects unlikely.

Those findings indicates that DGKα mediates the pro-invasive signaling promoted not only by tyrosine kinase receptors [22] but also by chemokine receptors involved in tumor cells metastatization, such as those of SDF-1α.

SDF-1α Stimulates DGKα Activity and Localization at Protrusions Sites

The previous findings that HGF, EGF and VEGF activate DGKα and promote its recruitment to the plasma membrane in epithelial and endothelial cells [15,17,22] suggest that SDF-1α may promote localized DGKα activation at ruffling sites. Despite its biological significance, the low level of DGKα expression in MDA-MB-231 cells hampers activation and localization studies of the endogenous protein with currently available antibodies.

Thus, for localization studies, MDA-MB-231 cells were stably infected with a lentiviral vector expressing myc-DGKα and plated on matrigel-coated coverslip to mimic the epithelial microenvironment. In unstimulated serum-deprived cells, myc–DGKα was mainly cytoplasmic, with some cells displaying very little accumulation at cell protrusions (Fig. 2A). Prolonged SDF-1α stimulation (50 ng/ml; 4 to 6 hours) resulted in the localization of DGKα at the tip of large protrusions (Fig. 2A and B). No detectable changes were observed at earlier time points (15 minutes, Fig. 2B).

For enzymatic activation assays, we infected MDA-MB-231 with a lentiviral vector expressing OneStrep-Tagged DGKα (OST-DGKα) under the control of a doxycycline-inducible promoter. Upon 48 hours doxycycline treatment (1 μg/ml), OST-DGKα was strongly overexpressed as compared to endogenous protein (Fig. S2A). Under these conditions the enzymatic activity of OST-DGKα was responsible for almost the entire DGK activity measured in cell homogenates. Both SDF-1α and HGF (a well known DGKα activator) induced a further moderate increase of OST-DGKα activity within 15 minutes of stimulation (Fig. 2C).

Altogether these data indicate that SDF-1α regulates DGKα activity and localization and suggest that DGKα plays a role in the formation and/or extension of cell protrusions induced by SDF-1α.

DGKα Mediates SDF-1α-induced Cell Invasion by Regulating aPKCs Recruitment to Cell Protrusions

DGKα, by producing PA, mediates aPKCs activation and recruitment to the cell surface induced by growth factors [23,28]. Thus, we set to investigate whether DGKα mediates SDF-1α-induced cell invasion by regulating aPKCs. To investigate the role of DGKα in regulating aPKCs localization, MDA-MB-231 cells were transiently transfected with control (siRNA-CTRL) or DGKα-specific siRNA (siRNA-DGKα). Upon 48 hours from transfection with siRNA-DGKα, the expression of DGKα was nearly undetectable as compared to its expression in cells transfected with control siRNA (Fig. 3C). Then, MDA-MB-231 cells were plated on matrigel-coated coverslips, serum starved and stimulated with 50 ng/ml SDF-1α for 6 hours. In control siRNA transfected cells, SDF-1α treatment significantly increased the percentage of cells displaying aPKCs at protrusions, while DGKα silencing strongly impaired aPKCs recruitment to the membrane (Fig. 3A and B). In order to verify the requirement for DGKα enzymatic activity, we carried out aPKCs localization assays in presence or in absence of 1 μM R59949, a rather specific DGKα inhibitor [16,29]. R59949 treatment completely abrogated aPKCs localization at protrusions induced by SDF-1α, while it did not affect aPKCs localization in unstimulated cells (Fig. 3D and E).

In order to investigate the role of aPKCs in SDF-1α-induced invasion through extracellular matrix, MDA-MB-231 cells were treated with 10 μM cell permeable PKCζ pseudosubstrate (PS-PKCζ). In a matrigel invasion assay aPKCs inhibition significantly reduced SDF-1α-induced invasion, while basal invasion was unaffected in unstimulated cells (Fig. 3F).

Altogether, these data demonstrate that in SDF-1α-stimulated breast carcinoma cells, localized activity of DGKα at pseudopodial tips provides a crucial localization lipid signal for aPKCs recruitment, thus mediating SDF-1α-induced invasive signaling.

DGKα and aPKCs Mediate SDF-1α-induced Recruitment of β1 Integrin to Protrusions Sites

Recycling and clustering of β1 integrin at the tip of invasive pseudopods is a key event sustaining the invasive properties of malignant cells [30]. Conversely, growth factors stimulate invasion both by inducing integrin clustering at actin-rich adhesive sites and lamellipodia and by stimulating integrin recycling [26,31]. Thus, we set to investigate whether the DGKα and aPKCs at protrusions promote local accumulation of β1 integrin. In serum starved MDA-MB-231 cells plated on matrigel-coated coverslips β1 integrin is mostly localized in intracellular vesicles in the perinuclear/Golgi area. Upon SDF-1α stimulation, β1 integrin also localized in clusters at the tip of cell protrusions (Fig. 4A, C and E). However, either siRNA-mediated silencing of DGKα or R59949-mediated inhibition of its enzymatic activity impaired SDF-1α-induced localization of β1 integrin at cell extensions

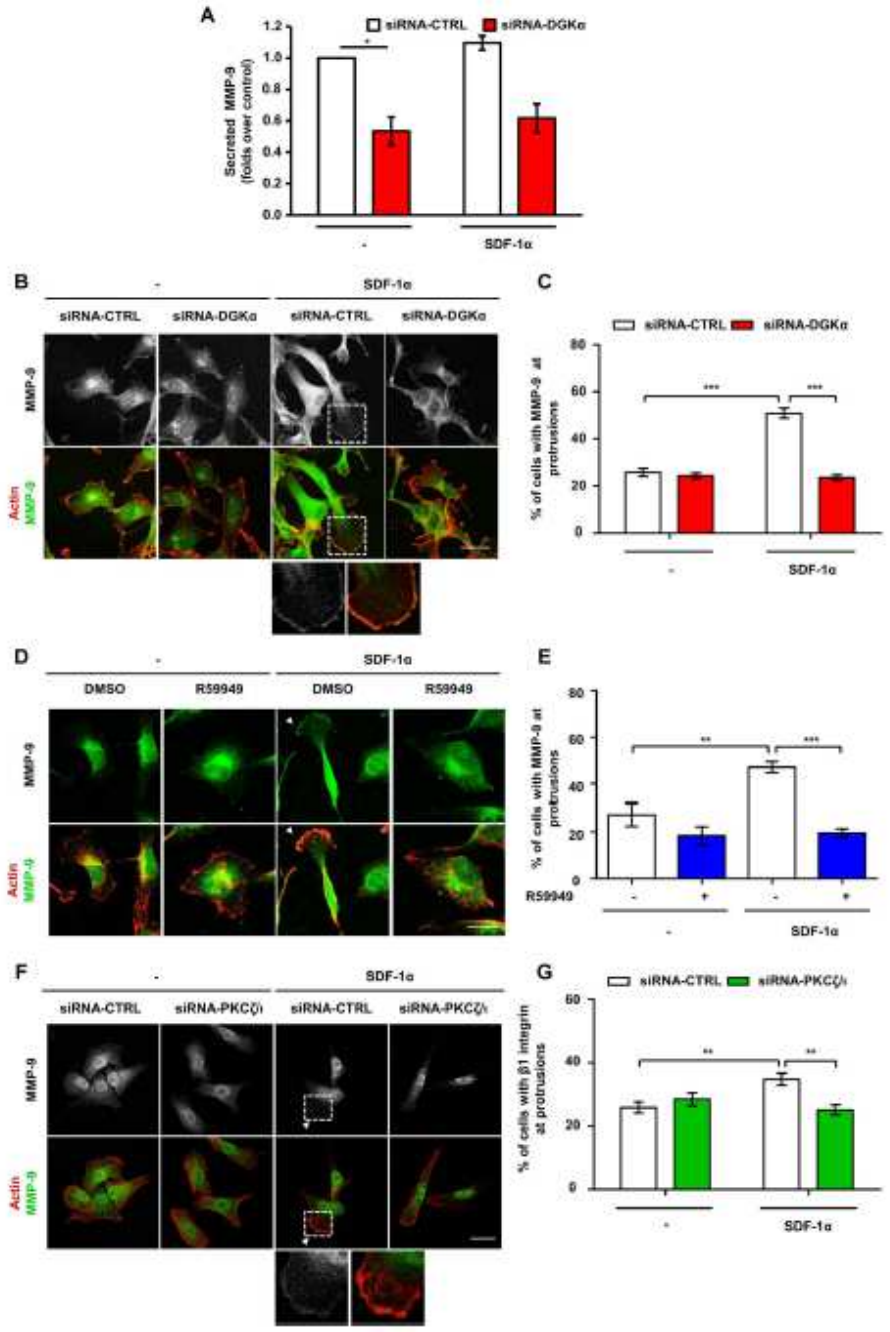

Figure 5. DGKα and aPKCs mediates MMP-9 secretion and localization at protrusions. A) MDA-MB-231 cells were transfected with CTRL or DGKα –specific siRNA and shifted to serum free media. After 24 hours cells were treated with 100 ng/ml SDF-1α in serum free medium for further 20 hours. MMP9 content in the supernatants was measured by ELISA assay, histogram reports secreted MMP-9 as mean ± SE of 3 independent

experiments normalized for control, with *t-test p<0.05. B) MDA-MB-231 cells were plated on matrigel-coated coverslips for 20 hours in FCS containing medium, transfected with CTRL or DGKα –specific siRNA and cultured for further 20 hours in serum free medium. Cells were stimulated for 6 hours with 50 ng/ml SDF-1α, fixed and stained for actin (red) and MMP-9 (green). Arrowhead indicates MMP-9 at protrusions. Scale bar 24 μm. C) Histogram reports the percentage of cells displaying MMP-9 at protrusions as mean ± SE of 3 independent experiments with ***t-test p< 0.0005. D) MDA-MB-231 cells were plated on matrigel-coated coverslips for 20 hours in FCS containing medium and cultured for further 20 hours serum free medium. Cells were stimulated for 6 hours with 50 ng/ml SDF-1α, in presence or in absence of 1 μM R59949, fixed and stained for actin (red) and MMP-9 (green). Arrowhead indicates MMP-9 at protrusions. Scale bar 24 μm. E) Histogram reports the percentage of cells displaying MMP-9 at protrusions as mean ± SE of 3 independent experiments with **t-test p<0.005, ***t-test p<0.01. F) MDA-MB-231 cells were plated on matrigel-coated coverslips for 20 hours in FCS containing medium, transfected with CTRL or PKCζ/ι –specific siRNA and cultured for further 20 hours in serum free medium. Cells were then stimulated for 6 hours with 50 ng/ml SDF-1α, fixed and stained for actin (red) and MMP-9 (green). Arrowhead indicates MMP-9 at protrusions. Scale bar 24 μm. G) Histogram reports the percentage of cells displaying MMP-9 at protrusions as mean ± SE of 3 independent experiments with *t-test p<0.05, **t-test p<0.005.
doi:10.1371/journal.pone.0097144.g005

(Fig. 4A, B, C and D). Interestingly SDF-1α stimulation and DGKα inhibition did not affect the expression of β1 integrin at the cell surface, as measured by FACS analysis (Fig. S4A). Since DGKα promotes Rac1 activation and membrane ruffles by regulating aPKCs [15] and as DGKα mediates SDF-1α-induced aPKCs recruitment to the membrane protrusions, we assessed whether aPKCs controls β1 integrin localization. Indeed, siRNA-mediated silencing of aPKCs (Fig. 4G) impaired SDF1-α-induced localization of β1 integrin at cell protrusions (Fig. 4E and F).

Altogether these data suggest that SDF-1α, by activating the DGKα/aPKCs pathway, stimulates the clustering of β1 integrin at cell protrusions, rather than stimulating its bulk translocation at the plasma membrane.

Since the expression of constitutively-membrane bound myr-DGKα stimulates cell invasion by triggering RCP-mediated recycling of integrin α5β1 [15], we set to investigate the role of β1 integrin in SDF-1α-promoted cell invasion. To this purpose we used shRNA mediated knockdown of β1 integrin which resulted in an 80% reduction of its expression in MDA-MB-231 cells (Fig. 4I). We found that, β1 integrin knock down severely impaired the ability of MDA-MB-231 cells to invade through matrigel in response to SDF-1α stimulation (Fig. 4H).

Altogether these data indicate that DGKα, by regulating aPKCs, controls chemokine-induced β1 integrin localization at protrusion sites in breast carcinoma cells, thus confirming the pivotal role of β1 integrin in SDF-1α-promoted matrix invasion.

DGKα and aPKCs Mediate SDF-1α-induced MMP-9 Secretion and Localization at Protrusions

Secretion of matrix metalloproteinases (MMPs) is involved in the extracellular matrix degradation required for invasion of cancer cells [32,33]. SDF-1α stimulates the secretion of MMP-9 in several cancer cells, including MDA-MB-231 cells [34,35]. In migrating cells, MMP-9 is addressed to the cellular extensions involved in cell migration and accumulates at their tips [36]. Thus, we investigated whether SDF1-α regulates intracellular localization and secretion of MMP-9 through the DGKα/aPKCs axis.

MDA-MB-231 cells presented a low, constitutive secretion of MMP-9 (40–80 pg/ml in the supernatant), which was not affected by SDF-1α but was severely reduced by siRNA-mediated silencing of DGKα (Fig. 5A). However, the mRNA levels of MMP-9 were not affected by either SDF-1α stimulation or DGKα inhibition, suggesting that this pathway does not regulate MMP-9 at the transcriptional level in these cells (Fig. S4C). Conversely, SDF-1α stimulated MMP-9 accumulation at protrusions of serum-starved MDA-MB-231 plated on matrigel-coated coverslips (Fig. 5B to E). We cannot rule out that MMP-9 staining may be associated to the plasma membrane, indeed FACS analysis of these cells detected low amounts of membrane-bound MMP-9 with a small increase in MMP-9 surface positive cells following SDF-1α stimulation (Fig. S4B). Silencing of DGKα impaired MMP-9 translocation induced by SDF-1α, while it did not affect its localization in unstimulated cells (Fig. 5B and C). Similarly, DGKα pharmacological inhibition with R59949, completely impaired MMP-9 recruitment induced by SDF-1α (Fig. 5D and E).

Altogether these data suggest that DGKα is essential for MMP-9 accumulation at protrusions and subsequent release in the extracellular space. Given the role of DGKα in regulating aPKCs, we investigated whether aPKCs mediates SDF-1α-induced regulation of MMP-9 localization. Indeed, siRNA-mediated silencing of aPKCs blunted SDF-1α induced MMP-9 localization at pseudopodial tips (Fig. 5F and G).

Altogether these data demonstrate that activation of the DGKα/aPKCs pathway drives both MMP-9 and β1 integrin localization at the pseudopodial tips, thus regulating the extension of invasive protrusions and sustaining the invasive behavior of MDA-MB-231 cells.

DGKα Overexpression Promotes aPKC/Rac Dependent Cell Elongation

We observed that prolonged SDF1α treatment (6 hours, 50 ng/ml) of matrigel plated MDA-MB-231 promotes the transition to an elongated shape with the extension of long protrusions. Interestingly both siRNA downregulation of DGKα and R59949-mediated inhibition impairs this change in shape (Fig. S3A to C) indicating the crucial requirement of DGKα activity.

Since the over-expression of membrane-bound myr-DGKα stimulates cell migration in untransformed cells [18] and pseudopod extension and invasion in A2780 ovarian cancer cells [15], we investigated whether wild type DGKα over-expression was sufficient to further stimulate invasion in MDA-MB-231 cells. The previously described inducible OST-DGKα construct in MDA-MB-231 cells allowed us to verify this issue as doxycycline treatment induced a 30-fold increase in DGKα expression (Fig. 6A and Fig. S2A), with an increase of about 300-fold of the enzymatic activity (Fig. 2C). However, over-expression of OST-DGKα was not sufficient to enhance migration of MDA-MB-231 in wound-healing assay or to increase invasion through matrigel (Fig. S2B and C). Nevertheless, over-expression of OST-DGKα led to elongation of serum-starved MDA-MB-231 cells, while doxycycline did not affect the cell length of empty vector-infected MDA-MB-231 cells (Fig. 6B and D). Both in elongated and in shorter cells, OST-DGKα is localized at the tip of cell protrusions (Fig. 6C) suggesting that despite the absence of cytokines and growth factors the strong up-regulation of DGKα activity is sufficient to recruit the signaling machinery for membrane extension and to establish a feed forward loop recruiting further DGKα.

Consistently, with the reported role of the aPKCs in mediating DGKα-dependent Rac activation and membrane protrusions [23], we observed that siRNA-mediated silencing of aPKCs (Fig. 6G) blunted cell elongation induced by OST-DGKα over-expression (Fig. 6E). Also the Rac inhibitor NSC23766 completely

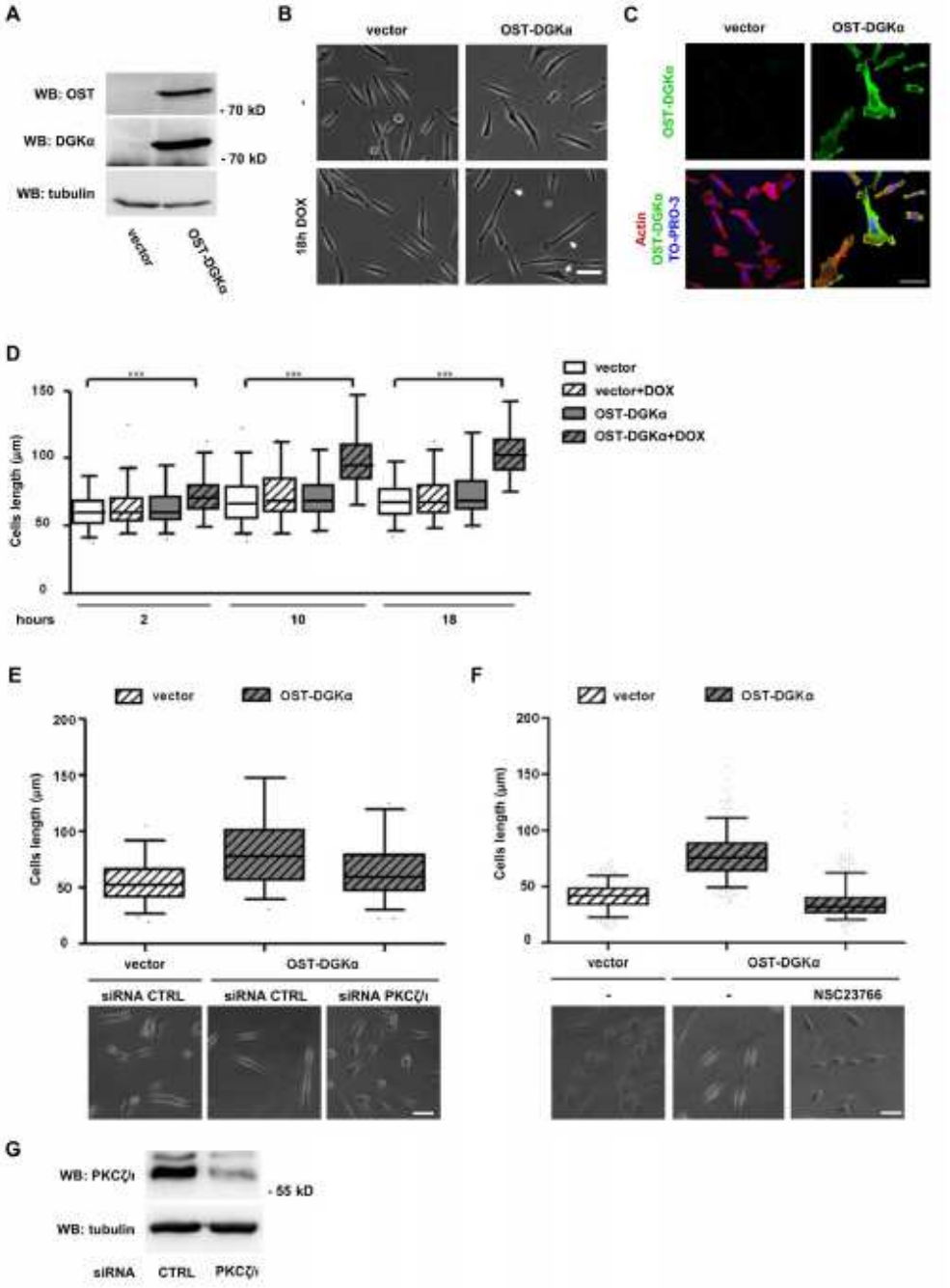

Figure 6. DGKα overexpression promotes a PKC-dependent cell elongation. MDA-MB-231 cells were infected with lentiviral vector expressing inducible OST-tagged DGKα or an empty vector. To induce DGKα expression, cells were treated overnight with doxycycline (1 µg/ml) in serum free medium. A) After cell lysis OST-DGKα induction was verified by western blotting with an antibody recognizing the OST-tag, while the

extent of overexpression was verified with anti DGKα antibodies. Tubulin was used as loading control. B) Phase contrast images of control and OST-DGKα cells cultured in presence or absence of doxycycline. Arrows indicate cells with long protrusions. Scale bar 50 μm. C) Confocal images of doxycycline induced cells showing OST-DGKα localization, cells were stained for actin (red) and OST (green). Scale bar 24 μm. D) Time course of cell elongation at 2, 10 and 18 hours with or without doxycycline treatment. Time lapse videos were recorded and total cell length measured. Box and whiskers plots (black lines show median, whiskers: 5–95 percentile) of data from 3 independent experiments are shown, ***p<0.0.001, 1 way ANOVA. E) MDA-MB-231 cells expressing OST-DGKα were transiently transfected with control or PKCζ/ι-specific siRNA. After 48 hours DGKα expression was induced by overnight treatment with doxycycline (1 μg/ml) in serum free medium. Images were acquired with a phase contrast microscope, representative images are shown. Scale bar 50 μm. Total cell length was measured for at least 100 cells and reported as box and whiskers plot. F) MDA-MB-231 cells expressing OST-DGKα were induced by overnight treatment with doxycycline (1 μg/ml) in serum free medium with or without NSC23766 (100 μM). Images were acquired with a phase contrast microscope, representative images are shown. Scale bar 50 μm. Total cell length was measured for at least 100 cells and reported as box and whiskers plot. MDA-MB-231 cells were transfected with CTRL and PKCζ/ι –specific siRNA and lysed. The efficiency of PKCζ/ι down-regulation by siRNA was verified by western blotting, tubulin was used as a loading control.
doi:10.1371/journal.pone.0097144.g006

blunted OST-DGKα induced elongation indicating the involvement of Rac family GTPases (Fig. 6F). Those findings confirm the relevance of aPKCs and Rac as DGKα downstream effectors promoting cytoskeletal remodeling and extension of membrane protrusions.

The expression of myr-DGKα drives pseudopodial extension by stimulating RCP-mediated recycling of β1 integrin in A2780 carcinoma cells [15]. However, siRNA-mediated silencing of either β1 integrin or RCP (Fig. S5C and D) did not affect protrusion elongation induced by wild type DGKα in serum starved MDA-MB-231 cells (Fig. S5A and B), suggesting that in this experimental model β1 integrin and its RCP-mediated recycling are not required for protrusion elongation.

These data indicate that up-regulation of DGKα activity by SDF-1α is sufficient to promote the extension of membrane protrusions through the aPKCs – RhoGDI – Rac pathway [22,23], but that additional signaling pathways and/or its localization at specific myrstyoilation-directed membrane compartment are required to trigger cells invasion.

Discussion

We and others established the relevance of DGKα activation and membrane recruitment in growth factors signaling [37]. In normal epithelia, endothelia and lymphocytes DGKα activity is required to convey proliferative [17,38,39] and migratory [16–18,22,23] signaling. Several studies pointed out DGKα involvement in cancer showing that its activity is necessary *in vivo* for glioblastoma and hepatocellular carcinoma progression [13], and *in vitro* for proliferation and survival of endometrial carcinoma [21], anaplastic large cell lymphoma [19], and melanoma [40]. Moreover, DGKα activity mediates matrix invasion sustained by p53 pro-metastatic mutations in cancer cells [15]. However, the molecular pathways by which DGKα controls carcinoma formation and metastatization are poorly known.

Inhere we investigated the role of DGKα in invasive signaling of SDF-1α, one of the key signals driving metastasis [41], whose receptor, CXCR4, is strongly associated to tumor growth and spontaneous metastasis formation [1]. We used MDA-MB-231 cells, a highly invasive human breast cancer cell line, whose invasiveness and tumorigenicity are dependent on the expression of SDF-1α receptor, CXCR4 [42–44]. In these cells we had previously shown that DGKα is required for EGF- [15] and HGF-induced [27] migration in a tridimensional environment.

Interestingly, we show here that DGKα is also regulated by SDF-1α, which stimulates its enzymatic activity and promotes its recruitment at ruffling sites (Fig. 2). Moreover, we show that activation of DGKα provides a key lipid signal required for SDF-1α pro-invasive activity in MDA-MB-231 cells (Fig. 1).

We previously showed that the PA generated by HGF-induced activation of DGKα recruits to the plasma membrane and activates aPKCs in a complex with RhoGDI and Rac1, thus mediating the release of Rac1 from RhoGDI, and its localization and activation at ruffle sites [23]. The aPKCs subfamily comprises the ζ and ι isoforms, which are activated by PA [28] but insensitive to DG.

Several pieces of evidence show that aPKCs and in particular PKCι, play a key role in cancer cell invasion and tumor progression [45]. Interestingly, PKCι is essential for K-Ras-driven invasion in colon cancer by regulating Rac1 [46], while aPKCs mediates EGF-induced cell migration of MDA-MB-231 breast cancer cells [47]. Altogether these data further suggest that the DGKα/aPKCs signaling axis contributes to pro-invasive signaling.

Accordingly, the finding that SDF-1α induces aPKCs localization at protrusion sites through activation of DGKα, indicates that the DGKα/aPKCs signaling axis mediates chemokine-driven mammary carcinoma invasiveness (Fig. 3). DGKα-dependent recruitment of aPKCs at protrusion is an essential signaling event, since the silencing of either DGKα or aPKCs impairs downstream events such as accumulation of β1 integrin and MMP-9 at the plasma membrane (Fig. 4 and 5). The functional relevance of aPKCs as a DGKα effector is further proved by the observation that its silencing impairs DGKα-induced cell elongation (Fig. 6E) and that its inhibition blocks SDF-1α-induced matrix invasion (Fig. 3F).

The findings that aPKCs, RCP and β1 integrin are all required for the invasiveness of MDA-MB-231 (Fig. 3F, 4H and ref. [15]), and that upon SDF-1α stimulation β1 integrin is concentrated at protrusion tips in a DGKα and aPKCs-dependent manner, are consistent with our previous data showing that DGKα-generated PA, through binding to RCP, docks α5β1 recycling vesicles to the tips of invasive pseudopods. Altogether these findings suggest that activation of aPKCs may also contribute to integrin recycling induced by chemokines and growth factors, although there is no experimental evidence for it.

Several pieces of evidence in different cell types indicate that activation of aPKCs regulates MMPs production and secretion [48]. For instance, PKCζ activation mediates MMP-9 secretion induced by SDF-1α in hematopoietic progenitors [11]. MMPs are key players in the tumor microenvironment and play a major role in invasion of extracellular matrix [49]. While some MMPs are transmembrane proteins, most of them are solubile and bind to the extracellular cell surface by interaction with several membrane proteins, including β1 integrin and CD44v [50–54].

Our finding that both DGKα and aPKCs are required for SDF-1α-induced release of MMP9 in the cell medium and for its accumulation at protrusions, provides further strength to our thesis that DGKα/aPKCs axis is a major component of chemokine pro-invasive signaling. Interestingly, in SDF-1α-stimulated cells, MMP-9 localization at cell surface superimposes with that of β1 integrin, suggesting that their function at protrusion tips is coordinately regulated by activation of DGKα/aPKCs signaling.

Finally, the observation that DGKα over expression drives by itself elongation of cell protrusions by regulating aPKCs is consistent with active PKCζ promoting wide cytoskeletal remodeling and protrusions in untrasformed cells [23]. The molecular mechanisms by which aPKCs induces cell elongation downstream to DGKα is still partially known. In line with our previous demonstration that activation of the DGKα/aPKCs signaling module stimulates the RhoGDI driven localization of both Rac1 and Cdc42 at membrane ruffles, we observed that the Rac inhibitor NSC23766 blunts DGKα induced cell elongation (Fig. 6G) and that SDF-1α-induced localization of Cdc42 at protrusions of MDA-MB-231 cells is significantly reduced by DGKα inhibition (Fig. S3D and E). Conversely, protrusion extension occurs even in the absence of β1 integrin and RCP, suggesting that DGKα-dependent activation of aPKCs regulates cytoskeletal remodeling independently from β1 integrin recycling and function, which are required, however, to enable cell migration through a 3D matrix (Fig. 4H). While it is clear that DGKα/aPKCs activity on cell elongation is independent on β1 integrin recycling, these data cannot rule out that accumulation of β1 integrin and MMP-9 at protrusion tips depends on DGKα/aPKCs-induced regulation of Rac1 or Cdc42 and cytoskeletal contractility [31].

Altogether we showed that activation of the DGKα/aPKCs/β1 integrin pathway plays a key role in chemokine-driven matrix invasion in breast cancer cells. Those observations suggest that DGKα inhibition or silencing could be effective not only in reducing primary tumor growth *in vivo* [13,14] but could potentially also reduce the metastatic potential of carcinoma cells.

Supporting Information

Figure S1 DGKα is necessary for SDF-1α-induced cell invasion. MDA-MB-231 cells were infected with lentiviral vectors expressing a shRNA against DGKα (shRNA-DGKα2) or an empty vector. A) Cells were lysed and the efficiency of DGKα down–regulation by shRNA was verified by western blot, tubulin was used as a loading control. B) 50,000 cells were plated on matrigel invasion chamber and incubated for 24 hours in presence or in absence of SDF-1α (100 ng/ml). Histogram reports mean ± SE of fold over control values from 3 independent experiments with *t-test $p<0.05$, ***t-test $p<0.0005$.
(TIF)

Figure S2 DGKα overexpression does not affect migration and invasion of MDA-MB-231 cells. MDA-MB-231 cells were infected with lentiviral vector expressing inducible OST-tagged DGKα or an empty vector. To induce DGKα expression, cells were treated overnight with doxycycline (1 μg/ml) in serum free medium. A) After cell lysis, the extent of DGKα overexpression was verified with anti DGKα antibodies, long and short exposures are shown. Actin was used as loading control. B) Cells were grown to confluence in 12 well plates and subjected to a wound healing assay for 24 hours in serum free medium. HGF (50 ng/ml) was used as a positive control. The cells were stained and those migrating inside 2.3 mm of wound counted. Histogram reports mean ± SE of fold over control values from 3 independent experiments with *t-test $p<0.05$. C) 50,000 cells were plated on matrigel invasion chamber and incubated for 24 hours in serum free medium. Medium with 10% FCS was used as positive control. Histogram reports mean ± SE of fold over control values from 3 independent experiments with *t-test $p<0.05$.
(TIF)

Figure S3 DGKα is required for SDF-1α-induced pseudopod elongation. A) MDA-MB-231 cells were plated on matrigel-coated coverslips for 20 hours in FCS containing medium, transfected with CTRL or DGKα -specific siRNA and cultured for further 20 hours in serum free medium. Cells were then stimulated for 6 hours with 50 ng/ml SDF-1α, fixed and photographed at phase contrast. B) Histogram reports protrusions length in μm as mean ± SE values of 4 independent experiments with *t-test $p<0.005$. C) MDA-MB-231 cells were plated on matrigel-coated coverslips for 20 hours in FCS containing medium and cultured for further 20 hours in serum free medium. Cells were then stimulated for 6 hours with 50 ng/ml SDF-1α, in presence or in absence of 1 μM R59949, fixed and photographed at phase contrast. Histogram reports protrusions length in μm as mean ± SE of 3 independent experiments with *t-test $p<0.005$. D) MDA-MB-231 cells were plated on matrigel-coated coverslips for 20 hours in FCS containing medium and cultured for further 20 hours serum free medium. Cells were stimulated for 6 hours with 50 ng/ml SDF-1α, in presence or in absence of 1 μM R59949, fixed and stained for actin (red) and Cdc42 (green). Arrowhead indicates Cdc42 at protrusions. Scale bar 24 μm. E) Histogram reports the percentage of cells displaying Cdc42 at protrusions as mean ± SE of 3 independent experiments with *t-test $p<0.05$.
(TIF)

Figure S4 SDF-1α is not affecting surface exposition of β1-integrin and MMP-9. A) Surface expression of β1 integrin was analyzed before (turquoise) and after (red) SDF-1α stimulation. Flow cytometry histogram overlay comparing the level of β1 integrin expression before and after SDF-1α expression. Isotype-matched controls mAb staining are given as dashed lines. MFI, median fluorescence intensity. B) Surface expression of MMP-9 was analyzed before (turquoise) and after (red) SDF-1α stimulation. Flow cytometry histogram overlay comparing the level of MMP-9 expression before and after SDF-1α expression. Isotype-matched controls mAb staining are given as dashed lines. MFI, median fluorescence intensity. C) MDA-MB-231 cells were plated on 6 wells dish for 20 hours in FCS containing medium and cultured for further 20 hours serum free medium. Cells were stimulated for 24 hours with 100 ng/ml SDF-1α, in presence or in absence of 1 μM R59949. MMP-9 mRNA was quantified by quantitative RT-PCR. Histogram reports the mean ± SE of 3 independent experiments.
(TIF)

Figure S5 DGKα promoted cell elongation is independent from β1 integrin and RCP. MDA-MB-231 cells were infected with lentiviral vector expressing inducible OST-tagged DGKα or an empty vector. A) Cells were transiently transfected with control or β1 integrin-specific siRNA. After 48 hours DGKα expression was induced by overnight treatment with doxycycline (1 μg/ml) in serum free medium. Images were acquired with a phase contrast microscope, representative images are shown. Scale bar 50 μm. Total cell length was measured for at least 100 cells and reported as box and whiskers plot. B) Cells were transiently transfected with control or RCP-specific siRNA. After 48 hours DGKα expression was induced by overnight treatment with doxycycline (1 μg/ml) in serum free medium. Images were acquired with a phase contrast microscope, representative images are shown. Scale bar 50 μm. Total cell length was measured for at least 100 cells and reported as box and whiskers plot. C) MDA-MB-231 cells were transfected with CTRL and β1 integrin-specific siRNA and lysed. The efficiency of β1 integrin down–regulation by siRNA was verified by western blotting, tubulin was used as a

loading control. D) MDA-MB-231 cells were transfected with CTRL and RCP-specific siRNA and lysed. The efficiency of RCP down-regulation by siRNA and of OST-DGKα induction was verified by western blotting, actin was used as a loading control. (TIF)

Acknowledgments

ShRNA-β1 integrin in pLKO were a kind gift of P. Defilippi [26]. We thank O. Acuto (Oxford, UK) for helpful discussions.

Author Contributions

Conceived and designed the experiments: E. Rainero GB AG JCN. Performed the experiments: E. Rainero CC PEP FC VM VB E. Ruffo MF FB DC WP IL. Analyzed the data: E. Rainero CC FC PEP VM VB E. Ruffo MF DC IL AB NF FS GB AG. Contributed reagents/materials/analysis tools: E. Rainero WP GB AG. Wrote the paper: E. Rainero GB AG.

References

1. Muller A, Homey B, Soto H, Ge N, Catron D, et al. (2001) Involvement of chemokine receptors in breast cancer metastasis. Nature 410: 50–56.
2. Korkaya H, Liu S, Wicha MS (2011) Breast cancer stem cells, cytokine networks, and the tumor microenvironment. J Clin Invest 121: 3804–3809.
3. Teicher BA, Fricker SP (2010) CXCL12 (SDF-1)/CXCR4 pathway in cancer. Clin Cancer Res 16: 2927–2931.
4. Burger JA, Kipps TJ (2006) CXCR4: a key receptor in the crosstalk between tumor cells and their microenvironment. Blood 107: 1761–1767.
5. Li H, Yang L, Fu H, Yan J, Wang Y, et al. (2013) Association between Grb2 and ELMO1/Dock180 connects chemokine signaling with Rac activation and metastasis. Nat Commun 4: 1706.
6. Yagi H, Tan W, Dillenburg-Pilla P, Armando S, Amornphimoltham P, et al. (2011) A synthetic biology approach reveals a CXCR4-G13-Rho signaling axis driving transendothelial migration of metastatic breast cancer cells. Sci Signal 4: ra60.
7. Azab AK, Azab F, Blotta S, Pitsillides CM, Thompson B, et al. (2009) RhoA and Rac1 GTPases play major and differential roles in stromal cell-derived factor-1-induced cell adhesion and chemotaxis in multiple myeloma. Blood 114: 619–629.
8. Kumar A, Kremer KN, Dominguez D, Tachi M, Hedin KE (2011) Gαi3 and Rho mediate endosomal trafficking of CXCR4 into Rab11+ vesicles upon stromal cell-derived factor-1 stimulation. J Immunol 186: 951–958.
9. Chen G, Chen SM, Wang X, Ding XF, Ding J, et al. (2012) Inhibition of chemokine (CXC motif) ligand 12/chemokine (CXC motif) receptor 4 axis (CXCL12/CXCR4)-mediated cell migration by targeting mammalian target of rapamycin (mTOR) pathway in human gastric carcinoma cells. J Biol Chem 287: 12132–12141.
10. Odemis V, Boosmann K, Dieterlen MT, Engele J (2007) The chemokine SDF1 controls multiple steps of myogenesis through atypical PKCzeta. J Cell Sci 120: 4026–4035.
11. Petit I, Goichberg P, Spiegel A, Peled A, Brodie C, et al. (2005) Atypical PKC-zeta regulates SDF-1-mediated migration and development of human CD34+ progenitor cells. J Clin Invest 115: 168–176.
12. Mérida I, Avila-Flores A, Merino E (2008) Diacylglycerol kinases: at the hub of cell signaling. Biochem J 409: 1–18.
13. Takeishi K, Taketomi A, Shimabe K, Toshima T, Motomura T, et al. (2012) Diacylglycerol kinase alpha enhances hepatocellular carcinoma progression by activation of Ras-Raf-MEK-ERK pathway. J Hepatol 57: 77–83.
14. Dominguez CL, Floyd DH, Xiao A, Mullins GR, Kefas BA, et al. (2013) Diacylglycerol kinase α is a critical signaling node and novel therapeutic target in glioblastoma and other cancers. Cancer Discov 3: 782–797.
15. Rainero E, Caswell PT, Muller PA, Grindlay J, McCaffrey MW, et al. (2012) Diacylglycerol kinase α controls RCP-dependent integrin trafficking to promote invasive migration. J Cell Biol 196: 277–295.
16. Cutrupi S, Baldanzi G, Gnocchi D, Maffè A, Schaap D, et al. (2000) Src-mediated activation of alpha-diacylglycerol kinase is required for hepatocyte growth factor-induced cell motility. EMBO J 19: 4614–4622.
17. Baldanzi G, Mitola S, Cutrupi S, Filigheddu N, van Blitterswijk WJ, et al. (2004) Activation of diacylglycerol kinase alpha is required for VEGF-induced angiogenic signaling in vitro. Oncogene 23: 4828–4838.
18. Baldanzi G, Cutrupi S, Chiarle F, Gnocchi V, Rainero E, et al. (2008) Diacylglycerol kinase-alpha phosphorylation by Src on Y335 is required for activation, membrane recruitment and Hgf-induced cell motility. Oncogene 27: 962–976.
19. Bacchiocchi R, Baldanzi G, Carbonari D, Caporaggi C, Colombo E, et al. (2005) Activation of alpha-diacylglycerol kinase is critical for the mitogenic properties of anaplastic lymphoma kinase. Blood 106: 2175–2182.
20. Baldanzi G, Pietronave S, Lozzarno D, Merlin S, Porporato P, et al. (2011) Diacylglycerol kinases are essential for HGF-dependent proliferation and motility of Kaposi's Sarcoma cells. Cancer Sci.
21. Filigheddu N, Santpietro S, Chiarale F, Porporato PE, Gaggianesi M, et al. (2011) Diacylglycerol kinase α mediates 17-β-estradiol-induced proliferation, motility, and anchorage-independent growth of Hec-1A endometrial cancer cell line through the G protein-coupled estrogen receptor GPR30. Cell Signal 23: 1988–1996.
22. Chiarale F, Cutrupi S, Rainero E, Baldanzi G, Porporato PE, et al. (2007) Diacylglycerol kinase-alpha mediates hepatocyte growth factor-induced epithelial cell scatter by regulating Rac activation and membrane ruffling. Mol Biol Cell 18: 4859–4871.
23. Chiarale F, Rainero E, Gianfelice G, Bettio V, Pighini A, et al. (2010) Diacylglycerol kinase alpha mediates HGF-induced Rac activation and membrane ruffling by regulating atypical PKC and RhoGDI. Proc Natl Acad Sci U S A 107: 4182–4187.
24. Schaap D, de Widt J, van der Wal J, Vandekerckhove J, van Damme J, et al. (1990) Purification, cDNA-cloning and expression of human diacylglycerol kinase. FEBS Lett 273: 151–158.
25. Tiscili R, Accornero P, Fellenni A, Mangano T, Morotti A, et al. (2005) RNAi technology and lentiviral delivery as a powerful tool to suppress Tpr-Met-mediated tumorigenesis. Cancer Gene Ther 12: 456–463.
26. Morello V, Cabodi S, Sigismund S, Camacho-Leal MP, Repetto D, et al. (2011) β1 integrin controls EGFR signaling and tumorigenic properties of lung cancer cells. Oncogene 30: 4087–4096.
27. Filigheddu N, Cutrupi S, Porporato PE, Riboni F, Baldanzi G, et al. (2007) Diacylglycerol kinase ε is required for HGF-induced invasiveness and anchorage-independent growth of MDA-MB-231 breast cancer cells. Anticancer Res 27: 1489–1492.
28. Lintsaria C, Schaap D, Monleman WH, van Blitterswijk WJ (1994) Phosphatidic acid activation of protein kinase C-zeta overexpressed in COS cells: comparison with other protein kinase C isotypes and other acidic lipids. Biochem J 304 (Pt 3): 1001–1008.
29. Sato M, Liu K, Sasaki S, Kunii N, Sakai H, et al. (2013) Evaluation of the selectivities of the diacylglycerol kinase inhibitors ε50922 and ε50949 among diacylglycerol kinase isozymes using a new non-radioactive assay method. Pharmacology 92: 99–107.
30. Desgrosellier JS, Cheresh DA (2010) Integrins in cancer: biological implications and therapeutic opportunities. Nat Rev Cancer 10: 9–22.
31. Trusolino L, Comoglio S, Angelini P, Ando M, Bertotti A, et al. (2000) HGF/scatter factor selectively promotes cell invasion by increasing integrin avidity. FASEB J 14: 1629–1640.
32. Nakashima K, Inoue T, Shimao Y, Sameshima T (2002) Matrix metalloproteinases in tumor invasion: role for cell migration. Pathol Int 52: 253–264.
33. Itoh Y, Nagase H (2002) Matrix metalloproteinases in cancer. Essays Biochem 38: 21–36.
34. Yuncheng Y, Xiaoyan X (2007) Stromal-cell derived factor-1 regulates epithelial ovarian cancer cell invasion by activating matrix metalloproteinase-9 and matrix metalloproteinase-2. Eur J Cancer Prev 16: 430–435.
35. Fernandis AZ, Prasad A, Band H, Klösel R, Ganju RK (2004) Regulation of CXCR4-mediated chemotaxis and chemoinvasion of breast cancer cells. Oncogene 23: 157–167.
36. Legrand C, Gilles C, Zahm JM, Polette M, Buisson AC, et al. (1999) Airway epithelial cell migration dynamics. MMP-9 role in cell-extracellular matrix remodeling. J Cell Biol 146: 517–529.
37. Mérida I, Avila-Flores A, Garcia J, Merino E, Almena M, et al. (2009) Diacylglycerol kinase alpha, from negative modulation of T cell activation to control of cancer progression. Adv Enzyme Regul.
38. Flores I, Canseco T, Martinez-A C, Kanoh H, Mérida I (1996) Phosphatidic acid generation through interleukin 2 (IL-2)-induced alpha-diacylglycerol kinase activation is an essential step in IL-2-mediated lymphocyte proliferation. J Biol Chem 271: 16384–10840.
39. Flores I, Jones DR, Cipres A, Diaz-Flores E, Sanjuan MA, et al. (1999) Diacylglycerol kinase inhibition prevents IL-2-induced G1 to S transition through a phosphatidylinositol-3 kinase-independent mechanism. J Immunol 163: 708–714.
40. Yamagiuwa K, Yamada S, Kai M, Imai S, Yamada K, et al. (2007) Diacylglycerol kinase alpha suppresses tumor necrosis factor-alpha-induced apoptosis of human melanoma cells through NF-kappaB activation. Biochim Biophys Acta 1771: 462–474.
41. Luker KE, Luker GD (2006) Functions of CXCL12 and CXCR4 in breast cancer. Cancer Lett 238: 30–41.
42. Kang H, Mansel RE, Jiang WG (2005) Genetic manipulation of stromal cell-derived factor-1 attests the pivotal role of the autocrine SDF-1-CXCR4 pathway in the aggressiveness of breast cancer cells. Int J Oncol 26: 1429–1434.
43. Kang H, Watkins G, Parr C, Douglas-Jones A, Mansel RE, et al. (2005) Stromal cell derived factor-1: its influence on invasiveness and migration of breast cancer

cells in vitro, and its association with progress and survival in human breast cancer. Breast Cancer Res 7: R402–410.
44. Lapteva N, Yang AG, Sanders DE, Strube RW, Chen SY (2005) CXCR4 knockdown by small interfering RNA abrogates breast tumor growth in vivo. Cancer Gene Ther 12: 84–89.
45. Murray NR, Kalari KR, Fields AP (2011) Protein kinase Cι expression and oncogenic signaling mechanisms in cancer. J Cell Physiol 226: 879–887.
46. Murray NR, Jamieson L, Yu W, Zhang J, Gokmen-Polar Y, et al. (2004) Protein kinase Ciota is required for Ras transformation and colon carcinogenesis in vivo. J Cell Biol 164: 797–802.
47. Sun R, Gao P, Chen L, Ma D, Wang J, et al. (2005) Protein kinase C zeta is required for epidermal growth factor-induced chemotaxis of human breast cancer cells. Cancer Res 65: 1433–1441.
48. Frederick LA, Matthews JA, Jamieson L, Justilien V, Thompson EA, et al. (2008) Matrix metalloproteinase-10 is a critical effector of protein kinase Ciota-Par6alpha-mediated lung cancer. Oncogene 27: 4841–4853.
49. Kessenbrock K, Plaks V, Werb Z (2010) Matrix metalloproteinases: regulators of the tumor microenvironment. Cell 141: 52–67.
50. Brooks PC, Stromblad S, Sanders LC, von Schalscha TL, Aimes RT, et al. (1996) Localization of matrix metalloproteinase MMP-2 to the surface of invasive cells by interaction with integrin alpha v beta 3. Cell 85: 683–693.
51. Yu WH, Woessner JF, McNeish JD, Stamenkovic I (2002) CD44 anchors the assembly of matrilysin/MMP-7 with heparin-binding epidermal growth factor precursor and ErbB4 and regulates female reproductive organ remodeling. Genes Dev 16: 307–323.
52. Redondo-Muñoz J, Escobar-Díaz E, Samaniego R, Terol MJ, García-Marco JA, et al. (2006) MMP-9 in B-cell chronic lymphocytic leukemia is up-regulated by alpha4beta1 integrin or CXCR4 engagement via distinct signaling pathways, localizes to podosomes, and is involved in cell invasion and migration. Blood 108: 3143–3151.
53. Redondo-Muñoz J, Ugarte-Berzal E, García-Marco JA, del Cerro MH, Van den Steen PE, et al. (2008) Alpha4beta1 integrin and 190-kDa CD44v constitute a cell surface docking complex for gelatinase B/MMP-9 in chronic leukemic but not in normal B cells. Blood 112: 169–178.
54. Redondo-Muñoz J, Ugarte-Berzal E, Terol MJ, Van den Steen PE, Hernández del Cerro M, et al. (2010) Matrix metalloproteinase-9 promotes chronic lymphocytic leukemia b cell survival through its hemopexin domain. Cancer Cell 17: 160–172.